IMPROVING *IN VITRO* PREDICTIONS OF *IN VIVO* PAH BIOAVAILABILITY

A Thesis Submitted to the College of

Graduate and Postdoctoral Studies

In Partial Fulfillment of the Requirements

For the Degree of Doctor of Philosophy

In the Toxicology Graduate Program

University of Saskatchewan

Saskatoon

By

KYLE JORDAN JAMES

PERMISSION TO USE

In presenting this thesis in partial fulfilment of the requirements for a Postgraduate degree from the University of Saskatchewan, I agree that the Libraries of this University may make it freely available for inspection. I further agree that permission for copying of this thesis in any manner, in whole or in part, for scholarly purposes may be granted by the professor or professors who supervised my thesis work or, in their absence, by the Head of the Department or the Dean of the College in which my thesis work was done. It is understood that any copying or publication or use of this thesis or parts thereof for financial gain shall not be allowed without my written permission. It is also understood that due recognition shall be given to me and to the University of Saskatchewan in any scholarly use which may be made of any material in my thesis.

Requests for permission to copy or to make other use of material in this thesis in whole or part should be addressed to:

Program Chair, Graduate Program of Toxicology

Toxicology Centre

University of Saskatchewan

44 Campus Drive

Saskatoon, Saskatchewan S7N 5A8

College of Graduate and Postdoctoral Studies

University of Saskatchewan

116 Thorvaldson Building, 110 Science Place

Saskatoon, Saskatchewan S7N 5C9

ABSTRACT

Exposure assessment for incident ingestion of polycyclic aromatic hydrocarbon (PAH) contaminated soil typically assumes an absorption factor of 100%. However, gastro-intestinal (GI) absorption of PAHs from soil is known to be less than 100% and will vary based on the soil. The research herein investigates factors affecting desorption of soil PAHs and absorption into mammalian systemic circulation in order to develop an *in vitro* bioaccessibility model that is predictive of *in vivo* bioavailability, aka the absorption factor. *In vivo* bioavailability is determined using the juvenile swine model, a mammalian system, to determine PAH soil bioavailability. The Fed organic estimation of the human simulation test (FOREhST) is the *in vitro* model compared against *in vivo* bioavailability. The hypotheses of this thesis are (1) PAH bioavailability can be partially explained by chemical partitioning, as measured by fugacity capacity, (2) PAH bioaccessibility measurements are dependent upon energetic input of the model, (3) PAHs interact with each other influencing partitioning, bioaccessibility and bioavailability, and (4) PAH-PAH interactions at the cellular level, using an intestinal porcine enterocyte cell line (IPEC-J2), alter partitioning into cellular components and rates of metabolism affecting bioavailability measurements.

Within a soil, fugacity predicts PAH exposure (Exposure = 0.21 log Fugacity + 0.68, r^2 = 0.96, $p < 0.005$, n=14), however between soils, fugacity does not predict plasma content of PAH compounds, with the exception of benzo(a)pyrene. Soil fugacity capacity predicts the PAH soil concentration for all five PAHs with an average slope of 0.30 (μg PAH g^{-1}soil) Pa^{-1} and r^2's of 0.64-0.73. As a result of soil fugacity capacity predicting soil concentration, soil fugacity capacity was correlated to PAH bioavailability for these historically contaminated soils, with r^2's of 0.45-0.66, however benzo(k)fluoranthene and benzo(a)pyrene had much weaker correlations with r^2 values of 0.13 and 0.14, respectively. These findings suggest that soil and chemical

dependent properties of fugacity and fugacity capacity can partially explain the variability associated with PAH exposure, soil concentration and bioavailability.

Shaking method significantly affected PAH bioaccessibility in the FOREhST model, with PAH desorption from the high energy FOREhST an order of magnitude greater compared to the low energy FOREhST. PAH-PAH interactions significantly influenced PAH bioavailability and when these interactions were used in a linear model, the model predicted benzo(a)anthracene bioavailability with a slope of 1 and r^2 of 0.66 and for benzo(a)pyrene bioavailability has a slope of 1 and r^2 of 0.65. When spiking low levels of benzo(a)anthracene into the FOREhST model with soil, a significant increase ($p < 0.05$) in bioaccessibile benzo(a)pyrene was observed. When spiking low levels of fluoranthene into the FOREhST model with soil, no significant differences in benzo(a)anthracene was observed.

Co-exposure of IPEC-J2 cells to fluoranthene/benzo(a)anthracene mixture significant increases the partitioning to media, opposed to partitioning to cellular components. Furthermore, a fluoranthene/benzo(a)anthracene mixture significantly increases the metabolism of benzo(a)anthracene from media when compared to solo exposure of benzo(a)anthracene. Notably, a chrysene/fluoranthene/benzo(a)anthracene mixture results in a significant increase of benzo(a)anthracene partitioning to media while no significant difference in the disappearance of benzo(a)anthracene from media was observed compared to solo benzo(a)anthracene exposure. Co-exposure of IPE-J2 cells to benzo(a)anthracene/benzo(a)pyrene mixture significantly increases the partitioning to media compared to solo benzo(a)pyrene exposure but no significant difference in benzo(a)pyrene metabolism.

PAH *in vivo* bioavailability is a function of a multitude of factors, including but not limited to PAH mixtures influencing PAH partitioning to soil, simulated intestinal fluid, and cellular

components, and PAH mixtures influencing their own relative metabolism. By accounting for the partitioning effects of PAH mixtures through the use of statistical modelling tools, co-inertia (COIA) and structural equation modelling (SEM), better *in vitro* predictions are made. PAHs mixtures influence PAH cellular partitioning and metabolism, influencing PAH bioavailability, however the simple 3 PAH mixtures used here may not wholly explain the complicated cellular interactions influencing partitioning and metabolism.

ACKNOWLEDGMENTS

I would like to thank my supervisor, Dr. Steven D. Siciliano for the continued support and guidance throughout my graduate career. I would also like to thank the members of my committee, Drs. Lynn Weber, David Janz, Markus Hecker, and Heather Wilson for their insight and scientific contributions. The students and staff of both the Soil Science Department and Toxicology Centre have been incredibly helpful throughout my tenure. Specifically, I would like to acknowledge the support of Richard Nhan and Roman Nosach for all their work in the lab. As we worked on a similar project, Rachel Peters, for bouncing ideas back and forth. Jordan Hamilton for doing his doctorate side by side with me and for forming a book club for coffee breaks. My fellow graduate students, Erin Karppinen and Katie Hyde, for their support and encouragement.

Lastly, but most certainly not least, I would like to acknowledge the unwavering support of my parents, KC and Marnie James, without your support none of this would have been possible.

TABLE OF CONTENTS

Page

LIST OF TABLES

LIST OF FIGURES

LIST OF ABBREVIATIONS

AhR	Aryl hydrocarbon receptor
ANT	Anthracene
ARNT	Aryl hydrocarbon nuclear translocator
ATSDR	Agency of Toxic Substances and Disease Registry
AUC	Area under the plasma concentration-time curve
B(a)A	Benzo(a)anthracene
B(a)P	Benzo(a)pyrene
B(b)F	Benzo(b)fluoranthene
B(ghi)P	Benzo(ghi)perylene
B(k)F	Benzo(k)fluoranthene
BGS	British Geological Survey
Caco-2	Human colon carcinoma
CCME	Canadian Council of Ministers of the Environment
CHR	Chrysene
COIA	Co-inertia analysis
CYP	Cytochrome P450
DIB	Dibenzo(ah)anthracene
DMSO	Dimethyl sulfoxide
EVA	Ethylene Vinyl Acetate
FLU	Fluoranthene
FOREhST	Fed organic estimator of the human simulation test
GI	Gastro-intestinal
GST	Glutathione S-transferases

GW	Gas Works
HepG2	Human hepatoma
HMW	Heavy molecular weight
HPLC-FD	High Pressure Liquid Chromatography coupled Fluorescence Detection
IPEC-J2	Intestinal porcine enterocyte cell line
IND	Indeno(123,cd)pyrene
IV	Intra venous
K_d	Soil-water partitioning coefficient
K_{oc}	Soil-organic carbon partitioning coefficient
K_{ow}	Octanol-water partitioning coefficient
K_{sim}	Soil-simulated fluid partitioning coefficient
LMW	Lower molecular weight
OC	Soil organic carbon
OSU-IVG	Ohio State University *in vitro* gastrointestinal method
PAH	Polycyclic aromatic hydrocarbon
PBET	Physiological based extraction test
PCA	Principle component analysis
PDMS	Poly(dimethylsiloxane)
PTFE	Polytetrafluoroethylene
PYR	Pyrene
RBALP	Relative bioaccessibility leaching procedure
SBET	Simplified based extraction test
SEM	Structure equation modeling

SHIME	Simulator of the human intestinal microbial ecosystem
SULT	Sulfotransferase
T-47D	Human breast cancer
TIM	TNO gastro-intestinal model
UGT	Uridine 5'-diphospho-glucuronosyltransferase
WP	Wood Preservation
XRE	Xenobiotics regulatory element
Z_{soil}	Fugacity Capacity of Soil
Z_{water}	Fugacity Capacity of Water

NOTE TO READERS

This thesis is organized and formatted to follow the University of Saskatchewan College of Graduate Studies and Research guidelines for a manuscript-style thesis. Chapter 1 is a general introduction, including objectives and hypothesis, Chapter 2 is the literature review, and Chapter 6 reviews the principle findings, synthesis, general discussion and conclusions tying the chapters together. Chapters 3, 4 and 5 of this thesis are organized as manuscripts for publication in peer-reviewed scientific journals. Chapter 2 has been published in Environmental Science and Technology, Chapter 4 has been published in Science of the Total Environment, and Chapter 5 has not been submitted for review. Full citations for the published research manuscripts are provided in the preface section to each chapter. As a result of the manuscript-style format, there is repetition of material in the materials and methods sections of the thesis. Tables, figures, supporting information and references cited in these research chapters have been reformatted here to a consistent thesis style. References cites in each chapter are combined and listed in the References section of the thesis. Supporting information associated with research chapters are presented in the Appendix section at the end of this thesis.

1 INTRODUCTION

Polycyclic aromatic hydrocarbon (PAH) soil contamination is a world-wide problem due to incidental ingestion of soil and the carcinogenic nature of PAHs. Risk assessors often assume an absorption factor of 100% for exposure assessment, however this is a conservative estimate, as gastro-intestinal (GI) absorption is known to vary based on the soil. *In vivo* animal bioavailability models are the gold standard for determining the PAH soil absorption factor, but these models are costly, time consuming, and ethically difficult to be used repeatedly. *In vitro* bioaccessibility models measure the amount of contaminant solubilized into simulated GI fluids, therefore they do not share the negatives of *in vivo* modeling and theoretically are a conservative estimate of *in vivo* bioavailability. Ideally, *in vitro* would replace *in vivo* models, but currently *in vivo* bioavailability across many soils cannot be predicted by *in vitro* models. The primary factors affecting PAH soil desorption between many soils is currently unknown. A confounding issue with PAH bioavailability is that PAHs are subject to metabolism via cytochrome P450 (CYP) enzymes which are highly conserved enzymes across species and tissues. Specific PAHs induce CYP enzymes and can increase the relative rate of metabolism based on the mixture of PAHs present, potentially altering the bioavailability measurements. While *in vivo* bioavailability models are affected by metabolism, *in vitro* bioaccessibility models typically do not contain biotic metabolizing components, and therefore do not account for metabolism. The research of this PhD thesis investigates factors influencing PAH desorption from soil in order to create an *in vitro* model that is predictive of *in vivo* bioavailability and to investigate the role of cellular PAH metabolism on bioavailability based on PAH mixture.

1.1 Objectives and Hypotheses

The global objective of this PhD research was to investigate the primary factors responsible for PAH desorption from soil in order to improve the accuracy of *in vitro* models predicting *in vivo* bioavailability. Over the course of the global objective stated, four sub hypotheses are evaluated: (1) PAH bioavailability can be partially explained by chemical partitioning, as measured by fugacity capacity, (2) PAH bioaccessibility measurements are dependent upon energetic input of the model, (3) PAHs interact with each other influencing partitioning, bioaccessibility and bioavailability, and (4) PAH-PAH interactions at the cellular level alter rates of metabolism affecting bioavailability measurements.

For the first hypothesis, the fugacity capacity of 11 PAHs across 14 soils was determined and compared to the *in vivo* exposure to swine and presented in Chapter 3 (Predicting Polycyclic Aromatic Hydrocarbon Bioavailability to Mammals from Incidentally Ingested Soils using Partitioning and Fugacity). To investigate the second hypothesis, bioaccessibility of the 14 soils was determined using two shaking methods and presented in Chapter 4 (*In vitro* Prediction of Polycyclic Aromatic Hydrocarbon Bioavailability of 14 Different Incidentally Ingested Soils in Juvenile Swine). The third hypothesis of PAH-PAH interactions was investigated using co-inertia analysis and is also presented in Chapter 4. Lastly, to test the fourth hypothesis, an intestinal cell line was exposed to various PAH mixtures and is presented in Chapter 5 (Polycyclic Aromatic Hydrocarbon Mixtures Effects on Metabolism and Binding to Cellular Components). Chapter 6 discusses future directions and implications associated with the current findings.

2 LITERATURE REVIEW

2.1 Polycyclic Aromatic Hydrocarbons

Polycyclic aromatic hydrocarbons are a large class of hydrophobic ubiquitous environmental contaminants consisting of two or more fused benzene rings. There are over 100 known individual PAH compounds, however the focus of the research presented here is limited to 12 compounds selected within the US EPA priority 16 PAHs, namely: phenanthrene, anthracene, pyrene, fluoranthene, benzo(a)anthracene, chrysene, benzo(b)fluoranthene, benzo(k)fluoranthene, benzo(a)pyrene, benzo(ghi)perylene, dibenzo(ah)anthracene, and indeno(123-cd)pyrene. Notably, phenanthrene and anthracene are typically classified as lower molecular weight (LMW) PAHs as they contain a series of three fused benzene rings, while pyrene, fluoranthene, benzo(a)anthracene, chrysene, benzo(b)fluoranthene, benzo(k)fluoranthene, benzo(a)pyrene, benzo(ghi)perylene, dibenzo(ah)anthracene, and indeno(123-cd)pyrene are typically classified as heavy molecular weight (HMW) PAHs as they contain a series of four or more fused benzene rings **(Figure 2.1**). The aforementioned PAHs are chosen as they are routinely analyzed for and have been widely studied. Additional PAHs that are not included in the USEPA priority 16 PAHs include nitro, alkyl, and oxy-PAH derivatives.

The source of many PAHs are broadly classified into either pyrogenic, products of incomplete combustion of organic matter, or petrogenic, by-products of petroleum processes. Specific sources of PAHs result in the production of PAHs at different ratios (Galarneau 2008; Li et al. 2003; Tobiszewski and Namiesnik 2012; Zhang et al. 2005). For example, pyrogenic sources generally have a higher contribution of HMW PAHs (4 and 5 rings) while petrogenic sources generally have a higher contribution of LMW PAHs (2 and 3 rings) (Zhang et al. 2005). More specifically, (Ravindra et al. 2008) has found that a fluorene to pyrene ratio (fluorene / (fluorene

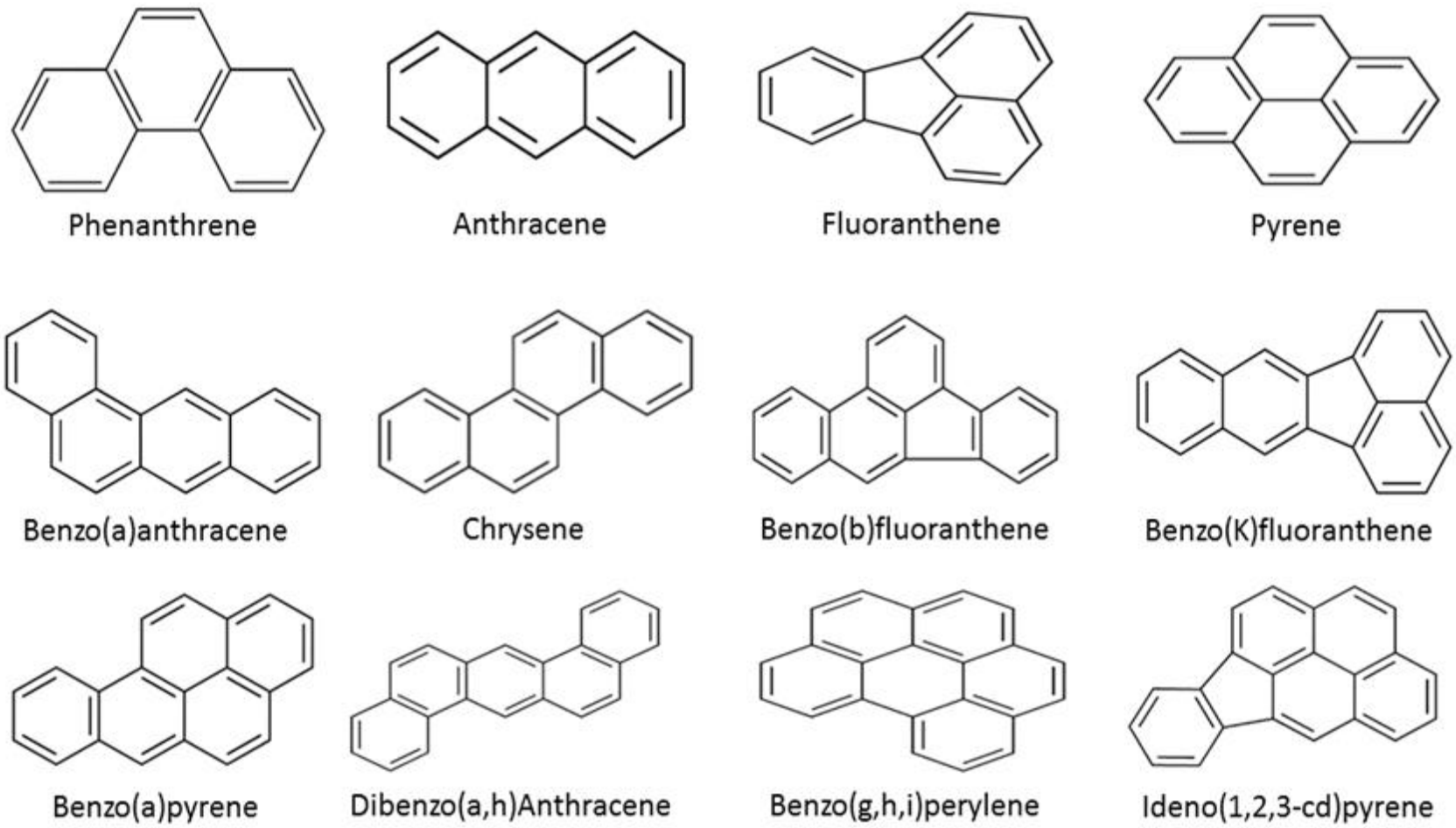

Figure 2.1 Structure of twelve common parent PAH compounds.

+ pyrene)) greater than 0.5 is attributed to petrol emissions, while a ratio of less than 0.5 is attributed to diesel emissions. Additional PAH ratios reported in the literature for source appointment include anthracene and phenanthrene, benzo(a)anthracene and chrysene, benzo(a)pyrene and benzo(e)pyrene, and indeno(123-cd)pyrene and benzo(ghi)perylene (Tobiszewski and Namiesnik 2012). Principal component analysis and canonical analysis are the primarily statistical tools used to decipher the source appointment based on the PAH ratios and the typical sources include combustion of fossil fuels, grass, wood, and coal (Tobiszewski and Namiesnik 2012).

PAHs are a broad class of hydrophobic contaminants and there are large differences in their physiochemical properties including but not limited to solubility, vapor pressure, octanol-water partitioning coefficient (K_{ow}), and molecular weight. As a result of these differences in physiochemical properties each individual PAH will behave somewhat differently, however despite these differences, the 12 PAHs selected here have a relatively low solubility and vapor pressure with relatively high K_{ow} values.

Due to the physiochemical properties of PAHs, soil is a major repository for PAHs. Estimated by Wild and Jones (1995), 90% of the total environmental PAHs in Great Britain are stored in the soil. PAHs will accumulate in soil over time, whereas the low water solubility of PAHs limits the concentration in water. Pyrogenic sources of PAHs, such as residential heating, vehicular emissions, coal combustion, and forest fires, emit PAHs into the atmosphere. Depending on the physiochemical properties of the PAH, the fate and transport PAHs in the atmosphere will change, however atmospheric deposition via rainfall or gravimetric settling transfers a substantial amount of atmospheric PAHs to the soil (Wilcke 2000). Direct PAH soil contamination results from industrial sites associated with the following activities (primarily

petrogenic in nature): gasworks, fuel processing, coke production, asphalt production, coal tar production, and wood preservation (Wild and Jones 1995).

2.1.1 Human Exposure to Polycyclic Aromatic Hydrocarbons

Human exposure to environmental contaminants occur through ingestion, inhalation or dermal absorption. Ingestion of PAHs can be from ingestion of PAH contaminated drinking water, contaminated food, and incidental ingestion of contaminated soil. Inhalation of PAHs can be from the inhalation of gaseous PAHs, however it is more common to inhale PAHs adhered to airborne particulate matter (e.g. dust or re-suspended soil). A prominent source of PAH exposure is through the inhalation of cigarette smoke, especially when individuals voluntarily inhale freshly combusted organic material deep into the lungs (Band et al. 2002). Occupational exposure is another important source for PAH exposure and exposure is primarily through inhalation, however dermal absorption can also be important (Boffetta et al. 1997; Brandt et al. 2003). Dermal absorption can occur from water (bathing or showering), soil (typically adhered to hands) or from consumer products. Of the three exposure routes, ingestion is typically the dominant exposure pathway as PAH concentration in the air is relatively small with dermal absorption relevant in certain situations (CCME 2010; James et al. 2012). Ingestion of contaminated food has consistently been found to be the most significant exposure route to humans (Bansal and Kim 2015; Domingo and Nadal 2015; Phillips 1999; Yebra-Pimentel et al. 2015). Whereas PAH transfer into cereal grains and vegetables from soil and water is limited, the relative PAH concentration and composition found in food is primarily linked to the cooking process (e.g. baked, grilled or barbequed) and the type of food being cooked (Bansal and Kim 2015; Domingo and Nadal 2015; Phillips 1999). Outside of individuals voluntarily inhaling cigarette smoke, consuming grilled or barbequed food, and occupational exposure, incidental

ingestion of PAH contaminated soil is one of the main drivers of human health risk assessment from environmental media.

2.1.2 Effects Characterization of Polycyclic Aromatic Hydrocarbons

The human health effects of PAHs have been well documented over the years (CCME 2010; Kim et al. 2013; ATSDR 1995). As a broad class of contaminant, PAHs exhibit carcinogenic, teratogenic, genotoxic, mutagenic, systemic, immunological, neurological, reproductive, and developmental effects (CCME 2010; Kim et al. 2013; ATSDR 1995). From this list of PAH exposure effects, the most sensitive endpoint is believed to be the carcinogenic mechanism of action, which drives the Canadian Soil Quality Guideline value of 0.6 mg kg^{-1} (mg PAH per kg bodyweight) and 5.3 mg kg^{-1} corresponding to an incremental lifetime cancer risk of 10^{-6} and 10^{-5} (CCME 2010).

Three well recognized mechanisms of PAH carcinogenic action include 1) PAH metabolism to epoxides and diol epoxides, 2) metabolism of PAH radical cations and 3) PAH metabolism into quinone intermediates (Penning et al. 1999; Ramesh et al. 2004). The formation of the aforementioned compounds leads to interactions with DNA, epoxides forming DNA adducts causing mutations, radical cations forming DNA adducts resulting in depurination, and quinones which can form DNA adducts resulting in depurination or by creating reactive oxygen species which subsequently attack DNA (Cavalieri and Rogan 1995; Harvey 1996; Penning et al. 1999; Singh et al. 2007).

Select PAHs elicit immunological responses, with immunosuppression relevant to the carcinogenic endpoint. While the three aforementioned carcinogenic mechanisms of action represent the initiation phase of carcinogenesis, immunosuppression acts via promotion of carcinogenesis. The immune response from PAH exposure is similar to the carcinogenic response, such that the effects require metabolic activation. Not all PAHs exhibit

immunosuppressive effects, whereas White et al. (1985) found that anthracene and chrysene were not immunosuppressive in mice, other HMW PAHs such as benzo(a)anthracene, benzo(a)pyrene, dibenzo(ah)anthracene, and a less routinely used PAH, 7,12-dimethylbenzo(a)anthracene, had significant immunosuppression. Benzo(a)pyrene and 7,12-dimethylbenzo(a)anthracene are regularly used to study immune effects and they have the potential to suppress B cell lymphopoiesis (Hardin et al. 1992), inhibit differentiation of blood monocytes into macrophages (Van Grevenynghe et al. 2003), decrease spleen and thymus weight (Miyata et al. 2001), and damage bone marrow subsequently depleting lymphocytes (Galvan et al. 2005). Taken together the aforementioned effects all influence the immune system, and thereby contribute to the promotion of carcinogenesis.

2.1.2.1 Activation/Detoxification of Polycyclic Aromatic Hydrocarbons

Associated with PAH carcinogenicity is the aryl hydrocarbon receptor (AhR). Many PAHs induce various phase I and phase II enzymes and it is likely that they act through the AhR (Lampen et al. 2004; Mathieu et al. 2001; Ramesh et al. 2004; Vakharia et al. 2001). Select PAHs bind to the AhR receptor and heterodimerize with the aryl hydrocarbon nuclear translocator (ARNT) and pass into the nuclear membrane to complex with the xenobiotics regulatory element (XRE) to illicit a biochemical response from the cell (Androutsopoulos et al. 2009; Rowlands and Gustafsson 1997). The AhR pathway induces phase I CYP enzymes, predominately CYP1A and CYP1B (Androutsopoulos et al. 2009; Ramesh et al. 2004) as well as phase II enzymes, sulfotransferases (SULTs), uridine 5'-diphospho-glucuronosyltransferases (UGTs), glutathione S-transferases (GSTs) (Buesen et al. 2003; Hessel et al. 2013). Generation of epoxide and quinone species occur as a result of phase I metabolism, whereas the products of phase II metabolism are much less hydrophobic and therefore are readily excreted (Ramesh et al. 2004).

Metabolism of PAHs by phase I enzymes, such as CYP1A1, is known to produce oxygenated reactive intermediates which are carcinogenic (Ramesh et al. 2004), but overall CYP1A1 plays a protective role against PAH toxicity (Nebert and Dieter 2000; Uno et al. 2004). For example, Uno et al. 2004 performed an *in vivo* B(a)P dosing study using mice, where oral B(a)P exposure to *Cyp1a1 (-/-)* knockout mice lead to lethality whereas there were no overt signs of toxicity to *Cyp1a1 (+/+)* mice. Furthermore, Uno et al. (2004) shows that there was four times more B(a)P in circulating blood in *Cyp1a1 (-/-)* mice and a 4 times slower clearance rate. In agreement with Uno et al. (2004), Arlt et al. (2008) found that *Cyp1a1 (-/-)* mice resulted in slower clearance of B(a)P compared to *Cyp1a1 (+/-)* mice, further, *Cyp1a1 (-/-)* mice had higher hepatic DNA adduct levels (4-fold) compared to *Cyp1a1 (+/-)* mice. PAH carcinogenesis requires metabolic activation and although cancer is not an ideal outcome, it is a likely a preferable outcome relative to lethality when there is no metabolic activation.

2.2 Bioavailability/Bioaccessibility in Human Health Risk Assessment

In human health risk assessment bioavailability/bioaccessibility measurements are used to better characterize exposure estimates. Typically a conservative estimate of 100% relative bioavailability is used, however the default assumption of 100% relative bioavailability can potentially lead to overestimating the risk to human health (Richardson et al. 2006). Within the context of risk assessment the term relative bioavailability refers to the bioavailability relative to the media from which the guideline *In vitro* bioaccessibility models estimate the contaminant fraction solubilized into simulated GI fluids that can potentially be absorbed by the GI epithelium. In theory the solubilized fraction from *in vitro* bioaccessibility models should be a conservative estimate of bioavailability, as the entire soluble fraction will not be absorbed, however Juhasz et al. (2014a) noted that this is not always the case. Ideally, *in vitro* bioaccessibility models would be used for human health risk assessments as *in vivo*

bioavailability models are comparatively time-consuming and costly (Rees et al. 2009). Additionally there is also the ethical issue of euthanasia of animals for the purpose of characterizing human health risk, as there are currently many contaminated sites and there will continue to be more sites caused through incidental release of pollutants. *In vitro* bioaccessibility models need to be validated against *in vivo* bioavailability models. In the case of exposure to contaminants found in soil, such as PAHs, the *in vitro* models need to be validated across many soils with contrasting soil properties.

2.2.1 *In vivo* Bioavailability

Currently, three animal models are commonly used to calculate mammalian oral bioavailability: juvenile swine (Casteel et al. 1997), monkey (Roberts et al. 2007), and mouse/rat (Budinsky et al. 2008; Smith et al. 2011). Three advantages of using swine include 1) their anatomically similar GI tracts (Patterson et al. 2008), 2) similar nutritional requirements (Cooper et al. 1997) as humans and 3) swine are routinely used as livestock. Historically monkeys have been used as they are non-human primates, and their physiology is similar to humans (Ikegami et al. 2003; Kararli 1995). However, there are ethical complications of using monkeys for bioavailability studies and typically they are not used. Lastly, the rat/mouse model is the most commonly used for bioavailability studies (Ramesh et al. 2004), as there is relative lower cost of housing and maintenance when compared to swine or monkeys.

Defining *in vivo* bioavailability is a complicated process that is dependent upon the nature of the toxicant. For example, for arsenic *in vivo* bioavailability, typically urine and feces are analyzed, as arsenic is primarily excreted via the urine (Buchet et al. 1981). For lead bioavailability, bone, blood, liver and kidney have been collected (Schroder et al. 2004). For PAHs, oral bioavailability is defined as the fraction of a compound that reaches the systemic circulation (Ruby et al. 1999); therefore, multiple studies have directly sampled from the

systemic circulation and analyzed whole blood or plasma (Budinsky et al. 2008; James et al. 2011; Rees et al. 2009). In contrast, Juhasz et al. (2014b) analyzed parent PAH compound recovered in the feces to estimate bioavailability. The oral bioavailable fraction of PAHs pass through the intestinal epithelium and is absorbed into either the bloodstream or the lymphatic system; for PAHs the bloodstream is the dominant pathway (Busbee et al. 1990; Laher et al. 1983). Kinetic desorption of PAHs from soil and subsequent absorption into systemic circulation is a time dependent process. As such, area under the plasma concentration-time curve (AUC) analysis can be used as it integrates the contaminant plasma concentration over multiple time points to estimate the total body burden over an extended period of time (Rees et al. 2009; Van Schooten et al. 1997).

2.2.2 *In vitro* bioaccessibility

In vitro bioaccessibility models are designed to mimic the chemical and physiological conditions present in the human GI tract. Common *in vitro* bioaccessibility models include, but are not limited to: Physiological Based Extraction Test (PBET) (Ruby et al. 1996), Simulator of the Human Intestinal Microbial Ecosystem (SHIME) (Van de Wiele et al. 2004), Ohio State University *In vitro* Gastrointestinal method (OSU-IVG) (Basta et al. 2007), Fed ORganic Estimation human Simulation Test (FOREhST) (Cave et al. 2010; Juhasz et al. 2014b), Relative Bioaccessibility Leaching Procedure (RBALP) (Drexler and Brattin 2007), Simplified Based Extraction Test (SBET) (Juhasz et al. 2008) and TNO Gastrointestinal Model (TIM) (Minekus et al. 1995). The majority of *in vitro* digestion models follow the same basic doctrine using standardized values for temperature, peristaltic mixing, pH, liquid-to-solid ratio, and transit times (Oomen et al. 2002). Temperature (37°C) is the only consistent value used across various models (Drexler and Brattin 2007; Oomen et al. 2002; Van de Wiele et al. 2007). Peristaltic mixing has been simulated with magnetic stir bars (Van de Wiele et al. 2004), end-over-end rotation

(Drexler and Brattin 2007), mixing of an inert gas directly into simulated fluids (Ruby et al. 1996), or horizontal shaking (Laird et al. 2007). The pH used for the various *in vitro* models in the stomach compartment range between 1.3 (Ruby et al. 1993) to 4.0 (Oomen et al. 2002), in the intestinal compartment range between 6.5 (Laird et al. 2007) to 7.8 (Oomen et al. 2002), while in the colon compartment it ranges between 5.6 to 5.9 (Laird et al. 2007). Liquid-to-solid ratios previously had a large discrepancy between models ranging between 10:1 (Ruby et al. 1993) to 5000:1 (Hamel et al. 1998); however current models favour using 100:1 ratio (Cave et al. 2010; James et al. 2011; Tilston et al. 2011a). Transit times for the gastric stages range between 1 to 3 hours (Oomen et al. 2002), whereas intestinal stages range between 2 to 6 hours (Oomen et al. 2002), and colon stages range between 8 hours (Tilston et al. 2011a) and last up to 18 hours (Laird et al. 2007). In a comparison between five *in vitro* digestion models for arsenic, cadmium and lead bioaccessibility, Oomen et al. (2002) identifies pH, residence time, liquid to solid ratios, filtration process, fed state, and bile concentrations as factors responsible for discrepancies between models. Similarly, Van de Wiele et al. (2007) found that fed vs fasted state and liquid to solid ratios were the main factors resulting in differences in lead bioaccessibility between five *in vitro* models.

One of the most notable differences between *in vitro* models is the number of compartments utilized and the relative chemical composition of each of these compartments. Less complex models such as the RBALP, contain only a single compartment consisting of a 0.4M glycine solution acidified to a pH of 1.5 (Drexler and Brattin 2007). The FOREhST is a slightly more complex model, totaling three compartments, where the simulated fluids consists of 25 various inorganic, organic or additional compounds (Cave et al. 2010) and the pH is modified at every stage. The TIM method is likely the most complex mechanical method as it is a dynamic model

that simulates the transit through the GI tract utilizing computer controlled transit times and secretion rates (Minekus et al. 1995).

Oftentimes, to improve the utility of bioaccessibility models modifications to the original design are implemented. Modifying an *in vitro* model occurs either to improve the accuracy of the model or to eliminate unnecessary steps for particular contaminants. When measuring PAH bioaccessibility, James et al. (2011) added an intestinal stage to the RBALP model, as well, in this same study a C18 membrane was added as a lipophilic sink. Similarly for PAH bioaccessibility, Tilston et al. (2011b) added a colon compartment to the PBET. Conversely, Juhasz et al. (2008) eliminated the intestinal stage in the SBET because arsenic bioaccessibility is greatest in the gastric stage. As another form of lipophilic sink, Gouliarmou and Mayer (2012) added silicone rods to the PBET model to influence partitioning and simplify the extracting procedure. Notably, ethyl vinyl acetate (EVA) thin films (Minhas et al. 2006; Vasiluk et al. 2007) and tenax beads (Li et al. 2015) have also been used as a lipophilic sink for PAH *in vitro* bioaccessibility.

In this thesis, the FOREhST model is chosen and modified to determine the *in vitro* bioaccessibility across multiple soils. The FOREhST model is an adaption of the fed state methods developed by the RIVM - The Netherlands National Institute for Public Health and the Environment (Versantvoort et al. 2004) and is intended for organic contaminants (Cave et al. 2010). The three compartments of the FOREhST model include saliva, gastric, and intestinal. The simulated fluids of each stage consist of inorganic salts (e.g. KCl, NaOH, or NaH_2PO_4), organic reagents (e.g. urea, bile, or pancreatin) that mimic the physiological conditions at each stage (**Table 2.1**). The fed state utilizes freeze dried porridge (~ 0.8 g), sunflower oil (50 µL), and 2.45 mL milli-Q water. If necessary the pH of the supernatant solution is adjusted at each

stage with NaOH or HCL to match the following conditions: saliva – 6.5 ± 0.5, stomach – 1.4 ± 0.3, intestinal – 6.3 ± 0.5. After the addition of each fluid, bottles are capped and incubated in a water bath (37°C) with end over end rotation (30 rpm). The transit time for the saliva phase is 5 minutes, while the gastric and small intestinal phases are 2 hours each.

Table 2.1 Components of FOREhST fluids

Reagent	Concentration (mg l^{-})	Compartment	Organic/Inorganic/ Additional
KCl	1792	Saliva	Inorganic
NaH_2PO_4	1776	Saliva	Inorganic
KSCN	400	Saliva	Inorganic
Na_2SO_4	1140	Saliva	Inorganic
NaCl	596	Saliva	Inorganic
NaOH	144	Saliva	Inorganic
Urea	400	Saliva	Organic
Amylase	145	Saliva	Additional
Mucin	50	Saliva	Additional
Uric Acid	15	Saliva	Additional
NaCl	5504	Gastric	Inorganic
NaH_2PO_4	533	Gastric	Inorganic
KCl	1649	Gastric	Inorganic
$CaCl_2$	799	Gastric	Inorganic
NH_4Cl	612	Gastric	Inorganic
HCl	8.3 ml of 37% HCl	Gastric	Inorganic
Glucose	1300	Gastric	Organic
Glucuronic acid	40	Gastric	Organic
Urea	170	Gastric	Organic
Glucoaminehydrochloride	660	Gastric	Organic
Bovine Serum Albumin	1000	Gastric	Additional
Mucin	3000	Gastric	Additional
Pepsin	1000	Gastric	Additional
NaCl	14024	Duodenal	Inorganic
$NaHCO_3$	11214	Duodenal	Inorganic
KH_2PO_4	160	Duodenal	Inorganic
KCl	1129	Duodenal	Inorganic
$MgCl_2$	100	Duodenal	Inorganic
HCl	180 µl of 37% HCl	Duodenal	Inorganic
Urea	200	Duodenal	Organic
$CaCl_2$	200	Duodenal	Additional
Bovine Serum Albumin	1000	Duodenal	Additional
Pancreatin	3000	Duodenal	Additional
Lipase	500	Duodenal	Additional
NaCl	10518	Bile	Inorganic
$NHCO_3$	11570	Bile	Inorganic
KCl	753	Bile	Inorganic
HCl	180 µl of 37% HCl	Bile	Inorganic
Urea	500	Bile	Organic
$CaCl_2$	222	Bile	Additional
Bovine Serum Albumin	1800	Bile	Additional
Bile	6000	Bile	Additional

2.3 Fugacity

A common way to view fugacity is as the thermodynamic equivalent to chemical potential. Lewis (1901) developed the concept of fugacity as an alternative to chemical potential when working with chemicals in multiple phases. Fugacity is a partial pressure and is measured in units of pressure such as pascals (Pa) or mm mercury (mm Hg). According to Lewis (1901), when a chemical present in one phase comes in contact with a second phase the chemical will have a tendency to escape to the second phase. This escaping tendency can be viewed as a pressure exerted by the chemical and therefore fugacity can be measured as a partial pressure. Lewis developed fugacity as it requires less rigorous calculations than using chemical potential and furthermore it consolidates the units of multiple phases. Whereas a chemicals' concentration in air, water and soil are measured in µg m^{-3} and µg L^{-}, and µg g^{-}, respectively, within the fugacity concept, units of concentration are unilaterally expressed as mol m^{-3}.

For many years, fugacity wasn't widely used until Mackay (1979) took interest and investigated the usefulness of fugacity. To summarize the relevant findings of Mackay (1979), it is generalized that fugacity calculations are most appropriate for persistent environmental chemicals and that at low concentrations, the concentration of most chemicals are linearly related to fugacity. The relationship between concentration and fugacity is as follows:

$$C_p = F \times Z_p \qquad \text{(Eqn 2.1)}$$

Where C_p = chemical concentration within a phase (mol m^{-3}), F = fugacity or escaping tendency (Pa), and Z_p = fugacity capacity of the phase (mol m^{-3} Pa^{-}). Notably, fugacity acts as a partial pressure and has units of Pa. Within the fugacity concept, when every phase obtains the same fugacity the system reaches equilibrium (Lewis 1901). Furthermore, the concept of fugacity functions such that a chemical will move from an area of high fugacity to an area of low

fugacity, similar to how chemicals move from a state of high resting energy to low resting energy. The fugacity capacity is akin to solubility as the fugacity capacity refers to the ability of a phase to absorb a chemical. Alternatively, fugacity capacity can be viewed as the potential of a medium to dissolve a chemical.

Applying the fugacity concept in practice can mainly be attributed to the work of MacKay (1979), Mackay and Patterson (1981), and Mackay and Patterson (1982). From the aforementioned articles, fugacity mainly applied to multimedia fate and transport models (MFTMs) (Kawamoto et al. 2001; MacLeod and Mackay 1999; MacLeod et al. 2001; Toose et al. 2004; Wania et al. 2006). Despite the popular use in MFTMs, Mackay (2004) states that the most valuable application of fugacity is the ability to explain bioconcentration, bioaccumulation, and biomagnification. Essentially, Mackay (2004) argues that fugacity can be used to explain an organism's exposure based on interactions with contaminants in environmental media. To support the ideas of Mackay (2004), Gobas et al. (1993) found that fugacity can explain intestinal absorption and biomagnification of organochlorines in both fish and humans. Conversely, Kelly et al. (2004) indicates that there are multiple factors outside of fugacity that influence the bioaccumulative potential of various commercial chemicals. Fugacity modelling does have limitations, and Mackay (1979) acknowledges that fugacity modelling does not allow for heterogeneity within a phase, such as changing soil parameters across a large ecoregion. A second major drawback is the assumption of first-order kinetics for many major processes within the model. Non-first order kinetics or nonlinear sorption isotherms can be accounted for within fugacity modelling, however the resulting complexity of the model may not be worth it (Mackay 1979). Lastly, fugacity modelling works best for persistent environmental chemicals at low

concentrations, therefore chemicals that are rapidly degraded, ionize into multiple forms, and are present in large quantities will not follow the linear relationship describe by Eqn 2.1.

2.4 Cell Cultures and Environmental Contaminants

Cell cultures can be used to examine the biochemical response resulting from exposure to environmental contaminants. Cell cultures can be used to examine a variety of biochemical responses, including but not limited to bioavailability, absorption, adsorption, metabolism, apical-basolateral transport, cytotoxicity, and interactions with probiotics and bacteria (Cencic and Langerholc 2010; Langerholc et al. 2011; Ramesh et al. 2004; Sergent et al. 2008). For biochemical responses to PAHs, human cell lines such as the human colon carcinoma (Caco-2) (Oomen et al. 2001; Vasiluk et al. 2007), human hepatoma (HepG2) (Bessette et al. 2005; Vakharia et al. 2001; Wu et al. 2003), and human breast cancer (T-47D) (Spink et al. 2002; Wu et al. 2003) are routinely used. It is important to note that these cell lines are of carcinogenic origin and as a result may show a significant alteration to various physiological properties related to cell functionality (Cencic and Langerholc 2010).

The caco-2 cell line has the most versatile uses regarding exposure to environmental contaminants. In a sense, caco-2 cells can be considered an *in vitro* digestion model, as it is used to measure the absorption and transport of contaminants (Minhas et al. 2006; Vasiluk et al. 2007). A sophisticated use of the caco-2 cells for bioaccessibility is to dose caco-2 cells with extracts from the simulated intestinal fluids of an *in vitro* digestion model (Oomen et al. 2001). Notably, this isn't the perfect replication of GI conditions, and highlighted by (Cui et al. 2016) the model lacks goblet cells which produce mucus to further interact with absorption. When using caco-2 cells in this manner, the cells are grown on culture plates of mixed cellulose esters (Oomen et al. 2001) or polycarbonate cell culture inserts (Vasiluk et al. 2007), both consisting of high pore density (~ 0.4 μm). Cells are incubated for three to four weeks until maximum

confluency is reached and cells differentiate into mature cells with distinct apical and basolateral domains (Oomen et al. 2001; Vasiluk et al. 2007). The caco-2 cells are exposed to a 1:1 mixture of simulated intestinal fluid containing PAHs and culture medium on the apical side. To assess bioaccessibility, measurements of PAH concentration are taken from the cells, as well as the apical and basolateral compartments over the course of 24 hours.

Intestinal metabolism of PAHs has the potential to influence the bioavailability of PAHs (Buesen et al. 2003). The bioavailability of individual PAHs can be dependent upon their lipophilicity (Cavret and Feidt 2005; Laher et al. 1983; Rahman et al. 1986) and CYP enzymes generally metabolize PAHs into less lipophilic compounds (Ramesh et al. 2004). Using caco-2 cells it has been demonstrated that PAH mixtures, PAH mixtures with metals, PAH mixtures with CYP inhibitors all influence PAH metabolism and subsequent bioavailability (Buesen et al. 2002; Buesen et al. 2003; Cavret and Feidt 2005; Hessel and Lampen 2010).

The intestinal porcine enterocyte cell line (IPEC-J2) is a non-transformed, permanent intestinal cell line isolated from the jejunal epithelium of a neonatal unsuckled piglet (Berschneider 1989). The IPEC-J2 cells mimic the processes of human intestinal epithelium closer than any other cell line of non-human origin and therefore is an ideal cell line for modelling human epithelial intestinal processes (Brosnahan and Brown 2012; Vergauwen 2015). Furthermore, a porcine intestinal cell line is the best representation of porcine intestinal absorption and metabolism when comparing to porcine bioavailability from soil. To date the cell line has reached over 100 passages without significant changes in cell growth or transport characteristics (GonzalezVallina et al. 1996; Vergauwen 2015). The IPEC-J2 cell line has been characterized mainly for immune responses, i.e. interleukins, tumour necrosis factor, nuclear factor kappa beta, major histocompatibility complexes, transforming growth factors (Brosnahan

and Brown 2012; Mariani et al. 2009; Schierack et al. 2006). Despite the IPEC-J2 cell line not being characterized for CYP enzymes, Hansen et al. (2000) confirms that porcine duodenal enterocytes contain CYP enzymes and that they are appropriate for studies investigating intestinal metabolism. Furthermore, IPEC-J2 is also established as an ideal cell line for investigating oxidative stress (Vergauwen et al. 2015).

Typical dosing for a cell culture involves the mixing of the contaminant of concern with an appropriate solvent for both the media and contaminant. For example, metals can simply be dissolved in water and mixed with cell media. Whereas organic contaminants are dissolved in dimethyl sulfoxide (DMSO) and then mixed with cell media. To ensure that the solvent does not influence experimental results, solvent controls are included in the experimental design for both cytotoxicity and for the experimental endpoint. Typical volume for solvent controls do not exceed 1% of the total media volume, i.e. 1µL of solvent in 100 µL media dosing, and ideally are as low as 0.01% (Berridge et al. 1996; Shimada et al. 2008; Vakharia et al. 2001). A major issue with cell culture exposure to organic contaminants is loss due to evaporation and adsorption/absorption to the sides of the plastic wells (Schreiber et al. 2008; Tanneberger et al. 2010). In an attempt to minimize the evaporative losses, sealplate, or adhesive tape can be applied (Schreiber et al. 2008; Vakharia et al. 2001). For sorption to the walls of plates, one can simply measure the recovery from plates made of different material, as Schreiber et al. (2008) found that a plexiglass plate prevented phenanthrene losses to 28% over a 48 hour period opposed to 94% losses from polystrene. An alternative method of dosing cell cultures is passive dosing. Passive dosing can be accomplished by loading a polymer such as silicone with the target chemical at high concentrations to maintain equilibrium with the dosing media (Gilbert et al. 2015; Kramer et al. 2010). Passive dosing relies on partitioning between the solid phase,

dosing polymer, and the liquid phase, cell media. With established partitioning parameters a high concentration in the solid phase will maintain a steady concentration of target contaminant in the liquid phase (Gilbert et al. 2015; Kramer et al. 2010). Therefore, when evaopartive or sorption losses occur, additional chemical will partition from polymer and maintain a constant concentration within the cell media (Kramer et al. 2010).

Taken together, cell cultures and the specialized techniques developed for cell cultures, allow for measuring cellular absorption, transportation, metabolism, and bioaccessibility of various chemicals which can be directly applicable to making *in vivo* to *in vitro* correlations.

3 PREDICTING POLYCYCLIC AROMATIC HYDROCARBON BIOAVAILABILITY TO MAMMALS FROM INCIDENTALLY INGESTED SOILS USING PARTITIONING AND FUGACITY

3.1 Preface

The following chapter has been accepted as a peer-reviewed article in the journal Environmental Science & Technology with the following co-authors:

Rachel Peters (University of Saskatchewan) – involved with experimental design, data analysis, and editorial;

Mark Cave (British Geological Survey) – involved with experimental design, statistical analysis, and editorial;

Mark Wickstrom (University of Saskatchewan) – involved with experimental design and editorial;

Eric Lamb (University of Saskatchewan) – aided with statistical analysis and editorial;

Steven D Siciliano (University of Saskatchewan) – supervisor involved with all aspects of project oversight.

As the lead author, Kyle James, was involved in every aspect of the article. More specially, Kyle was preformed approximately 30% of the animal work (feeding, dosing, and sampling), 30% of the lab work (chemical extraction), 50% of the data analysis and 95% of the manuscript writing.

James K, Peters RE, Cave MR, Wickstrom M, Lamb EG, Siciliano SD. 2016. Predicting polycyclic aromatic hydrocarbon bioavailability to mammals from incidentally ingested soils using partitioning and fugacity. Environmental Science & Technology 50:1338-1346. DOI: 10.1021/acs.est.5b05317

This chapter focuses on how chemical partitioning, via fugacity, influences PAH bioavailability from soil. The objective of the chapter was to explore how soil properties may

explain PAH bioavailability from soil and to examine inter-correlations between soil properties, chemical properties, and soil bioavailability. Fugacity capacity of 11 PAHs was determined for 14 soils and compared against *in vivo* PAH bioavailability to juvenile swine. The 14 soils collected had a wide range of PAH contamination as well as soil physiological characteristics to represent various exposure scenarios. The research suggests that both soil and chemical properties influence in vivo bioavailability.

3.2 Abstract

Soil and dust ingestion is one of the major human exposure pathways to contaminated soil; however, pollutant transfer from ingested substances to humans cannot currently be confidently predicted. Soil polycyclic aromatic hydrocarbon (PAH) bioavailability is likely dependent upon properties linked to chemical potential and partitioning such as fugacity, fugacity capacity, soil organic carbon and partitioning to simulated intestinal fluids. We estimated the oral PAH bioavailability of 19 historically contaminated soils fed to juvenile swine. Between soils, fugacity does not predict PAH blood content, with the exception of benzo(a)pyrene. In contrast, between individual PAHs, fugacity predicts PAH blood content (Area under the Curve = 0.47 log Fugacity + 0.34, $r^2 = 0.68$, $p < 0.005$, $n = 14$). Soil fugacity capacity predicts PAH soil concentration with an average slope of 0.30 (μg PAH g^{-1}soil) Pa^{-1} and r^2's of 0.61-0.73. Because PAH blood content was independent of soil concentration, soil fugacity correlated to PAH bioavailability via soil fugacity's link to soil concentration. In conclusion, fugacity predicts PAH uptake from a soil into blood. However, something other than partitioning is critical to explain the differences in PAH uptake into blood between soils. The kinetically constrained desorption of PAHs from carbonaceous geosorbents, i.e. black carbon, coupled with the short transit time in the gastro-intestinal tract, may explain differences between soils. Alternatively, soil, chyme and

ileum biochemical interactions may be specific to each PAH, which would explain why fugacity predicts the blood uptake of some PAHs, such as benzo(a)pyrene, but not others.

3.3 Introduction

How do pollutants move from soil to our blood? Such a question is what drove us to collect 19 contaminated soils from across the world and feed these soils to swine. This question is essential to answer because the transfer of pollutants from soil to blood following ingestion can be the dominant pathway for human exposure at contaminated sites. For example, incidentally ingesting soil exposes humans to 100 times more carcinogens than inhaling air particles (James et al. 2012). Yet, we have still not developed an acceptable model to quantify movement of carcinogens, such as polyaromatic hydrocarbons (PAHs), from an ingested particle to the human bloodstream.

In his pivotal 1979 paper titled "Finding Fugacity Feasible", Professor Don Mackay popularized the use of fugacity to characterize how pollutant movement occurs between environment phases and organisms (Mackay 1979). PAH uptake into human cells (Caco-2) (Minhas et al. 2006; Vasiluk et al. 2007) and PAH uptake into juvenile swine blood (James et al. 2011) can be predicted using fugacity. But using a mouse model, Juhasz et al. (2014b) could not use fugacity to model uptake. Fugacity modelling can be done at both equilibrium and non-equilibrium as well as steady state and non-steady state. Minhas et al. (2006) and Vasiluk et al. (2007) calculate fugacity by measuring concentrations over a time course allowing for fugacity calculations at equilibrium and non-equilibrium, whereas Juhasz et al. (2014b), like us, did not measure fugacity, instead used published K_{oc}/K_{ow} to calculate fugacity. Minhas et al. (2007) reports that steady state conditions between soil and aqueous phase (simulated intestinal fluids) is reached after 2 hours. Notably, the mean transit time through the stomach (~1.5 hours) and

small intestines (~3.5 hours) equates to ~5 hours (Madsen 1992), suggesting that steady state conditions are reasonable for modelling gastro-intestinal uptake.

At environmentally relevant concentrations, the concentration (C_{phase}) of a compound is linearly related to fugacity (f) via the fugacity capacity (Z_{phase}).

$$C_{phase} = Z_{phase} \times f \quad \text{(Eqn 3.1)}$$

Mackay (1979) derived the soil fugacity capacity (Z_{soil}) of a compound to be:

$$Z_{soil} = Z_{water} \times \text{soil organic carbon} \times K_{oc} \times \text{soil particle density} \quad \text{(Eqn 3.2)}$$

Where Z_{water} is calculated as solubility divided by vapour pressure. Assuming a constant soil-organic carbon partitioning coefficient (K_{oc}) between soils allows one to calculate fugacity capacity by determining soil organic carbon content. Routinely, our group and others, would use this assumption because it provided useful results (Cachada et al. 2014; James et al. 2011; Juhasz et al. 2014b; Mackay and Fraser 2000). Results from Hawthorne et al. (2006) suggest that K_{oc} values are not constant between sediments. Across 114 PAH contaminated sediments, K_{oc} values for individual PAHs ranged between 2 and 3 orders of magnitude. Hence, the ability of fugacity models to predict blood uptake may be linked to using a more precise estimate of soil fugacity capacity. To achieve this, one needs to experimentally determine K_{oc}. K_{oc} is the soil-water partitioning coefficient (K_d) normalized to organic carbon content:

$$K_{oc} = K_d \div \text{soil organic carbon} \quad \text{(Eqn 3.3)}$$

Substituting equation 3.3 into equation 3.2 we obtain equation 3.4 which eliminates soil organic carbon from the fugacity capacity equation.

$$Z_{soil} = Z_{water} \times K_d \times \text{soil particle density} \quad \text{(Eqn 3.4)}$$

Therefore, if Z_{water} and soil particle density remain relatively constant, soil fugacity capacity is primarily dictated by K_d, which can be directly estimated.

But our intestines contain intestinal fluid rather than the pure water used to estimate K_d. Intestines contain ingested particles suspended in fluids and these fluids differ in their lipophilicity from pure water. Hence, estimating K_{sim}, i.e. the partitioning between soil and a synthetic intestinal fluid, should further improve the precision of estimating fugacity for ingested particles (Cave et al. 2014). Improved estimates of fugacity ought to enhance calculations of PAH bioavailability based on partitioning theory.

Here, we define bioavailability as the fraction of an administered dose that is present in systemic circulation for a specific time frame (Semple et al. 2003), in our case 48 hours. One can estimate PAH bioavailability by measuring urinary metabolites, PAHs in feces, and PAHs or metabolites in blood (see review by Ramesh et al. (2004)). The use of blood concentrations of parent compounds is criticized because ingested PAHs enter the body via the portal vein, where many PAHs are metabolized by liver enzymes. A series of recent papers (Shimada and Guengerich 2006; Uno et al. 2004) explored how AhR activity, which signals various PAH metabolizing enzymes (Ioannides and Lewis 2004), is linked to toxicity. Hepatic toxicity and detoxification depend on metabolism by CYP enzymes yet systemic parent PAH compounds cause non-hepatic toxicity. Thus, parent PAHs that reach systemic circulation are what can cause non-hepatic toxicity. This does not suggest that metabolites do not cause toxicity in systemic circulation, only that the majority of systemic toxicity is likely the result of parent compounds metabolizing to reactive species at the site of toxic effect. Thus parent PAHs in the blood provide a meaningful estimate of bioavailability because these PAHs are what pose a risk to the remainder of the body, i.e. not the liver or small intestine which are directly exposed to PAHs and metabolites during ingestion.

Mice, rats and juvenile swine are common animal models used for bioavailability research. The mouse model has several advantages over the swine model, namely less dilution into body volume of ingested PAHs (thereby lowering the detection limit of bioavailability studies), and that some cancer slope factors are derived from mouse based studies (Culp et al. 1998). However, there are certain limits to the mouse model compared to juvenile swine models. For example, the mouse AhR is ~10 times more sensitive than the human AhR to AhR ligands such as 2,3,7,8-Tetrachlorodibenzo-p-dioxin (TCDD) (Flaveny and Perdew 2009), whereas the swine AhR is comparable to human AhR for benzo(a)pyrene and TCDD (Lesca et al. 1994). Further, the juvenile swine's digestive tract is very similar to human toddlers (Miller and Ullrey 1987; Patterson et al. 2008), typically the critical human receptor of concern. In this study, we wished to characterize how toxicokinetics and digestive physiology influenced PAH uptake from soil. Thus, juvenile swine are a good animal model for this purpose.

In the core of the manuscript, we focus on the results of five carcinogenic PAHs. Because of their carcinogenicity, these five PAHs are drivers of the majority of contaminated soil risk assessments. Similar results were obtained with another six PAHs, but with less emphasize on their results. Other PAHs were not robustly or routinely detected and thus, not included in our discussion.

3.4 Materials

3.4.1 Soils

A total of 19 soils contaminated with hydrocarbons were obtained from sites in the United Kingdom (n = 12), Canada (n = 5) and Sweden (n = 2), as described previously in James et al. (2011) and Cave et al. (2010). Soil pH, soil organic carbon content, and particle size were analyzed as previously described by Siciliano et al. (2009).

3.4.2 PAH Soil Extraction

The extraction of PAHs from each soil sample was prepared by weighing approximately 2 g of soil into a pre-cleaned 50 mL Teflon centrifuge tube. To the tube a 5 mL of a 6:1 (v/v) mix of methanol: toluene was added and the tube was sealed with Teflon lid. The vial was gently shaken to suspend the contents and then sonicated in an ultrasonic bath for 2 hours at 50°C. To separate the supernatant solution, the tubes were centrifuged at ~ 3000 rpm (1000 g) for 15 min and filtered through Whatman GMF 0.45 μm filters into a 15 mL amber glass vial. A 0.15 mL aliquot of the solvent extract was diluted with 1.35 mL acetonitrile into labeled 2 mL amber HPLC vials and kept at -20°C until analysis. For the quantification of PAHs from soil a sand matrix spike was analyzed every ten samples and the average recovery ranges from 77% to 94% with a standard deviation of 12%. Benzo(b)chrysene, present only in very low concentrations in the environmental samples, was added as an internal standard and the recovery ranged between 90-110% with a standard deviation of 11%.

3.4.3 Bioavailability of Ingested PAHs to Swine

Female Landrace cross swine (8 week-old; ~20kg) were obtained and housed at the Prairie Swine Centre near Saskatoon, Saskatchewan. The animals were housed in individual pens (1.5 x 1.0 x 1.0 m) to prevent cross contamination and for ease of sampling and exposure. The diet consists of standard grower ration, two meals a day, with total daily intake rate limited to 4% body weight. Drinking water was provided *ad libitum* via self-activated watering nozzles present in each pen. Swine were allowed to acclimate for one week prior to dosing and were trained daily to eat a dough ball treat consisting of molasses, flour, oats and pig feed as described by Casteel et al. (1997).

Swine were randomly allocated into treatment groups (n = 6) each week for five weeks. At the start of each week the pigs were weighed and fed accordingly. Treatment groups

consisted of 1 of 19 soils individually mixed into dough balls, 40 μg of each 16 priority PAHs intra venous (IV) dose in a glycerol tri-octanoate vehicle (each week), and control group receiving no PAH dose. In subsequent weeks, groups were crossed over such that each group was assessed as a control and IV dose at some point during the experiment. Controls were used to quantify background levels and IV dose groups were used to ensure consistency between treatment groups over progressive weeks.

Blood samples were collected from the jugular vein at 2, 4, 6, and 8 hours post exposure where n = 4 for each treatment group, while at 0, 12, 24, and 48 hours post exposure, n = 3 for each treatment group. Blood samples were collected from each animal a maximum of five times per week to preserve the integrity of the veins for subsequent weeks. Approximately 10-15 mL of blood was collected using heparinized vacutainer tubes, which prevents the blood from coagulating. Plasma was separated from the blood within one hour after sampling by centrifuging at ~ 3000 rpm (1000 g) for 15 minutes and was stored after decanting at -20˚C until solid phase extraction. PAH tissue concentrations have also been collected and are reported in Peters et al. (2015).

PAH bioavailability was calculated according to the following equation

$$\text{Bioavailability (\%)} = \frac{\text{AUC}_{\text{Soil Dose 48 H}}\ (\mu g)}{\text{PAH administered from soil (}\mu g\text{)}} \times 100\% \qquad \text{(Eqn 3.5)}$$

$\text{AUC}_{\text{Soil Dose 48 H}}$ was determined using area under the plasma concentration curve (AUC) analysis over a 48 hour period and PAH administered was the amount of PAHs in contaminated soil ($\mu g\ g^{-1}$). Area under the curve calculations used the plasma concentration time course for each compound in individual pigs. AUC was calculated to the 48 hour time point with the MESS package (Ekstrom and Ekstrom 2012) in statistical program R (R Core Team 2013) using the trapezoidal rule and thus, AUC units convert from $\mu g\ g^{-1}\ 48h^{-1}$ to $\mu g\ g^{-1}$.

3.4.4 PAH Plasma Extraction

The extraction of PAHs from plasma follow the procedures of James et al. (2011) with minor modifications. To remove impurities from plasma, all samples were extracted using Waters Oasis HLB solid phase extraction columns (waters Corporation, Milford MA). Approximately 5 mL of plasma was diluted with 0.1 M nitric acid (1:2 plasma: nitric acid) and sonicated for 15 min in an ultra-sonic bath. The columns were conditioned with 2 mL of Milli-Q water and then with 2 mL methanol. Approximately 5 mL of acidified plasma was run through the column, rinsed with 2 mL of methanol and was eluted with 9 mL of acetonitrile. The eluate was evaporated to near dryness, re-suspended in 2 mL of acetonitrile, and filtered through Whatman GMF 0.45 μm filters into labeled 2 mL amber HPLC vials and kept at -20°C until analysis. Plasma samples were analyzed in duplicate and the value reported was the average of duplicate samples. In addition, for every 10 samples, we assessed a blank and a matrix spike. For the quantification of PAHs in plasma extracted by SPE columns, a matrix spike was analyzed every ten samples using control plasma and the average recovery ranges from 60% to 75% for individual PAHs with the highest standard deviation of 6.3% for a PAH. The average recovery of PAHs recovered in plasma separated from whole blood ranged from 43% to 59% compared to PAHs recovered from whole blood. Plasma values have been corrected to reflect recovery from whole blood and matrix spike recovery from plasma.

3.4.5 Simulated Fluids

The simulated fluids used here follows the composition of the Fed ORganic Estimation human Simulation Test (FOREhST) described by Cave et al. (2010). To summarize, the simulated fluids of the FOREhST model mimic the physiological conditions of the human gastro-intestinal tract during the fed state. There are three stages which include saliva, gastric and intestinal (duodenal and bile) phases where the temperature was held constant at 37°C.

3.4.6 Soil-Water and Soil-Simulated Fluid Partitioning Coefficient (K_d and K_{sim})

The K_d was determined by weighing approximately 3 g of soil into pre-cleaned 50 mL Teflon centrifuge tubes. To the tube, 8 mL of de-ionized water was added and the tubes were sealed and placed into a shaker at ~ 30 rpm (0.1 g) for a period of fourteen days. To separate the supernatant solution, tubes were centrifuged at ~3000 rpm (1000 g) for 15 minutes and the overlaying water was decanted and filtered through Whatman GMF 0.45 μm filters into 15 mL amber vials. Approximately 1 mL of toluene was added to the water and the mixture was evaporated to near dryness and re-suspended in 2 mL of acetonitrile and transferred into labeled 2 mL amber HPLC vials. The leftover soil pellet was air-dried overnight and the PAHs remaining in soil were extracted using a 6:1 mix of methanol: toluene in an ultrasonic bath for 2 hours at 50°C. To separate the supernatant solution, the tubes were centrifuged at ~ 2000 rpm (600 g) for 15 min and were filtered through Whatman GMF 0.45 μm filters into a 15 mL amber glass vial. A 0.15 mL aliquot of the methanol: toluene mixture was diluted with 1.35 mL acetonitrile into labeled 2 mL amber HPLC vials and kept at -20°C until analysis. The K_{sim} was determined similarly to the K_d, except only 0.3 g of soil was used with 30 mL of simulated fluids to mimic the procedures of Cave et al. (2010).

The K_d and K_{sim} was calculated by dividing the PAH concentration remaining in the soil by the concentration of PAHs in the water and simulated fluids, respectively.

3.4.7 Fugacity Analysis

The soil fugacity capacity (Z_{soil}) was calculated as described by Mackay (2001). Solubility and vapour pressure (i.e. Z_{water}) for each PAH are the median values obtained from Mackay et al. (2006). Fugacity capacity was calculated using equation 3.4 and measured K_d values. Soil particle density was assumed to be 2.65.

$$Z_{soil} = Z_{water} \times K_d \times \text{soil particle density} \quad \text{(Eqn 3.4)}$$

3.4.8 HPLC

Prepared PAH samples were analyzed using an Agilent 1260 Infinity High Pressure Liquid Chromatography coupled with Fluorescence Detection (HPLC-FD) (Marriott et al. 1993). A 10 µL aliquot was injected onto an Agilent PAH Pursuit column (3 µm particle size, 100mm length, and 4.6 mm internal diameter) guarded with an Agilent Pursuit C18 MetaGuard (3 µm particle size, 2mm internal diameter). The column temperature was maintained at 25°C for the duration of the 25 min run. The mobile phase consists of acetonitrile and water with a flow rate of 1.5 mL min^{-1}. At the start of the run the solvent gradient was 60:40 acetonitrile: water, gradually increases to 95:5 acetonitrile: water at 20 m, and was held constant until the end of the run. The fluorescence detector employs a constant excitation wavelength of 260 nm and four emission wavelengths of 350, 420, 440, and 500 nm. Detection limits for anthracene was 0.70 pg µL, fluoranthene was 1.71 pg µL, pyrene 0.43 pg µL, benzo(a)anthracene was 2.45 pg µL, chrysene was 5.27 pg µL, benzo(b)fluoranthene was 5.58, benzo(k)fluoranthene was 2.77 pg µL, benzo(a)pyrene was 13.02 pg µL, dibenzo(ah)anthracene was 7.79 pg µL, benzo(ghi)perylene was 1.78 pg µL, and indeno(123-cd)pyrene was 1.80 pg µL.

3.4.9 Statistical Analysis

We selected regression analysis for our estimates of the nature of the relationship between blood content, bioavailability and soil fugacity because (i) we wished to imply causality and (ii) the variation in soil concentration, measured soil fugacity, or soil fugacity capacity was much less than that associated with bioavailability or blood content. Where the variability of the x-axis exceeds the variability on the y-axis 95% confidence intervals are provided. Regression analyses were performed in SigmaPlot (version 10.0).

Structure equation modeling (SEM) was performed using R software (R Core Team 2013) and the 'lavaan' (Rosseel 2012) package. SEM is a statistical approach similar to path

analysis and is used for testing hypotheses where the relationships between many variables are confounded by inter-correlations (Lamb et al. 2011). Soil organic carbon content was removed from the fugacity capacity equation (see equation 3.4) however soil organic carbon is known to influence both partitioning (Chiou et al. 1998) and soil PAH concentration (Tang et al. 2005). Furthermore, K_d and K_{sim} were correlated due to similar experimental conditions. Using SEM, the influence of soil organic carbon on partitioning and soil concentration can be accounted for, while simultaneously accounting for the correlation between K_d and K_{sim}. The initial SEM was set up with soil organic carbon as an endogenous variable. Direct paths from soil organic carbon to soil PAH and simulated fluid partitioning were included because soil organic carbon is known to influence partitioning (Chiou et al. 1998) and soil concentration (Tang et al. 2005). Soil simulated fluid partitioning and soil fugacity capacity are inherently related due to partitioning (Cave et al. 2014; Chiou et al. 1998). Soil fugacity was then included as a direct cause of soil PAH concentration based on results generated within. Finally, all four variables, soil organic carbon, soil fugacity capacity, soil simulated fluid partitioning and soil PAH concentration were included as direct causes of PAH exposure. PAH exposure (AUC48 plasma content) was calculated with R software with the 'MESS' (Ekstrom and Ekstrom 2012) package using the trapezoidal rule.

The assumptions of normality were tested using the Shapiro-Wilk test. All data that were not normally distributed were typically log-normally distributed therefore they were log-transformed prior to analysis. Data which were not log-normally distributed were transformed to normality using box-cox transformations.

3.5 Results

The *in vivo* bioavailability estimates of the 5 PAH compounds analyzed from the 19 soils were largely below 30% with an average bioavailability of 12% for benzo(a)anthracene, 11% for

chrysene, 29% for benzo(b)fluoranthene, 27% for benzo(k)fluoranthene, and 21% for benzo(a)pyrene. Five of the soils, COT1-COT5, had very low PAH soil concentrations, ranging from 0.008 to 0.02 μg/g (**Table 3.1**). Because of low soil PAH concentrations in these soils, a non-detect in plasma led to bioavailability of 0% whereas a detection in plasma led to bioavailability of 100%. BGS2 was the only other soil that had a 0% bioavailability for benzo(k)fluoranthene. Trimming these samples from the data set, results in lower average bioavailability of 12% for benzo(a)anthracene, 11% for chrysene, 8.8% for benzo(b)fluoranthene, 6.5% for benzo(k)fluoranthene, 4.4% for benzo(a)pyrene. The soil concentration and bioavailability of anthracene, fluoranthene, pyrene, dibenzo(ah)anthracene, benzo(ghi)perylene, and indeno(123-cd)pyrene are presented in **Table A1**.

Table 3.1 Physiochemical properties and PAH bioavailability soils used in this study

	Particle Size (%)				Soil Concentration (µg/g)					Bioavailability (%)				
	Sand	Silt + Clay	OC[1]	pH	B(a)A[2]	CHR[2]	B(b)F[2]	B(k)F[2]	B(a)P[2]	B(a)A[2]	CHR[2]	B(b)F[2]	B(k)F[2]	B(a)P[2]
BGS1	84	16	1.3	6.7	1.5	1.4	3.7	2.0	2.5	38	10	27	32	11
BGS2	77	23	8.8	6.7	23	27	84	22	56	2.5	8.6	3.45	0	0.8
BGS3	54	46	8.2	6.5	19	24	86	22	35	7.1	6.9	4.9	3.1	2.1
BGS4	67	33	6.8	n/a	50	49	101	33	61	6.2	11	4.8	0.3	2.6
BGS5	57	43	3.3	n/a	18	18	46	16	18	14	19	7.0	3.9	0.7
BGS6	59	41	12	6.5	19	26	40	14	17	5.4	6.3	6.7	0.8	4.1
BGS7	49	51	7.8	6.6	6.8	11	22	8	10	31	27	8.5	1.9	9.1
BGS8	70	30	13	2.0	32	39	80	19	25	8.8	14	6.6	4.0	0.5
BGS9	38	62	3.9	6.2	16	16	36	13	22	9.1	14	5.2	0.9	0.3
BGS10	90	10	4.8	6.3	75	86	77	32	41	6.5	4.5	6.9	6.5	13
BGS11	39	61	4.9	6.3	54	60	73	29	48	1.3	9.8	4.5	0.3	14
BGS12	63	37	33	n/a	390	340	410	160	290	0.2	0.007	0.2	0.01	0.1
WP1	42	58	2.4	5.7	51	45	39	15	18	3.2	4.2	9.6	26	2.0
GW2	59	41	4.6	6.7	3.7	4.0	5.7	2.2	4.5	40	22	29	4.9	1.4
COT1			0.8	7.1	ND	ND	<LOQ	0.004	ND	-	-	-	0	-
COT2			0.9	6.8	<LOQ	<LOQ	0.02	0.002	0.005	-	-	100	100	100
COT3			0.7	6.8	ND	ND	0.02	0.004	ND	-	-	100	100	-
COT4			0.8	6.8	<LOQ	<LOQ	0.01	0.01	0.09	-	-	100	100	100
COT5			1.6	6.8	ND	<LOQ	0.008	0.008	0.02	-	-	100	100	100
Average[3]	60	40	6.3	6.3	57	56	61	21	41	12	11	8.8	6.5	4.4
Geometric Mean[3]	59	36	3.7	6.1	25	27	7.5	2.0	5.0	6.2	6.2	5.8	1.7	2.0
Standard Deviation[3]	16	16	7.9	1.4	100	86	94	36	67	14	7.4	8.3	10	5.1

[1]Organic carbon reported as percent (w/w).

[2]Abbreviations are as follows: B(a)A is benzo(a)anthracene, CHR is chrysene, B(b)F is benzo(b)fluoranthene, B(k)F is benzo(k)fluoranthene, and B(a)P is benzo(a)pyrene

[3]The average, geometric mean and standard deviation values for bioavailability do not include the 5 COT soils

ND indicates a non-detection of PAH in soil

<LOQ indicates a value below the limit of quantification

As a pre-requisite to calculating fugacity capacity, we determined the partitioning coefficients. As expected, between soils, the PAH partitioning coefficient between soils and water (K_d) varied over five orders of magnitude. For example, for benzo(a)pyrene, the log K_d varied between 1.34 and 5.05 (**Table A2**). In contrast, between PAHs within a soil, log K_d values varied at most one order of magnitude.

Partitioning between simulated intestinal fluid (K_{sim}) and soils remained relatively similar between soils. For example, for benzo(a)pyrene, the log K_{sim} only varied between 1.59 and 2.97. The K_{sim} between PAHs was also relatively similar with K_{sim} varying slightly less than an order of magnitude within a soil (**Table A3**). The two measures of partitioning were not linked to one another across soils. For example, K_d and K_{sim} did not correlate ($r < 0.1$) for all PAHs, except benzo(a)pyrene in which K_d and K_{sim} were negatively correlated ($r = -0.43$, $p < 0.05$).

Soil fugacity capacity predicts, with an average slope of 0.30 with standard error of the slopes between 0.054-0.073, soil PAH concentration (r^2 between 0.61-0.73, $p < 0.001$) (**Figure 3.1**). The average soil fugacity capacity for these soils was $1.4 \pm 0.70 \times 10^9$ mol m^{-3} Pa^{-1} for benzo(a)anthracene, $1.3 \pm 0.60 \times 10^9$ mol m^{-3} Pa^{-1} for chrysene, $1.2 \pm 0.52 \times 10^7$ mol m^{-3} Pa^{-1} for benzo(b)fluoranthene, $7.5 \pm 2.9 \times 10^9$ mol m^{-3} Pa^{-1} for benzo(k)fluoranthene, and $5.0 \pm 2.0 \times 10^8$ mol m^{-3} Pa^{-1} for benzo(a)pyrene (mean ± SE) with an average soil concentration of 55 ± 27μg g^{-1} for benzo(a)anthracene, 53 ± 23μg g^{-1} for chrysene, 79 ± 27μg g^{-1} for benzo(b)fluoranthene, 28 ± 11μg g^{-1} for benzo(k)fluoranthene, and 46 ± 19 μg g^{-1} for benzo(a)pyrene (mean ± SE). Soil PAH concentrations were normally distributed between ~1-100 μg/g between the soils for five PAHs with the exception of BGS 12, which has soil PAH concentrations between 160-490 μg/g.

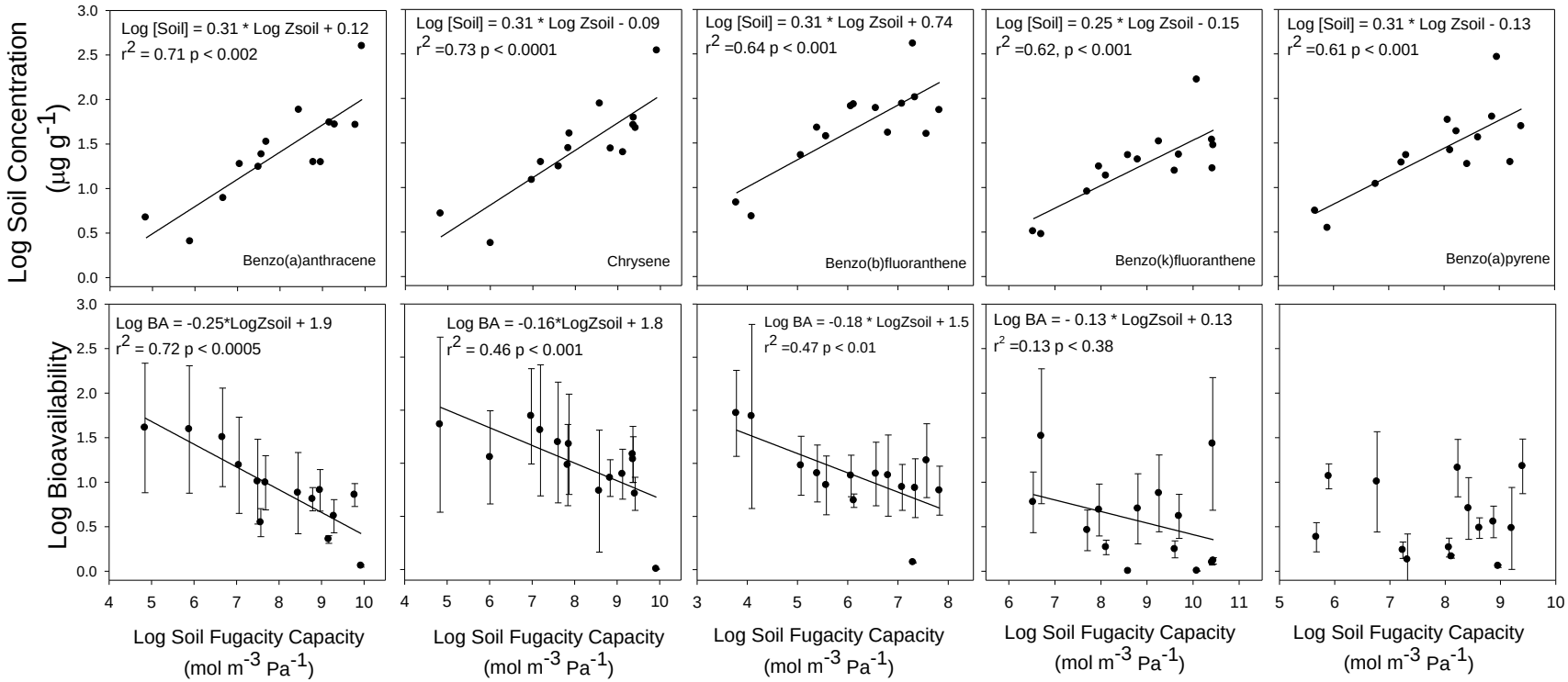

Figure 3.1 Comparison between soil concentration (top) or log bioavailability (bottom) and soil fugacity capacity of five PAHs in 14 soils historically contaminated with hydrocarbons. Lines indicates line of best fit. Data points represent the mean (n =6) of mammalian bioavailability and (n=3) estimates of soil concentration or (n=3) estimates of fugacity capacity. Fugacity capacity was calculated using experimentally determined K_d values. Bioavailability was calculated as the quotient of Area under the Curve (µg PAHs recovered in plasma per gram of soil over a 48 hour time period) divided by the total amount of PAHs in the dosed soil multiplied by 100%. Error bars represent the standard error of the mean and were obscured for soil concentration and fugacity capacity.

Soil fugacity capacity correlated strongly with PAH bioavailability (**Figure 3.1**). However as the K_{ow} of the PAH increases, the relationship between the soil fugacity capacity and bioavailability declines in strength. For example, soil fugacity explains ca. 60% of the variation between soils for low K_{ow} PAHs but explained variance decreases remarkably down to ca. 13% for benzo(k)fluoranthene or benzo(a)pyrene. In contrast with soil fugacity capacity, the K_{sim} was not as closely linked to bioavailability, however as the K_{ow} of PAHs increase the correlation with K_{sim} increases, but not by a significant amount **(Figure A2)**. Notably, neither PAH fugacity **(Figure A3)** nor PAH fugacity capacity **(Figure 3.2)** correlated to AUC48 (area under the plasma concentration time curve over a 48 hour time period) with the exception of benzo(a)pyrene which had a weak to moderate correlation ($r^2 \sim 0.4$-0.5). As soil concentration, fugacity, soil organic carbon and partitioning coefficients are all inter-correlated, we used structural equation modeling (SEM) to assess the strength of individual parameters. Specifically, we investigated if soil organic carbon, fugacity capacity (estimated by K_d), K_{sim}, and/or soil PAH content was linked to PAH exposure. Our conceptualized causal network adequately represented the data with our SEMs having low chi-squared values (acceptable model parameters) and highly non-significant P values (individual analysis was not significantly different than the model) (**Table 3.2**). Therefore, considering that PAH exposure was not directly correlated to soil organic carbon, soil PAH concentration, fugacity capacity or K_{sim} (**Figure 3.2**; **Table A4**), the relationship of soil fugacity capacity predicting bioavailability was merely a consequence of soil fugacity capacity predicting soil PAH concentration (**Figure 3.1**). Thus, correlations between soil fugacity capacity and soil concentrations were non-causal and should not be used in a predictive fashion. There was one exception to this indirect correlation, the soil fugacity capacity of benzo(a)pyrene's blood content were strongly ($P<0.001$) and tightly (a slope of 0.78)

linked to fugacity capacity (**Figure 3.2**). In only one case, anthracene, the partitioning between soil and simulated intestinal fluid (K_{sim}) was causally linked to blood content (**Table 3.6).** Notably, soil organic carbon also predicts soil PAH concentration, but not as well as soil fugacity capacity, as indicated by the standardized coefficient (**Table 3.2**; **Figure 3.2**).

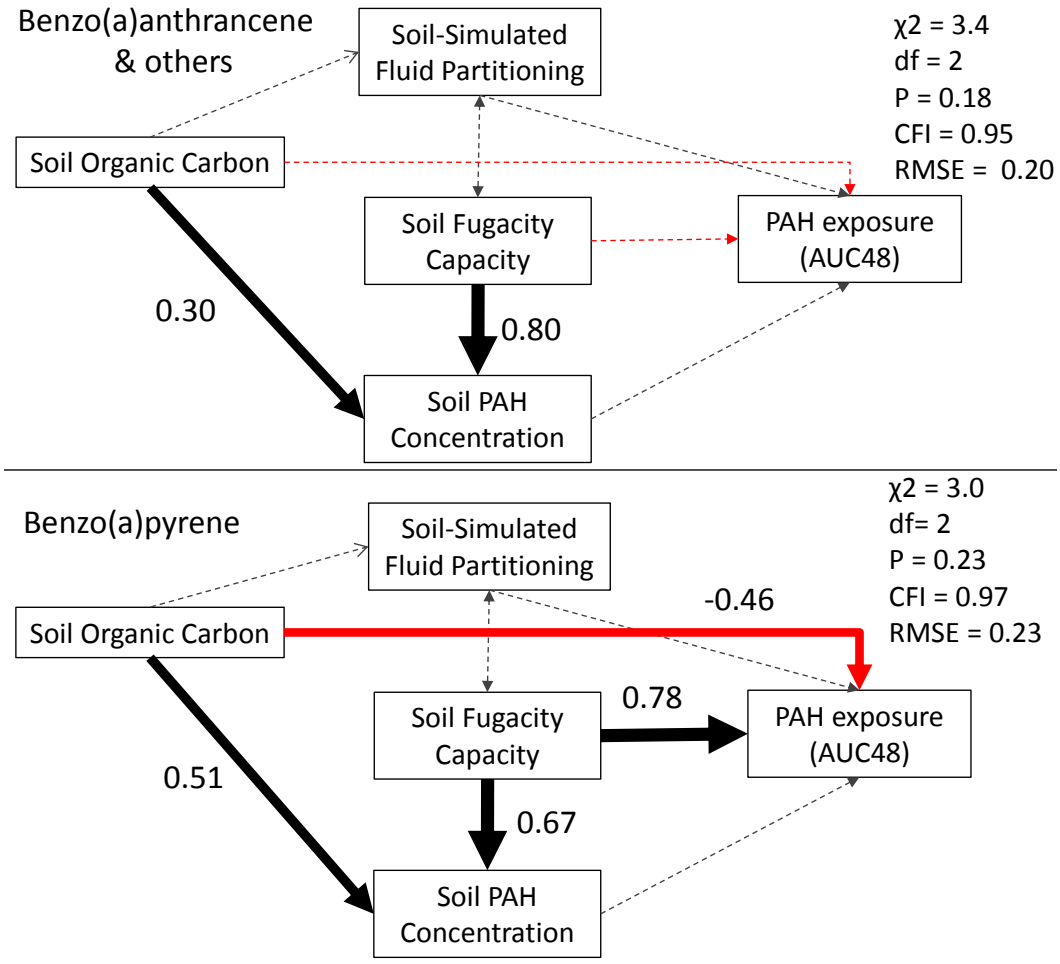

Figure 3.2 Diagram of the structure equation model (SEM) for the relationships between soil fugacity capacity, PAH soil concentration, soil-simulated fluid partitioning soil organic carbon and PAH exposure. Single headed arrows indicate that a change in the variable at the tail causes a direct change to the variable at the head. Double headed errors indicate non-directed causality. Dashed lines indicate a non-significant (P>0.05) path, whereas red arrows indicate a negative relationship. Arrow width corresponds to the strength of the relationship between variables with standardized coefficients provided for significant paths.

Table 3.2 Summary of Significant Collinear Data

PAH	Model Parameters			Significant Relationship	P value	Standardized Coefficient
	Chi-square	DF	P-Value			
Benzo(a)anthracene	3.4	2	0.18	Z_{soil} predicts [Soil]	0.001	0.80
				OC predicts [Soil]	0.035	0.30
Chrysene	3.2	2	0.20	Z_{soil} predicts [Soil]	0.001	0.79
				OC predicts [Soil]	0.004	0.37
Benzo(b)fluoranthene	3.7	2	0.15	Z_{soil} predicts [Soil]	0.001	0.69
				OC predicts [Soil]	0.001	0.55
Benzo(k)fluoranthene	3.0	2	0.22	Z_{soil} predicts [Soil]	0.001	0.69
				OC predicts [Soil]	0.001	0.50
Benzo(a)pyrene	3.0	2	0.23	Z_{soil} predicts [Soil]	0.001	0.67
				OC predicts [Soil]	0.001	0.51
				Z_{soil} predicts AUC48	0.001	0.78
				OC predicts AUC48	0.010	-0.46

[1]Abbreviations are as follows: Z_{soil} is the soil fugacity capacity, [Soil] is the soil PAH concentration, OC is the soil organic carbon, and AUC48 is the area under the curve exposure up to 48hours

Averaged across 14 soils, the fugacity of 11 PAH compounds predicts the AUC48 of individual PAHs **(Figure 3.3)**. As the fugacity of PAHs within a soil increases, the AUC48 increases proportionally ($r^2 = 0.68$, $p<0.005$) with a slope of 0.47 Log fugacity. The average log fugacity of PAHs between soils was 1.49 ± 0.29 nPa for anthracene, 2.47 ± 0.28 nPa for fluoranthene, 1.59 ± 0.25 nPa for pyrene, 0.62 ± 0.18 nPa for benzo(a)anthracene, 0.57 ± 0.18 nPa for chrysene, 2.25 ± 0.23 nPa for benzo(b)fluoranthene, 0.16 ± 0.06 nPa for benzo(k)fluoranthene, and 0.58 ± 0.14 nPa for benzo(a)pyrene 0.27 ± 0.16 nPa for dibenzo(ah)anthracene, 0.40 ± 0.22 nPa for benzo(ghi)perylene, 0.76 ± 0.24 nPa for indeno(123-cd)pyrene. However, for individual soils this relationship was not consistent for all fourteen soils. For example, for 4 of the 14 soils (BGS2, BGS3, BGS10, and BGS11) there was not a strong correlation between the AUC48 and fugacity of individual PAH compounds with r^2 values between 0.01-0.09, whereas the remaining ten soils had individual r^2 values between 0.18 and 0.65.

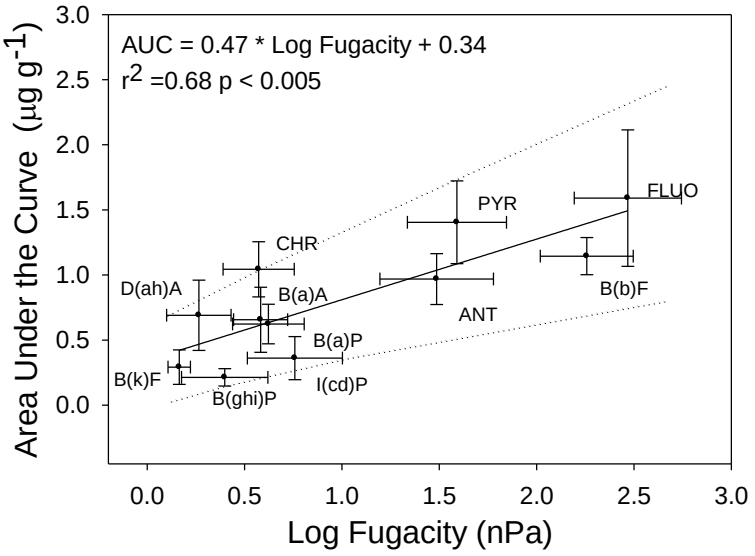

Figure 3.3 Regression between the Area Under the Curve exposure in µg PAH recovered per gram of soil against the fugacity of individual PAHs averaged across all 14 soils historically contaminated with hydrocarbons. Fugacity units were reported in nano-fugacity or 10^{-9} Pa and was calculated from soil concentration and soil fugacity capacity. Error bars represent the standard error of this mean. Dotted lines represent the 95% confidence intervals. Abbreviations are as follows: ANT is anthracene, FLU is fluoranthene, PYR is pyrene, B(a)A is benzo(a)anthracene, CHR is chrysene, B(b)F is benzo(b)fluoranthene, B(k)F is benzo(k)fluoranthene, and B(a)P is benzo(a)pyrene, DIB is dibenzo(ah)anthracene, B(g)P is benzo(ghi)perylene, and IND is indeno(123-cd)pyrene.

3.6 Discussion

Our study dosing juvenile swine with PAH-contaminated soils shows that although soil properties influenced soil PAH concentration (**Figure 3.6**), they did not reliably predict the 48-h plasma AUC. The only exception to this was benzo(a)pyrene. Using soil fugacity capacity predicts 40% of the variation in benzo(a)pyrene blood content (Log (AUC) =0.16 * Log (Z_{soil}) - 0.9: r^2=0.41, $p<0.05$, n=14). Further, all measures of bioavailability incorporate soil PAH concentration, typically as a denominator. Thus, if we use any soil property such as fugacity, fugacity capacity or K_d / K_{oc} / K_{sim}, to predict bioavailability, we cannot be certain if the predictive link was merely due to co-linearity with soil concentration or if it was truly a predictive link. Structural equation modeling unraveled this knot of causality and revealed that soil properties predict soil concentration, not uptake into the blood, barring benzo(a)pyrene. We

are not surprised by this result; fugacity superbly predicts soil, water and atmospheric concentrations as demonstrated by 40 years of research. In our study we use partitioning to pure water (K_d) and simulated intestinal fluid (K_{sim}) to explain mammalian exposure because typical exposure to contaminated soil occurs via ingestion of the soil particles that adhere to hands or are partially inhaled. Hence, partitioning was occurring between the soil particle and intestinal fluid, i.e. there was minimal partitioning between ingested soil and groundwater. For estimating the terrestrial fate of PAHs at a contaminated site, pure water is not well suited for partitioning estimates because partitioning is dependent upon site specific criteria such as the dissolved organic carbon and ionic strength of solution (Duan and Naidu 2013; Gouliarmou et al. 2012)

Mammalian internal exposure displayed no linkage to external exposure according to the partitioning behavior of soil bound PAHs. The inability of partitioning to explain differences between soils leads one to question, what other soil properties might influence mammalian PAH uptake. Soil texture may be one such clue. Duan et al. (2014) suggest that the bioavailability of benzo(a)pyrene was correlated to fine particle associated carbon (calculated as (% silt + % clay)/soil organic carbon). In our current study, no relationship exists between any PAHs and the fine particle associated carbon (**Figure A4**). Thus, soil texture may not be the key factor.

In model digestive systems, fugacity has a mixed record of predicting PAH release. Fugacity underestimates bioavailability in mice fed, aged spiked soils (Juhasz et al. 2014b). Conversely, James et al. (2011) predicted swine uptake using fugacity. In James et al. (2011) uptake was expressed in benzo(a)pyrene equivalents, which was benzo(a)pyrene driven. In the present study, benzo(a)pyrene was the only PAH where fugacity capacity was linked to exposure, thus explaining the success of our previous work (James et al. 2011) in linking fugacity but not the present results. Minhas et al. (2006) spiked chrysene into soil and Vasiluk et al.

(2007) spiked benzo(a)pyrene into pristine soil and used a field contaminated sediment. The use of a single PAH is problematic because the solubility of a single compound in simulated fluids is variable compared to the solubility of PAH mixtures. Juhasz et al.(2014b) PAH mixtures exhibit an intriguing dynamic with solubility and Chun et al. (2002) reports solubility of phenanthrene was enhanced in the presence of naphthalene yet reduced in the presence of pyrene. Chun et al. (2002) speculate that more hydrophobic compounds have greater solubility as they are held in the core of the micelle whereas less hydrophobic compounds are only solubilized in the interfacial medium, thus limiting solubility. However, the solubility experiments of Chun et al. (2002) used PAH concentrations at excess rates of solubility which are much greater than environmentally relevant concentrations. Minhas et al. (2006) and Vasiluk et al. (2007) report that the fugacity gradient drove PAH release in model digestive systems, however these were *in vitro* systems consisting of soil, aqueous phase and either EVA thin films or Caco-2 cells and the results are not surprising. What is particularly interesting from Vasiluk et al. (2007) was that both a low and high organic matter soil (11% and 29%) were spiked with the same concentration of [^{14}C]-benzo(a)pyrene and while the low organic matter soil released more [^{14}C]-benzo(a)pyrene at 5 hours, there was no significant difference of the [^{14}C]-benzo(a)pyrene in either EVA thin film or Caco-2 cells at equilibrium (~12 hours). These results suggest that a fugacity gradient was more prominent under non-equilibrium conditions and that partitioning measurements, i.e. K_d and K_{sim}, would be most appropriate at physiologically relevant times, i.e. non-equilibrium over equilibrium.

The early work on black carbon's role in PAH bioavailability (Pignatello and Xing 1996), has been refined (Burgess and Lohmann 2004) and developed into the dual-mode sorption concept (Cornelissen et al. 2005). Soil sorption of organic compounds follows either absorption

to amorphous organic matter or adsorption to carbonaceous geosorbents. Absorption to amorphous organic matter follows linear, non-competitive binding with fast desorption kinetics whereas adsorption to carbonaceous geosorbents (i.e. black carbon, kerogen, unburned coal and coke) follows non-linear, competitive binding with slow desorption kinetics. Fugacity predictions of soil concentrations incorporate both modes of sorption but are ill suited for estimating desorption in a short time frame. The lack of a (linear) correlation implies these PAHs are extensively bound to carbonaceous geosorbents and exposure will be dictated as a function of desorption rate constant specific to carbon source (Tang et al. 2006). Further, the competitive binding aspect of carbonaceous geosorbents may further explain differences between PAHs.

The soil-water and soil-simulated fluid partitioning coefficients are complementary pieces in the bioavailability puzzle. In our experiments, K_d (fugacity capacity) effectively predicted soil concentration but not bioavailability. If kinetics drive soil bioavailability, K_{sim} can model these short term kinetics and hydrophobic restraints (K_d vs K_{sim}) occurring in the mammalian gastrointestinal tract. Kinetic release depends upon the energetic inputs associated with simulated fluids such as ambient temperature, shaking method, and relative concentration of intestinal components (Oomen et al. 2002; Tang et al. 2006). Thus, K_{sim} can be estimated under conditions similar to gastrointestinal release in terms of energetic inputs. In this case, it may be worthwhile to consider estimating K_{sim} in dynamic *in vitro* digestion models such as 'TIM' (Oomen et al. 2002). Alternatively, the estimation of uptake of PAHs from soil into blood may require more sophisticated models than, the simple, first-order fugacity model used here.

Systemic parent PAH compounds are responsible for non-hepatic and non-intestinal toxicity (Shimada and Guengerich 2006; Uno et al. 2004). Metabolites internal to the organ of

interest, are responsible for organ toxicity, thus measuring metabolites at the site of toxic action would alter our bioavailability estimates. However we are unsure how one could measure internal organ metabolites over a time course in a non-lethal manner. In contrast, assessing biomarkers of exposure such as a CYP1A1 induction may be an alternative method of assessing exposure. For example, using three PAH contaminated soils Roos et al. (2002) found that hepatic CYP 1A1 induction in mini-pigs appeared to correlate with five and six ring PAH content of soils, but no correlation was found with total PAH content. This suggests that these biomarkers of exposure may be an alternative means of assessing bioavailability. Although, other soil compounds, such as metals interact with the systems CYP (Kaminsky 2006; Vakharia et al. 2001) confounding the use of these biomarkers for soil bioavailability studies. Lastly, PAH metabolism is specific to each PAH and increased metabolism leads to increased bioavailability (Cavret and Feidt 2005).

By predicting soil concentration, fugacity explains up to 65% of the variation in PAH bioavailability in historically contaminated soils. In reality, one is simply predicting soil concentration based on partitioning, or essentially, confirming the fugacity ideas outlined by Mackay in 1979. We speculate that due to the short transit times, the soil-PAH-chyme-ileum system does not come to equilibrium. As a consequence, the kinetic limitations of PAH desorption from carbonaceous geosorbents may be the critical driver of PAH bioavailability between soils. A K_{sim} specifically designed to mimic the energetic inputs that occur on the mammalian gut, may allow us to use partitioning predict bioavailability between soils.

PREFACE

4 *IN VITRO* PREDICTION OF POLYCYCLIC AROMATIC HYDROCARBON BIOAVAILABILITY OF 14 DIFFERENT INCIDENTALLY INGESTED SOILS IN JUVENILE SWINE

4.1 Preface

The following chapter has been accepted as a peer-reviewed article in the journal Science of the Total Environment with the following co-authors:

Rachel Peters (University of Saskatchewan) – involved with experimental design, data analysis, and editorial;

Mark Cave (British Geological Survey) – involved with experimental design, statistical analysis, and editorial;

Mark Wickstrom (University of Saskatchewan) – involved with experimental design and editorial;

Steven Siciliano (University of Saskatchewan) – supervisor involved with all aspects of project oversight.

As the lead author, Kyle James, was involved in every aspect of the article. Kyle performed approximately 30% of the animal work (feeding, handling, dosing, and sampling), 100% of the *in vitro* bioaccessibility testing, 100% of the data analysis, and 95% of the manuscript writing. James K, Peters RE, Cave MR, Wickstrom M, Siciliano SD. 2018. In vitro prediction of polycyclic aromatic hydrocarbon bioavailability of 14 different incidentally ingested soils in juvenile swine. Science of The Total Environment 618:682-689.

The main focus of the chapter is to evaluate how energetics and co-inertia analysis (COAI) can be used to improve *in vitro* estimations of *in vivo* PAH bioavailability. Specifically, a high and low energetic shaking method was used for *in vitro* bioaccessibility testing to compare the relative PAH release from soil. Building on the results of Chapter 3, where

correlations to PAH soil concentration does not correlate to PAH exposure, the high and low shaking methods are compared to soil concentration and *in vivo* bioavailability. Due to the predictability of PAH bioavailability between PAHs in Chapter 3, COIA is used to account for PAH interactions affecting partitioning to create a predictive model of PAH bioavailability. To confirm PAH interactions influencing partitioning, and by extension bioavailability and bioaccessibility, additional PAHs were spiked into *in vitro* bioaccessibility tests to examine PAH release from soil.

4.2 Abstract

Predicting mammalian bioavailability of PAH mixtures from in vitro bioaccessibility results has proven to be an elusive goal. In an attempt to improve in vitro predictions of PAH soil bioavailability we investigated how energetic input influences PAH bioaccessibility by using a high and low energetic shaking method. Co-inertia analysis (COIA), and Structural Equation Modeling (SEM) were also used to examine PAH-PAH interactions during ingestion. PAH bioaccessibility was determined from 14 historically contaminated soils using the fed organic estimation of the human simulation test (FOREhST) with inclusion of a silicone rod as a sorption sink and compared to bioavailability estimates from the juvenile swine model. Shaking method significantly affected PAH bioaccessibility in the FOREhST model, with PAH desorption from the high energy FOREhST almost an order of magnitude greater compared to the low energy FOREhST. PAH-PAH interactions significantly influenced PAH bioavailability and when these interactions were used in a linear model, the model predicted benzo(a)anthracene bioavailability with an slope of 1 and r2 of 0.66 and for benzo(a)pyrene bioavailability has a slope of 1 and r2 of 0.65. Lastly, to confirm the effects as determined by COIA and SEM, we spiked low levels of benzo(a)anthracene into historically contaminated soils, and observed a significant increase in benzo(a)pyrene bioaccessibility. By accounting for PAH interactions, and reducing the

energetics of in vitro extractions, we were able to use bioaccessibility to predict bioavailability across 14 historically contaminated soils. Our work suggests that future work on PAH bioavailability and bioaccessibility should focus on the dynamics of how the matrix of PAHs present in the soil interact with mammalian systems. Such interactions should not only include the chemical interactions discussed here but also the interactions of PAH mixtures with mammalian uptake systems.

4.3 Introduction

Polycyclic aromatic hydrocarbons (PAHS) are carcinogenic compounds produced from incomplete combustion of organic material. Due to their relatively low solubility and vapour pressure PAHs will accumulate in soil over time and humans are exposed to PAHs through the incidental ingestion of PAH contaminated soil. The default assumption for exposure assessment is that all of the ingested PAHs have been solubilised and absorbed (i.e. 100% bioavailable) from the gastrointestinal tract, however a significant fraction of PAHs are strongly bound to soil constituents and are not released within the gastrointestinal tract (James et al. 2016; Juhasz et al. 2014b).

PAH bioavailability from soil is estimated by monitoring uptake of PAHs into the bloodstream of a model organism, e.g. mice, swine or rats. Animals should, ethically, not be used for routine site assessments and thus, substantial effort has gone into developing *in vitro* bioaccessibility models to predict bioavailability. Current models for organic contaminants include Physiologically Based Extraction Test (PBET) (Gouliarmou et al. 2013; Li et al. 2015; Ruby et al. 2002), Colon-extended PBET (Tilston et al. 2011a), Fed Organic Estimation human Simulation Test (FOREhST) (Cave et al. 2010; Juhasz et al. 2014b), Relative Bioaccessibility Leaching Procedure (RBALP) (James et al. 2011), as well as simulation of the human intestinal microbial ecosystem (SHIME) (Cave et al. 2010). To ensure that hydrophobic organic

contaminant soil release is not limited to the compound solubility for the simulated intestinal fluids, a sorption sink such as C18 membranes (Hurdzan et al. 2008; James et al. 2011), tenax beads (Li et al. 2015), ethyl vinyl acetate thin films (Vasiluk et al. 2007), and silicone rods (Gouliarmou and Mayer 2012) are incorporated into the models. These models can often predict the bioavailability of different PAHs within a soil (James et al. 2016), but typically are not successful in estimating bioavailability between soils.

Juhasz et al. (2014a) noted that maximizing estimated bioaccessibility is not necessarily the most conservative measure of bioavailability (i.e. bioaccessibility can be less that bioavailability). Bioaccessibility is dependent upon the desorption conditions within the *in vitro* model, i.e. shaking method, temperature, desorption media, and desorption time (Oomen et al. 2002; Reichenberg and Mayer 2006). PAH release in *in vitro* models is linked to the activation energy of the desorption process (Enell et al. 2005) as well as organic matter composition (Crampon et al. 2014; Zhang et al. 2010). PAHs bind to either amorphous organic matter with non-competitive fast desorption kinetics or to carbonaceous geosorbents with competitive slow desorption kinetics (Cornelissen et al. 2005). A typical soil has both amorphous and carbonaceous geosorbents and regardless of carbon type, longer desorption times typically lead to greater desorption (Oomen et al. 2002). The RBALP model, which utilizes end-over-end rotation, can be coupled with a lipid sink and leads to high PAH release from soil (James et al. 2011). Under such conditions, PAH bioaccessibility closely tracks PAH soil concentration but not PAH bioavailability (James et al. 2011). *In vitro* models that use reduced energetic input, such as the TIM model (Van de Wiele et al. 2007), will result in lower PAH release and perhaps this release is linked more closely to bioavailability. Our rationale for this hypothesis is that the current generation of *in vitro* models assumes that maximizing bioaccessibility will better predict

bioavailability. While possible, our experience is that these *in vitro* approaches closely mirror chemical activity but not bioavailability. Hence, we modified the existing FOREhST model to reduce energetic inputs during extraction and compared this release to *in vivo* bioavailability results.

PAHs are present as mixtures and depending on the source of the PAHs, e.g. pyrogenic, petrogenic, etc., the relative ratios of each PAH will change (Tobiszewski and Namiesnik 2012). The nature of this PAH mixture is a major factor influencing PAH bioaccessibility/bioavailability (Juhasz et al. 2016). It is thought that these mixture effects occur because PAHs interact with other PAHs and influence their partitioning behavior. For example, phenanthrene solubility in various surfactants was enhanced in the presence of naphthalene yet reduced in the presence of pyrene (Chun et al. 2002). Benzo(a)pyrene concentrations in gut fluids increased in the presence of cholesterol (137%), phenanthrene (154%), lecithin (140%) and hexadeconal (232%) (Voparil et al. 2003). Given that PAHs interact with each other, it is likely that linking PAH bioaccessibility to PAH bioavailability between soils requires that we explicitly link the matrices of PAH accessibility to PAH bioavailability.

Co-inertia analysis is statistical method developed to study the common structure of multiple sets of paired data (Thioulouse 2011). Co-inertia analysis is a non-directional approach to identify individual variables within each matrix that influence the other corresponding matrix and is well suited to situations where the number of samples is low relative to the number of predictor variables. Here we use co-inertia to identify key PAHs in the bioaccessibility matrix that are influencing other PAHs in the bioavailability matrix. However, co-inertia analysis is largely an exploratory statistical approach, and thus we tested if these PAHs were significantly influencing bioavailability using structural equation modelling. Structural equation modelling

(SEM) is well suited for assessing a hypothesis that links collinear variables in a causal network to predict a dependent variable (Lamb et al. 2011). Furthermore, unlike multiple regression approach, structural equation modelling explicitly accounts for collinearity and thus, allows one to estimate, not only the significance, but the strength of a relationship linking predictors (such as the bioaccessibility of single PAHs) to the bioavailability of a PAH.

Our goal here was to combine the concepts of bioaccessibility and bioavailability as outlined by Juhasz et al. (2014a) and Reichenberg and Mayer (2006), with explicit multivariate predictive approaches, to develop a numerical prediction of bioavailability based on a widely adopted bioaccessibility protocol. We then evaluated the robustness of this prediction by spiking PAHs into water or soil and confirming that the drivers identified by the multivariate approaches were indeed occurring in *in vitro* settings.

4.4 Materials and Methods

4.4.1 Soils

A total of 14 PAH contaminated soils have been collected from the United Kingdom (n = 12) and Sweden (n =2) as previously described by Cave et al. (2010) and James et al. (2011). Soil pH, organic carbon, and particle size were analyzed as previously described by Siciliano et al. (2009).

4.4.2 Sorptive sink

Silicone rods, poly(dimethylsiloxane) (PDMS), were chosen to act as a PAH sorption sink as they have established partitioning properties for PAHs and have been previously used for *in vitro* bioaccessibility testing (Gouliarmou et al. 2013; Juhasz et al. 2016). The silicone rod (Altec, Cornwall, United Kingdom) has a diameter of 2.87-3.13 with a mass of 8.0 g m^{-3}. To prepare the silicone rods for experimental use, the procedures of Gouliarmou and Mayer (2012) were followed, where the silicone was cleaned by soaking once overnight with ethyl acetate,

three times overnight with methanol, 3 times overnight with acetone, and 4 times overnight with Milli-Q water.

4.4.3 FOREhST Shaking Method/Energetic Input

To investigate the effects of energetic inputs two shaking methods were employed. The first was the standard high energy FOREhST where 125 mL glass bottles were rotated 30 rpm end-over-end inside of a water bath held at 37°C. The second method uses a less aggressive process to create a massaging motion that utilizes 2 – 1.5" rotating spherical balls moving back and forth horizontally (**Figure B1**). Modified polytetrafluoroethylene (PTFE) bags (5"x4"- 5.0 Mil thick, Welch Fluorocarbon, Dover, New Hampshire) were used with this lower energy method, as their inherent flexibility allows for a massaging technique. In the low energy method, the FOREhST fluids were warmed up to 37°C prior to use and cool down to 28-32°C after 2 hours.

The FOREhST model described here follows the detailed procedures of Cave et al. (2010). The FOREhST model is an adaption of the fed state methods developed by the RIVM - The Netherlands National Institute for Public Health and the Environment (Versantvoort and Rompelberg 2004) and is intended for organic contaminants (Cave et al. 2010). The fed state is the most conservative estimate of bioaccessibility for organic contaminants (Oomen et al. 2000). The compartments of the FOREhST model are saliva, gastric and intestinal, which consist of simulated fluids modeled to the physiochemical conditions present at each stage.

To each experimental unit, 0.3 g of contaminated soil was added, followed by approximately 0.8 g of HIPP creamy porridge™, 2.45 mL of deionized water, 50 µL sunflower oil, and 1 m silicone rod. Saliva fluid, 4.5 mL, was added to each unit and shaken for 5 min. Afterwards, 9 mL of gastric fluid was added and incubated for 2 hours. Finally, 9 mL of duodenal fluid and 4.5 mL of bile fluid were added, followed by an additional 2 hour incubation.

Post incubation, silicone rods were removed from the extraction units, washed with Milli-Q water and gently dried with lint free tissue paper. PAHs were extracted by soaking silicone rods in approximately 50 mL of acetone twice for 24 hours (Gouliarmou and Mayer 2012). The 100 mL acetone was evaporated using nitrogen gas to near dryness, re-constituted into 1.8 mL of acetonitrile into 2 mL HPLC vials and stored at -20°C until analysis.

4.4.4 Co-Solubility Experiments

Phenanthrene (96%), pyrene (98%), and benzo(k)fluoranthene (99%) were obtained from Sigma Aldrich, while benzo(a)pyrene was obtained from MRI Global. Bioaccessibility experiments were conducted using de-ionized water and bile fluid. Bile fluid was prepared by dissolving 12.5 g L^{-1} bile and 6 g L^{-1} $NaHCO_3^-$ into de-ionized water. To each experimental unit, 1 m of silicone rod was inserted into a 125 mL amber glass jar. To the jar, approximately 35 ± 5 mg of PAH was added, followed by 100 mL of either de-ionized water or bile fluid. Notably, the solubility limits of these PAHs in water was less than 1.2 mg L^{-1}(ATSDR 1995). The amber jar was then gently shaken on a horizontal shaker for 4 hours, the time was chosen to be representative of the gastric and intestinal transit time of the FOREhST model.

4.4.5 Low Energy FOREhST Spiking

The low energy FOREhST was repeated for five soils and spiked with benzo(a)anthracene (99%, Sigma-Aldrich) or fluoranthene (99%, Sigma-Aldrich) dissolved in 100 µL of acetonitrile. The spiking consisted of five concentrations for each benzo(a)anthracene and fluoranthene. Soils were also spiked with 100 µL of clean acetonitrile as a solvent control. Spiking solution was added directly to the FOREhST media, in the mixture containing soil, water, food, saliva and silicone rod.

4.4.6 *In vivo* Swine Oral Bioavailability

The oral bioavailability and area under the plasma concentration curve over a 48 hour time period (AUC48) of PAHs to swine has been previously reported in section 3.2.3 Bioavailability of Ingested PAHs to Swine.

4.4.7 Quality Assurance - Quality Control

To quantify the PAH recovery from soil, a sand matrix spike was added every 10 samples and the average recovery ranges from 77% to 94% with a standard deviation of 12%. Benzo(b)chrysene was present at very low concentrations in all soils and was used as an internal standard and the recovery ranged from 90% to 110% with a standard deviation of 11%. For the *in vitro* digestors, a blank sample (no soil) was included every 8 samples. Average blank samples recovered a range of 0 to 120 pg from the high energy FOREhST, 110 to 810 pg from the low energy FOREhST, and 0 to 120 pg from the low energy FOREhST spiked with acetonitrile. Residual PAHs adhering to PTFE bags range from 0 to 1400 pg.

4.4.8 Statistical analysis

4.4.8.1 Co-Inertia Modelling

Co-Inertia analysis (COIA) was performed using R software (R Core Team 2013) and the "ade4" (Dray and Dufour 2007) package. Co-inertia analysis developed by Doledec and Chessel (1994) was reviewed by Thioulouse (2011) and compared with canonical correspondence analysis by Dray et al. (2003) Co-inertia analysis is an alternative method to canonical correspondence analysis when number of samples is low relative to the number of predictor variables. Co-inertia analysis investigates the common structure of paired data tables by maximizing the covariance of the row scores between the tables. High co-inertia occurs when simultaneously high values (or inverse) occur in both tables, whereas low co-inertia occurs either when they vary independently or they do not vary. Thus, high scores indicate that parameters,

such as a specific PAH, were concordant between two sets of data tables, whereas low scores indicate that these specific PAHs were discordant (or in other words, PAHs behaving dissimilarly between the two data tables, which in this case would be the soil concentration data table consisting of different soils versus different PAHs bioaccessibility compared to the data table of different PAH's bioavailability).

PAHs have the ability to interact with each other and affect the solubility of each other, and in the environment PAHs are present as mixtures. When investigating the bioavailability of PAHs it is likely that the bioavailability of one PAH will affect the bioavailability of another, the same can be said for bioaccessibility; however the goal was to use bioaccessibility to predict bioavailability. In addition to bioaccessibility, other environmental variables such as soil PAH concentration, organic matter, soil texture, and soil metal concentrations may be used as predictive variables of PAH bioavailability. In one table there is bioavailability of individual PAHs, in columns, by soil samples, in rows. In another table there are the predictor variables, including bioaccessibility of individual PAHs, as well as PAH concentration , organic matter, soil texture, and soil metal concentrations, in columns, by the same soil samples in rows.

The two data sets were first studied separately with Principal Components Analysis (PCA), and eventually analyzed as PCA-PCA COIA. In a PCA-PCA COIA, the two PCA's on the original two data sets reduces their dimensionalities by selecting the dominant components (axes). COIA uses the principle components from each data set and merges the complied data into a new multidimensional space such that the covariance between axes of each data set is maximized. The data tables were not transformed prior to analysis.

4.4.8.2 Model Selection

Co-inertia analysis provides the primary components for predicting PAH bioavailability. Using the results from co-inertia analysis, a general linear model is constructed consisting of the

dependent variable, $AUC48_{PAH}$, being regressed on by $FOREhST_{PAH}$, $[soil]_{PAH}$, and the top five variables as given by co-inertia analysis. Non-significant variables were then stepwise removed using the "stepAIC" function from the "MASS" package (Venables and Ripley 2002) with R software (R Core Team 2013) until the best final model was chosen. The "stepAIC" function was combined with an ANOVA to examine significant differences between model fits based on Akaike Information Criterion (AIC). Model residuals were plotted against predicted values and visually inspected as per Osborne and Waters (2002) to ensure homoscedasticity.

4.4.8.3 Structure Equation Modelling

Structure equation modelling was performed using R software (R Core Team 2013) with the additional "laavan" (Rosseel 2012) package. SEM is a statistical method akin to path analysis which allows for testing of hypotheses were the relationship is confounded by many variables inter-correlated. The application of SEM was to determine the relative strength of the coefficient that each predictor variable has on the dependent variable in the presence of collinearity. After removing non-significant variables, SEM was used to account for collinearity between variables and to determine the path coefficients. The structure equation model was built similarly as outlined by James et al. (2016), where there was a high degree of collinearity between predictor variables, such as between bioaccessible FOREhST PAHs, they are set to co-vary. Where one predictor variable predicts another, such as total organic carbon predicting soil PAH concentration, the model reads PAH soil concentration was regressed on by total organic carbon. Finally, each predictor variable was included as a direct cause of $AUC48_{PAH}$. A detailed SEM diagram complete with all relative pathways is available in Appendix B (**Figure B6**).

4.5 Results

In the standard high energy FOREhST model the PAH release correlates moderately to strongly (r^2 between 0.43-0.62) with soil concentration (**Figure 4.1**), whereas no correlation was

found between the low energy FOREhST and soil concentration (**Figure B2**). The average bioaccessibility (mean ± standard deviation in parentheses) from the high energy FOREhST was 23% (8.0 ± 9.5 µg) for benzo(a)anthracene, 29% (9.2 ± 8.1 µg) for chrysene, 20% (11 ± 7.9 µg) for benzo(b)fluoranthene, 21% (4.4 ± 2.7 µg) for benzo(k)fluoranthene, and 13% (5.6 ± 5.8 µg) for benzo(a)pyrene while the average bioavailability from the low energy FOREhST was 3.7% (0.76 ± 0.65 µg) for benzo(a)anthracene, 5.0% (1.2 ± 0.96 µg) for chrysene, 3.0% (0.99 ± 0.58 µg) for benzo(b)fluoranthene, 3.4% (0.38 ± 0.24 µg) for benzo(k)fluoranthene, 1.6% (0.41 ± 0.30 µg) for benzo(a)pyrene. Individual PAH bioaccessibility for each soil is available for both the high and low energy FOREhST in Appendix B (**Table B3** and **Table B4**).

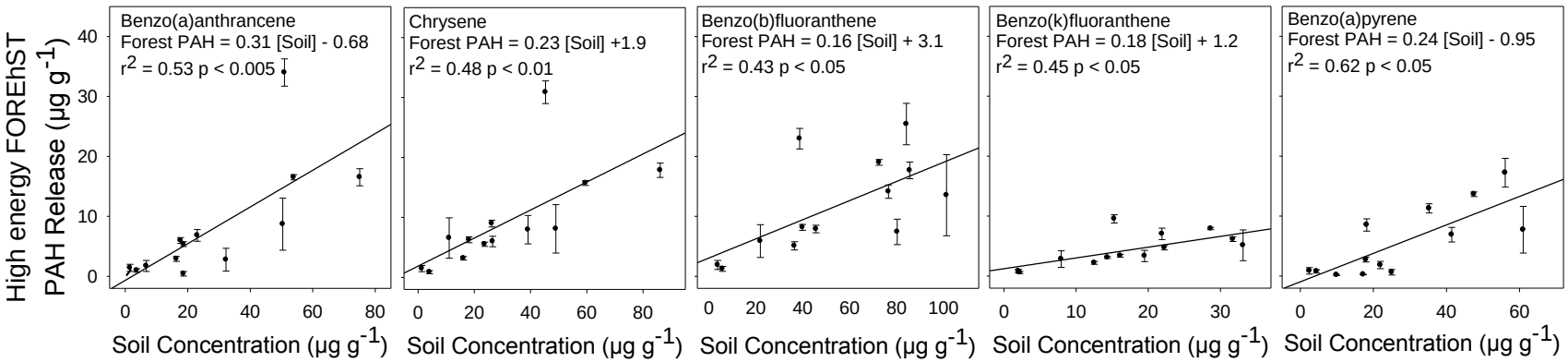

Figure 4.1 Comparison between FOREhST PAH release and soil concentration of five PAHs in 14 soils historically contaminated with hydrocarbons. Lines indicate line of best fit. Data points represent the mean (n=3) for FOREhST PAH release and error bars represent the standard error of this mean.

Between soils, neither the low or high energy FOREhST model predicts *in vivo* AUC48 juvenile swine exposure for individual PAHs (**Figure B3**). However, within a soil, both the low and high energy FOREhST predict *in vivo* AUC48 exposure between PAHs (**Figure 4.2**). Within a soil, desorption of PAHs was predictable likely due to the physiochemical properties of the PAH, as such they desorb from soil at a relative rate, however between soils, the PAH release cannot be predicted. The low energy FOREhST predicts exposure between PAHs with a slope of 1.9 ($r^2 = 0.64$, $p < 0.01$) while the high energy FOREhST predicts exposure between PAHs with a slope of 0.34 ($r^2 = 0.81$, $p < 0.005$). Notably, the energetic input does not appear to affect all PAHs equally. In **Figure 4.2**, the high energy FOREhST does not accurately predict anthracene, fluoranthene and pyrene AUC48, however the only outlier in the low energy FOREhST model was fluoranthene. PAH bioavailability data is provided in supplemental material (**Table B2**).

Co-Inertia Analysis

The PCA on PAH bioavailability reduces the data set to six principal components that explain 94.9% of the variance (**Table B5**) while the PCA on predictor variables (PAH bioaccessibility, PAH soil concentration, and soil properties) reduces the data set to five principle components that explain 90.2% of the variance (**Table B6**). COIA indicates that the primary variables predicting PAH *in vivo* exposure were FOREhST release of chrysene, fluoranthene, anthracene, and benzo(a)anthracene, followed by soil arsenic concentration, and then FOREhST release of pyrene and benzo(k)fluoranthene. The relative rankings of the individual predictor variables were determined using the 'Strength' of the predictive vector as determined by the canonical weights of COIA (**Table B7; Figure B5**).

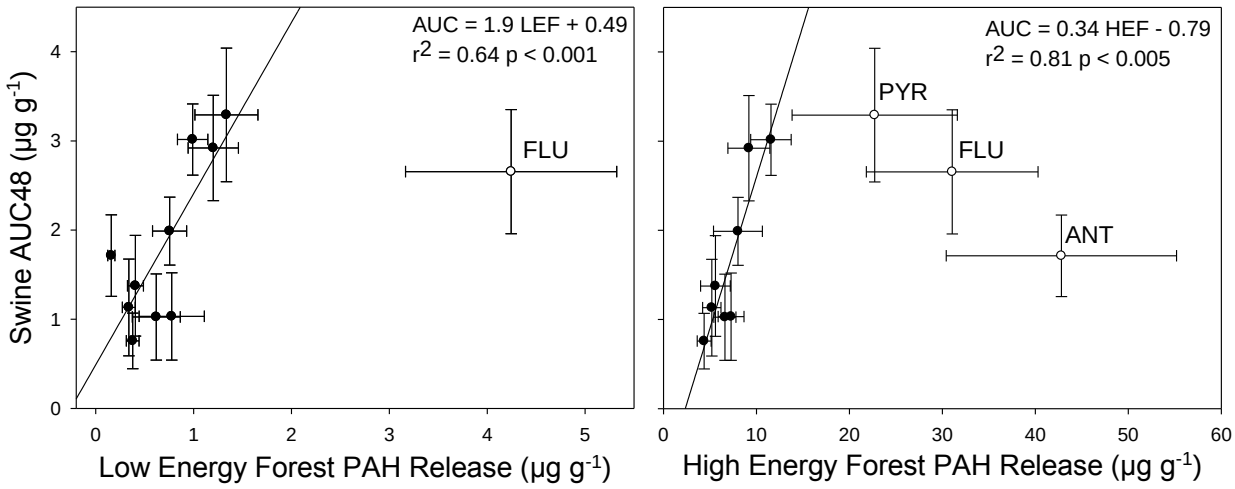

Figure 4.2 Regression between *in vivo* swine PAH area under the plasma concentration curve over 48 hours in units of µg PAH recovered in plasma per gram of soil ingested (AUC48) against *in vitro* FORE(h)ST PAH release in Low energy (left) and High energy (right). Each data point represents the mean bioavailability of a single PAH from 14 soils historically contaminated with PAHs and error bars were the standard error of this mean. Abbreviations are as follows: ANT is anthracene, FLU is fluoranthene, and PYR is pyrene.

Model Selection

The top five variables given from COIA predicting PAH *in vivo* exposure were FOREhST release of chrysene, fluoranthene, anthracene, and benzo(a)anthracene, followed by soil arsenic concentration. We evaluated these variables as well as soil concentration and FOREhST release of the individual PAH (either benzo(a)anthracene or benzo(a)pyrene) for their ability to predict bioavailability. After removing non-significant predictor variables, the most parsimonious model for benzo(a)anthracene AUC48 includes FOREhST release of benzo(a)anthracene, fluoranthene and chrysene, while the most parsimonious model for benzo(a)pyrene AUC48 includes FOREhST release of benzo(a)pyrene and benzo(a)anthracene (**Figure 4.3**). COIA does not evaluate information criterion and thus, will identify multiple predictors, whereas stepwise regression eliminates predictors based on their information content. When combining significant predictor variables into a general linear model ($B(a)A_{AUC48} \sim B(a)A_{FOR} + FLU_{FOR} + CHR_{FOR}$), the predicted AUC48 values were compared to observed

AUC48 resulting in a slope of 1.0, r^2 of 0.66, and p <0.0005. For benzo(a)pyrene, the general linear model predicts observed AUC48 with a slope of 1.0, r^2 of 0.65, and p <0.0005.

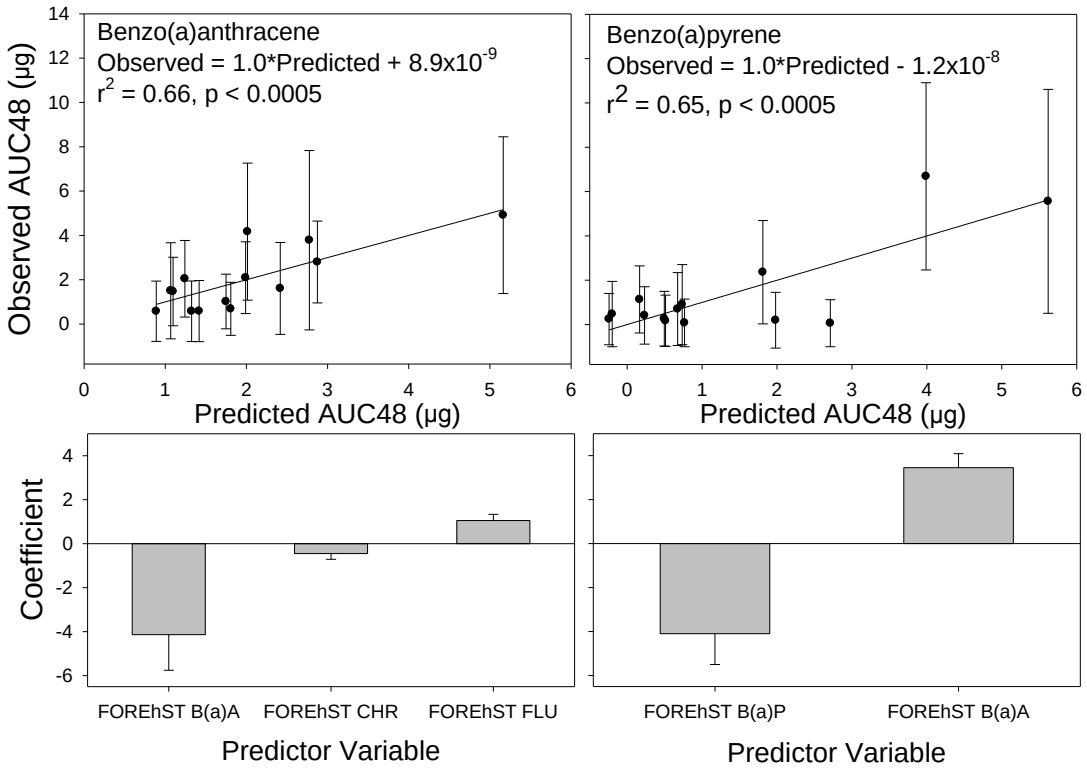

Figure 4.3 Comparison of observed AUC48 (area under the 48 hr plasma concentration curve) versus linear model predicted AUC for benzo(a)anthracene and benzo(a)pyrene PAHs (top) and the corresponding coefficient for each predictor variable (bottom). Coefficients were determined using structure equation modelling. Data points for observed AUC48 represent the mean of 6 measurements while error bars represent the standard error of this mean. Abbreviations are as follows: B(a)A is benzo(a)anthracene, CHR is chrysene, FLU is fluoranthene, and B(a)P is benzo(a)pyrene.

Structure Equation Modelling

Our hypothesized causal network linking bioaccessibility to bioavailability was congruent (P = 0.11 for benzo(a)anthracene and P = 0.13 for benzo(a)pyrene) with the data (**Table B8**). A non-significant P value for a SEM indicates the likelihood that a completely random models fits the data better than the hypothesized causal network. Other SEM fit values, e.g. CFI and RMSE, all indicate that the SEM represented the data reasonably well (**Figure B6**).

Only PAH bioaccessibility and not soil organic carbon content were significant predictors of bioavailability (**Table B8**). The standardized coefficients, used for comparing within a model, predicting benzo(a)anthracene AUC48 given by structure equation modelling were -1.8 for FOREhST benzo(a)anthracene, -0.29 for FOREhST chrysene, and 2.5 for FOREhST fluoranthene. The standardized coefficients predicting benzo(a)pyrene AUC48 were -0.56 for FOREhST benzo(a)pyrene and 1.0 for FOREhST benzo(a)anthracene. The SEM coefficients suggest that benzo(a)anthracene and fluoranthene counter-act each other in predicting benzo(a)anthracene bioavailability. In contrast, benzo(a)anthracene and benzo(a)pyrene counter-act each other in predicting benzo(a)pyrene bioavailability.

Co-solubility

In the absence of soil (i.e. only water or bile), PAHs significantly decreased the bioaccessibility of other PAHs. The amount of benzo(a)pyrene solubilized in 100 mL of de-ionized water was 94 ± 14 µg (mean ±SE), was reduced to 39 ± 15 µg in the presence of phenanthrene, significantly ($p<0.05$) reduced to 15 ± 4.8 µg in the presence of phenanthrene and pyrene, and 13 ± 6.1 µg in the presence of phenanthrene, pyrene and benzo(k)fluoranthene (**Figure 4.4**). The amount of bioaccessibile benzo(a)pyrene in 100 mL of simulated bile fluid was 36 ± 17 µg, and was significantly ($p<0.05$) reduced to 8.0 ± 2.5 µg in the presence of phenanthrene, 1.3 ± 2.1 µg in the presence of phenanthrene and pyrene, and 8.1 ± 2.1 µg in the presence of phenanthrene, pyrene and benzo(k)fluoranthene (**Figure 4.4**).

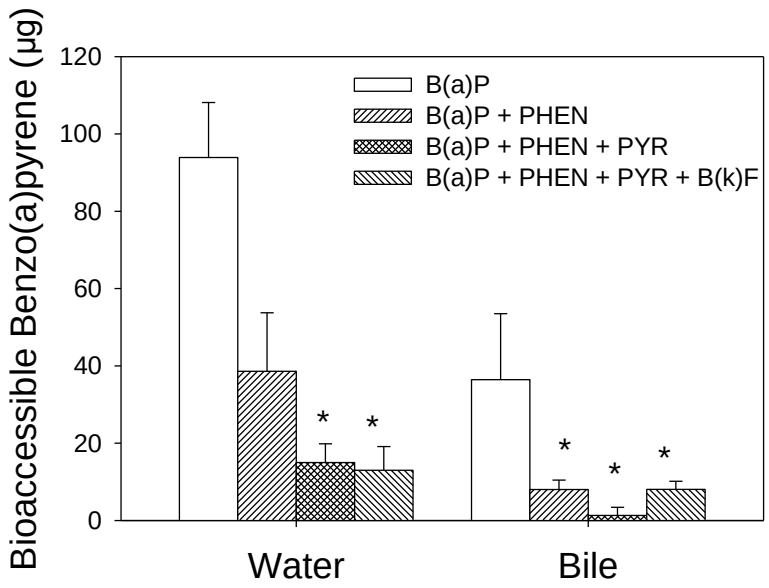

Figure 4.4 Bioaccessible fraction of benzo(a)pyrene in either water or bile in the presence of other PAHs. Approximately 30 mg of each PAH was added to the respective treatment which was above the solubility limit for the PAHs. Abbreviations are as follows: B(a)P is benzo(a)pyrene, PHEN is phenanthrene, PYR is pyrene, and B(k)F is benzo(k)fluoranthene. * indicates a significant ($p<0.05$) difference from bioaccessibility in the presence of only benzo(a)pyrene, i.e. only benzo(a)pyrene by itself.

Low-Energy FOREhST of Spiked Field Contaminated Soils

In contrast to the results in water and bile, PAH interactions in the presence of soil can increase the bioaccessibility of other PAHs. Benzo(a)anthracene was spiked into the low energy FOREhST model at 0, 0.38, 0.75, 1.5, 3.0 and 6.0 µg, resulting in a significant increase ($p < 0.05$) in the amount of benzo(a)pyrene bioaccessibility when spiking 3.0 and 6.0 µg benzo(a)anthracene (**Figure 4.5**). Fluoranthene was spiked into the low energy FOREhST model at 0, 2.3, 4.5, 9.0, 18 and 36 µg, resulting in no significant difference in benzo(a)anthracene bioaccessibility (**Figure 4.5**).

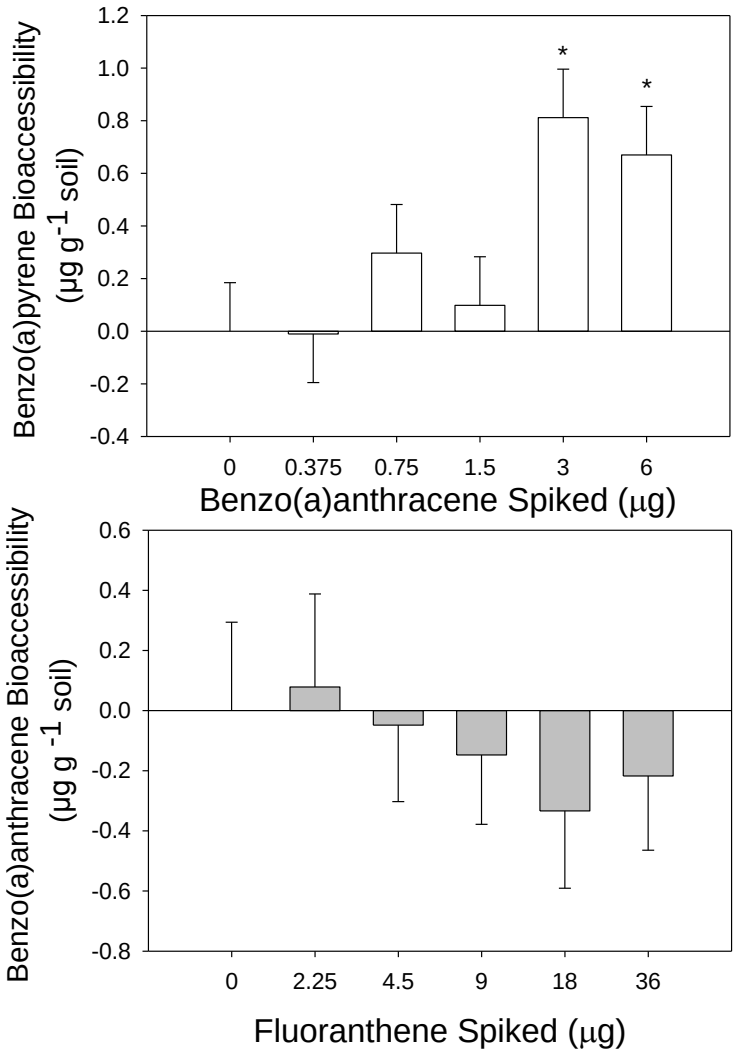

Figure 4.5 Top – Amount of benzo(a)pyrene released from soil in FOREhST fluids in the presence of increasing amounts of benzo(a)anthracene. Bottom – Amount of benzo(a)anthracene released in the presences of increasing amounts of fluoranthene. Each bar was the mean release from 5 soils and error bars represent the error of this measurement with the entire experiment duplicated. . '*' denotes a significant difference from acetonitrile control spike at $p < 0.05$.

4.6 Discussion

The FOREhST model successfully predicts 66% of the variance in benzo(a)anthracene and 65% of the variance in benzo(a)pyrene internal exposure across 14 soils polluted with a mixture of PAHs. To our knowledge, this was the first successful application of *in vitro* digestor results to estimate PAH bioavailability across multiple soils. We achieved this by: (i) incorporating PAH-PAH interactions into the predictive algorithm, and (ii) altering the energetic

input of the *in vitro* digestors. We were led to these modifications by building on key concepts outlined by Reichenberg and Mayer (2006) that chemical activity, bioaccessibility and bioavailability are conceptually distinct. Specifically, bioaccessibility was a combination of chemical activity and solubility, and thus, human *in vitro* digestors should not be designed to solely estimate chemical activity because factors, other than chemical activity, can influence bioaccessibility.

At environmentally relevant concentrations, PAH-PAH interactions can influence bioaccessibility and bioavailability. Phenanthrene, pyrene, and benzo(a)pyrene were used based on previous work that demonstrated the importance of this PAH-PAH interactions (Chun et al. 2002; Voparil et al. 2003). For example, Chun et al. (2002), attribute the change in PAH solubility from PAH-PAH interactions to PAH-micelle interactions. Using benzo(a)pyrene and phenanthrene in both artificial sea water and *Arenicola marina* gut fluid, Voparil et al. (2003) found that phenanthrene did not significantly change the benzo(a)pyrene concentration in the artificial sea water, whereas benzo(a)pyrene concentration was increased to 154% in *Arenicola marina* gut fluid in the presence of phenanthrene, alluding to the importance of the PAH-micelle interaction. Using phenanthrene, pyrene and fluoranthene with various surfactants and water, Prak and Pritchard (2002) found that PAH-micelle interactions was a significant factor but also that PAH-PAH interactions influenced the water solubility of fluoranthene.

Typically PAH-PAH experiments are in reduced mixtures of only 1 to 3 PAHs, e.g. Chun et al. (2002), Voparil et al. (2003), Prak and Pritchard (2002), etc. In contrast, our dosed soils contained more than 11 PAHs. Thus, an alternate numerical method was needed to incorporate PAH-PAH interactions because we were comparing two matrices, bioaccessibility and bioavailability which contained 14 soils by 11 PAHs. Co-inertia analysis is one such method.

We used co-inertia to link the matrix of PAH bioaccessibility with PAH internal exposure and identified that FOREhST release of chrysene, fluoranthene, anthracene, and benzo(a)anthracene were the principle components governing PAH uptake *in vivo*. For benzo(a)pyrene, we confirm that benzo(a)anthracene influences benzo(a)pyrene soil bioaccessibility. In contrast, fluoranthene does not increase benzo(a)anthracene soil bioaccessibility as predicted by statistical modelling bioaccessibility (**Figure 4.5**). Notably, PAH-PAH interactions are not limited to just desorption (White et al. 1999) and solubility (Chun et al. 2002; Prak and Pritchard 2002; Voparil et al. 2003), as PAH interactions are also relevant with cellular responses. DNA damage to HepG2 cells is modulated based on specific binary PAHs mixtures (Tarantini et al. 2011). Furthermore, induction of PAH metabolizing enzymes, CYP1A1 and CYP1A2, are dependent upon exposure to specific PAHs (Vakharia et al. 2001).

The collinearity of individual PAH bioavailabilities or bioaccessibilities likely reflects fundamental chemical-chemical interactions. PAHs with similar molecular weight, ring number, and structure have strong influences on each other. For example, Liu et al. (2013) reports a significant correlation for PAH soil concentration of all 16 PAHs examined but a stronger correlation for PAHs of similar molecular weight. Similarly, the PAH ratio of compounds w used in PAH source appointment because ratios of similar PAHs are consistently found based on source (Tobiszewski and Namiesnik 2012; Yunker et al. 2002). Although our results suggest the importance of chrysene, fluoranthene, benzo(a)anthracene, this may be limited to our sample set of 14 soils. In other soils, factors such as PAH source (Juhasz et al. 2016; Tobiszewski and Namiesnik 2012; Yunker et al. 2002), PAH concentration, sorption sink (Vasiluk et al. 2007), desorption media (Oomen et al. 2002; Reichenberg and Mayer 2006), soil physio-chemical properties (Cornelissen et al. 2005), dietary constituents (Voparil et al. 2003), and co-

contaminants (Voparil et al. 2003) may further influence the partitioning dynamic of PAHs and thus, may influence the equations describing the link between *in vitro* bioaccessibility and *in vivo* internal exposure.

Energetic input through shaking method was responsible for up to 99% of PAHs released from *in vitro* models. PAH release from the low energy FOREhST was between 0.66% (anthracene) and 31 % (fluoranthene) with an average of 19% between PAHs compared to the high energy FOREhST. PAH kinetic desorption from soil will be dependent upon the energy of the system, both kinetic and thermal, interacting with the PAH-soil binding media, amorphous organic matter and carbonaceous geosorbents. Given the limited desorption time of the FOREhST model, i.e. 4 hours, the majority of desorbed PAHs were likely bound to the rapidly desorbing amorphous organic matter as opposed to the slowly desorbing recalcitrant carbonaceous geosorbents. However, these rapidly released PAHs from amorphous geosorbents may in turn, influence PAH release from carbonaceous geosorbents. For example, White et al. (1999) observed that freshly spiked anthracene or pyrene into soil leads to increased aged phenanthrene extraction by a mild solvent and increased biodegradation, suggesting that PAHs compete for and interact at the slow desorption sites of carbonaceous geosorbents. Within the FOREhST model, it is uncertain if a similar interaction is occurring between the rapidly desorbed PAHs competing with the recalcitrant PAHs to influence bioaccessibility. If this interaction is occurring, this may explain the energetic disparity between the low and high energy FOREhST with PAH desorbed from amorphous organic matter in the high energy FOREhST increasing PAH desorption rate from the carbonaceous geosorbents. In either case the high energy FOREhST desorbs PAHs at a rate such that there is a strong correlation to soil PAH concentration, and we've repeatedly observed that soil concentration does not correlate with

bioavailability (James et al. 2011; James et al. 2016). As a product of the desorption kinetics and desorption time of *in vitro* models, energetic input becomes a dominant factor linking PAH desorption from soil in an *in vitro* model to mammalian PAH uptake into the blood stream. Yet oddly, this factor has not been identified in the round robins of *in vitro* digestor performance that have been performed previously (Oomen et al. 2002; Van de Wiele et al. 2007). Notably, the energetic input does not appear to affect all PAHs equally. In **Figure 4.5**, the high energy FOREhST does not accurately predict anthracene, fluoranthene and pyrene AUC48, whereas only fluoranthene was not predicted in the low energy FOREhST model. Suggesting that for these relatively lower molecular weight PAHs, energetic input was not a dominant factor.

When considered as single contaminants, PAH bioaccessibility and bioavailability was strongly linked to soil characteristics (Duan et al. 2014; Minhas et al. 2006; Vasiluk et al. 2007). When considered as a mixture, PAH-PAH interactions dominate. Our work suggests that future work on PAH bioavailability and bioaccessibility should focus on the dynamics of how the matrix of PAHs present in the soil interact with mammalian systems. Such interactions should not only include the chemical interactions discussed here but also the interactions of PAH mixtures with mammalian uptake systems.

5 POLYCYCLIC AROMATIC HYDROCARBON MIXTURES: EFFECTS ON METABOLISM AND BINDING TO CELLULAR COMPONENTS

5.1 Preface

The following chapter has been prepared in the style of a peer-reviewed journal article with the Steven D Siciliano as a co-author. Currently the chapter has not been submitted to a peer-reviewed journal, but would ideally be submitted to Environmental Toxicology and Chemistry.

Steven Siciliano (University of Saskatchewan) – supervisor involved with all aspects of project oversight.

As the lead author, Kyle James, performed 100% of the lab work, 100% of the data analysis, and 95% of the manuscript writing.

In the following chapter PAH biochemical interactions are investigated using an intestinal porcine cell line (IPEC-J2). Building on the results founded in Chapter 3, where PAH bioavailability was dependent upon soil and PAH physiochemical properties, and furthered examined in Chapter 4 where accounting for PAH physiochemical interactions improves predictions of PAH bioavailability, Chapter 5 investigates PAH mixtures from a biochemical persepctive. In Chapter 5, IPEC-J2 cells were exposed to PAH mixtures outlined in Chapter 4 to investigate the same PAH mixtures from a biochemical perspective. Biochemical measurement endpoints included metabolism and cellular partitioning of PAHs. The research suggests that while PAH interactions will affect PAH cellular partitioning and metabolism, they did not consistently agree with predicted values from co-inertia analysis and structure equation modelling found in Chapter 4.

5.2 Abstract

PAH interactions influence partitioning between soil and simulated intestinal fluid, affecting PAH release from soil and improving predictions of PAH bioavailability. In an attempt

to provide further insight regarding PAH interactions, an intestinal porcine enterocyte cell line (IPEC-J2) was exposed to PAH mixtures to investigate the relative rate of PAH metabolism and PAH partitioning to cellular components. When IPEC-J2 cells are exposed to a benzo(a)anthracene/fluoranthene mixture, the amount of benzo(a)anthracene remaining after 2 hours is significantly reduced from 65 ± 9.0% to 54 ± 9.1% for the benzo(a)anthracene/fluoranthene mixture, however in a tertiary mixture of benzo(a)anthracene/fluoranthene/chrysene 64 ± 15% of the benzo(a)anthracene remained after the 2 hour exposure. A significant increase of benzo(a)pyrene partitioned to cellular components was observed for solo benzo(a)pyrene exposure (0.23 ± 20) compared to a benzo(a)pyrene/benzo(a)anthracene mixture (0.68 ± 0.58). Exposure to PAH mixtures resulted in PAH interactions which affected both metabolism and cellular partitioning. The PAH interactions were PAH dependent and occurred in a limited number of mixtures. The work here suggests that PAH mixtures can be a crucial factor for PAH studies examining PAH metabolism and PAH partitioning, particularly PAH bioavailability.

5.3 Introduction

Polycyclic aromatic hydrocarbons (PAHs) are widespread carcinogenic environmental contaminants produced worldwide through biogenic, petrogenic and pyrogenic sources (Page et al. 1999; Tobiszewski and Namiesnik 2012; Yunker et al. 2002). PAHs found in the environment are present as complex mixtures and the mixture composition is attributed to source profile (Tobiszewski and Namiesnik 2012; Yunker et al. 2002). PAHs interact with each other from a physiochemical perspective influencing desorption from soil (White et al. 1997; White et al. 1999) and from a biochemical perspective by inducing or inhibiting their own metabolism (Lampen et al. 2004; Shimada et al. 2003; Shimada and Guengerich 2006; Spink et al. 2008). Furthermore, PAHs can competitively bind proteins within the cell as demonstrated by Merchant

et al. (1992), where benzo(ghi)perylene out competes benzo(a)pyrene for protein adsorption, resulting in higher concentrations of free cellular benzo(a)pyrene. Such physiochemical and biochemical interactions likely influence PAH exposure to humans.

For orally ingested PAHs, the enterocytes of the small intestine form the first tissue encountered with the capacity to metabolize PAHs. After uptake, PAHs are metabolized by CYP enzymes, such as CYP1A1, 1A2, 1B1 and 3A4 which creates various metabolites such as epoxide, quinone, and hydroxyl molecules (Ding and Kaminsky 2003; Ramesh et al. 2004; Shimada and Guengerich 2006). Whereas CYP3A4 is the dominant enzyme in hepatic tissue, CYP1A1, 1A2, and 1B1 are the prominent enzymes in extra-hepatic tissue, such as enterocytes of the small and large intestine (Ding and Kaminsky 2003).

Incorporating the metabolism of PAH mixtures may be a key component in developing an *in vitro* digestion bioaccessibility model to mimic *in vivo* bioavailability of PAHs. *In vivo* bioavailability measurements are influenced by metabolism (Juhasz et al. 2014; Ramesh et al. 2004; Ruby et al. 2016), whereas many *in vitro* digestion models, such as PBET, FOREhST, and SHIME do not contain biotic PAH metabolizing systems (Cave et al. 2010; Ruby et al. 2002). Oomen et al. (2001) and Vasiluk et al. (2007) extracted contaminants from soil with simulated intestinal fluids using the PBET model and exposed a confluent monolayer of caco-2 (human colon carcinoma) cells to a 1:1 mix of simulated and culture media to determine bioaccessibility. For Vasiluk et al. (2007), [14C]-labeled B(a)P was used therefore metabolism was not influencing the measurements and Oomen et al. (2001) did not believe caco-2 metabolism of lindane was significant relative to hepatic metabolism, and thus was not addressed.

PAH-PAH interactions influence partitioning, bioaccessibility and bioavailability (James et al. 2016). These PAH-PAH interactions can potentially occur by altering chemical adsorption

characteristics or chemical metabolic fate. For example, benzo(a)anthracene spiked into soil increased benzo(a)pyrene desorption from soil, thus increasing bioaccessibility (James et al. 2018) via a chemical competitive adsorption process. Alternatively, PAHs, and PAH metabolites, depending on the specific compound, can induce or inhibit CYP enzymes (Iwanari et al. 2002; Shimada et al. 2003; Shimada and Guengerich 2006). Benzo(a)anthracene inhibits human CYP1A1, 1A2, and 1B1 activity (Shimada and Guengerich 2006), suggesting a possible biochemical interaction with benzo(a)pyrene co-exposure. Other PAHs, such as chrysene and fluoranthene, induce CYP enzymes (Iwanari et al. 2002; Shimada et al. 2003). Notably, CYP enzyme induction/inhibition is not only PAH dependent, but can be species, tissue and cell specific (Iwanari et al. 2002; Shimada et al. 2003; Vondracek et al. 2017), as fluoranthene in fish can inhibit CYP1A activity (Willet et al. 2001). However, little is known about PAH-PAH interactions that occur during incidental soil ingestion. Our previous work demonstrated that there were chemical adsorption interactions; this work, explored the biochemical effects of PAH mixture ingestion.

We used an intestinal porcine enterocyte cell line (IPEC-J2) to investigate PAH-PAH biochemical interactions and provide results comparable to James et al. (2016) and James et al. (2018) which used the juvenile swine model. Within a mammalian cell, a contaminant resides in at least two compartments, free and bound (Lesca et al. 1994; Merchant et al. 1992; Raha et al. 1990), with the amount between these two compartments described by a distribution coefficient (Lesca et al. 1994). Thus, building on the work of Merchant et al. (1992), we investigated how the proportion of bound-PAH is influenced by PAH mixture using an intestinal cell line model system and hypothesize that PAH mixture will influence the partitioning between compartments as well as the relative rate of metabolism.

5.4 Materials and Methods

5.4.1 Chemicals and Reagents

Dimethyl sulfoxide (DMSO), benzo(a)anthracene (99%), chrysene (98%), and fluoranthene (99%) were all obtained from Sigma-Aldrich. Benzo(a)pyrene was obtained from MRI global. Stock solutions of each PAH were prepared by dissolving PAHs in DMSO. Stock solutions were stored at room temperature and dilutions were made immediately prior to use.

5.4.2 Intestinal Porcine Enterocyte Cell Line (IPEC-J2)

The IPEC-J2 cells were graciously donated by Dr. Natacha Hogan, University of Saskatchewan, were grown in DMEM/F12 (Dulbecco's modified Eagle medium/ Ham's F-12 mixture), supplemented with 5% fetal bovine serum (v/v), 1% penicillin/streptomycin (v/v), and 0.1% epidermal growth factor (v/v). The IPEC-J2 cell cultures were maintained in 250 mL tissue culture flasks, in a 5% CO_2 incubator at 37°C. When necessary, cell cultures nearing confluency were removed from the flask using TrypLE Express 1X Disassociation Reagent (Gibco – Lifetech), an alternative to trypsin, centrifuged and diluted back into culture flasks. For exposure conditions, cell cultures nearing confluency were removed from the flask using TrypLE Express 1X Disassociation Reagent, plated onto 96-well plates at a density of 1×10^5 cells/well, and grown for 48 hours to a density of 1×10^6 cells/well. At approximately 48 hours post plating, the IPEC-J2 cells were treated according to their respective experimental sections.

5.4.3 PAH Recovery from Glass and Plastic 96-Well Plates

To determine ideal experimental methodology, the abiotic recovery of PAHs present in 100 µL of media was determined for 1, 2, 4, 8, and 24 hour incubations with both glass and plastic 96-well plates. Glass and plastic 96-well plates were obtained from ThermoFisher Scientific. To prevent evaporative losses, breathable sterile rayon film is used to seal the 96-well

plates. For each endpoint there were three experimental replicates and each experimental replicate consisted of six technical replicate samples with the 96-well plate.

5.4.4 WST-1 Assay

Cell viability was evaluated using the WST-1 assay that utilizes colorimetric differences to determine cytotoxicity. Metabolically active cells produce NADPH, which triggers the cleavage of the WST-1 tetrazolium salt to produce a formazan dye (Berridge et al. 1996). Incubations were for 24 hours and treatments consist of 100 µL media, media with DMSO (0.01% total volume), or media with PAHs dissolved in DMSO into 200 µL 96-well plates. PAH treatments consists of three dose levels (0.2 µM, 1 µM, and 10 µM) for each PAH, benzo(a)pyrene, benzo(a)anthracene, chrysene, and fluoranthene. Previous researchers have exposed mammalian cells to PAH concentrations between 0.5-10 µM (Bessette et al. 2005; Vakharia et al. 2001; Larrson et al. 2012). The exposure concentrations for the WST-1 assay were chosen as 0.2 µM is an environmental relevant concentration based on bioaccessible PAH concentrations from James et al. (2018), 1 µM provides greater statistical power based on analytical sensitivity for metabolism and cellular partitioning experiments, and 10 µM is a high exposure scenario to purposefully strain IPEC-J2 cells.

After 24 hours, media was aspirated off and to each well, 100 µL media containing 10% (v/v) WST-1 reagent was added. The plate was incubated for an additional 3 hours and readings were taken at 0.5, 1, 2, and 3 hours using a spectrophotometric plate reader at 440 nm and background reference wavelength at 620 nm, according to the manufacturer's instructions. The percentage of viability was calculated relative to a media treatment control wells from triplicate observations. For each endpoint there were three experimental replicates and each experimental replicate consisted of six technical replicate samples with the 96-well plate.

5.4.5 PAH Metabolism by IPEC-J2

The metabolism of benzo(a)pyrene and benzo(a)anthracene by IPEC-J2 cells was determined using 100 µL of treated media in plastic 96-well plates at 1 and 2 hour incubations of cells with PAH mixtures. Cells were plated at a density of 1×10^5 cells/well, and grown for 48 hours to a density of 1×10^6 cells/well. Treatment groups consist of 1µM concentrations of: benzo(a)pyrene, benzo(a)pyrene/benzo(a)anthracene, benzo(a)anthracene, benzo(a)anthracene/ fluoranthene, benzo(a)anthracene/chrysene, and benzo(a)anthracene/fluoranthene/chrysene. At each time interval 100 µL of medium was removed from six replicate wells and samples were diluted with 1.7 mL of acetonitrile in 2 mL amber HPLC vials. Each well was washed with 100 µL of acetonitrile three times. Samples were stored at -20 °C until analysis, diluted with 1.7 mL of acetonitrile in 2 mL amber HPLC vials. In addition to the six replicates wells per experimental unit, there were five experiment units for each treatment.

PAH metabolism is estimated by measuring parent PAHs remaining after 2 hour exposure by HPLC. To account for PAH losses due to evaporative losses as well as absorption/adsorption, the total amount of PAHs recovered is corrected to the recovery of abiotic controls (see Section 5.4.8 Quality Assurance Quality Control). By accounting for the abiotic losses, it is assumed that all additional PAH losses is the result of metabolism.

5.4.6 PAH Binding to Cellular Components

Measuring benzo(a)pyrene and benzo(a)anthracene binding to cellular components was performed similarly to PAH metabolism. Cells were plated at a density of 1×10^5 cells/well, and grown for 48 hours to a density of 1×10^6 cells/well. After the 48 hour growth period, cells were killed by removing the media and subsequent 1 hour UV light exposure. Post UV exposure, cells were exposed to 100 µL of media in 96-well plates for incubations of 1 and 2

hours with PAH mixtures. Treatment groups consist of 1µM concentrations of: benzo(a)pyrene, benzo(a)pyrene/benzo(a)anthracene, benzo(a)anthracene, benzo(a)anthracene/fluoranthene, benzo(a)anthracene/chrysene, and benzo(a)anthracene/fluoranthene /chrysene. At the designated incubation time, media was removed from the well and placed in microtubes. Each well was then incubated with 100 µL of 0.25% TrypLE Express in PBS. The cell suspension was then added to the appropriate microtube and centrifuged at 14,600 g for 10 min. The supernatant media (~200 µL) was diluted with 1.6 mL of acetonitrile in 2 mL amber HPLC vials. The cell pellet was washed with 100 µL of acetonitrile and diluted with 1.7 mL of acetonitrile in 2 mL amber HPLC vials. A diagram of the method is available in Appendix C (**Figure C1**). Samples were stored at -20 °C until analysis. For each endpoint there were five experimental replicates and each experimental replicate consisted of six technical replicate samples with the 96-well plate.

5.4.7 HPLC

Prepared PAH samples were analyzed using an Agilent 1260 Infinity High Pressure Liquid Chromatography coupled with Fluorescence Detection (HPLC-FD) (Marriott et al. 1993). A 10 µL aliquot was injected onto an Agilent PAH Pursuit column (3 µm particle size, 100mm length, and 4.6 mm internal diameter) guarded with an Agilent Pursuit C18 MetaGuard (3 µm particle size, 2mm internal diameter). The column temperature was maintained at 25°C for the duration of the 25 min run. The mobile phase consists of acetonitrile and water with a flow rate of 1.5 mL min^{-1}. At the start of the run the solvent gradient was 60:40 acetonitrile: water, gradually increases to 95:5 acetonitrile: water at 20 m, and was held constant until the end of the run. The fluorescence detector employs a constant excitation wavelength of 260 nm and four emission wavelengths of 350, 420, 440, and 500 nm. Detection limits for fluoranthene was 1.71

pg µL, benzo(a)anthracene was 2.45 pg µL, chrysene was 5.27 pg µL, and benzo(a)pyrene was 13.02.

5.4.8 Quality Assurance Quality Control

To account for evaporative losses and adsorption/absorption of PAHs to plate walls, the PAH recovery of each experimental unit was corrected to abiotic controls measuring PAHs recovered from media without IPEC-J2 cells. The average recovery of benzo(a)anthracene, benzo(a)pyrene, and fluoranthene from abiotic controls throughout all experiments ranged from 72.6% to 107% with the highest standard deviation of 18.6%. The maximum difference between PAH recovery in a single experimental unit was 13.6% (86.2% for fluoranthene and 72.6% for benzo(a)anthracene) PAH metabolism and partitioning experiments are corrected to the parallel abiotic controls relative to their experimental unit where the average standard deviation was 8.6%. The average recovery of chrysene ranged from 9.5% to 38.9%.

5.4.9 Statistical Analysis

All data that was non-normally distributed typically were log-normally distributed and therefore was log-transformed prior to analysis. Tests of significant difference were performed using either one way ANOVA ($p < 0.05$) or student's t-test with a Bonferroni correction where appropriate ($p < 0.05$).

5.5 Results

Glass and Plastic PAH Recovery

The abiotic PAH recovery from plastic 96-well plates after 1 and 2 hour incubation averages 77.6% to 90.0%, except for chrysene, for which recovery averages 27.7% to 31.3% (**Table 5.1**). PAH recovery from glass 96-well plates after 1 and 2 hour incubation averages 54.6% to 89.6%, except for chrysene, for which recovery averages 17.4% to 27.8%. Incubations times of 4 hours and longer had significantly lower PAH recovery ($p < 0.05$) (**Table 5.1**).

WST-1 Cytotoxicity

The PAHs fluoranthene, benzo(a)anthracene, chrysene, and benzo(a)pyrene display no overt signs of cytotoxicity to IPEC-J2 cells from doses of 0.2 μM up to 10 μM according to WST-1 viability results (**Figure 5.1**). Whereas the control cultures of 0.01% and 0.001% triton resulted in an average cell viability of under 30% (**Figure 5.1**). Triton control groups were significantly different from PAH exposure groups, but not from each other (ANOVA, $p < 0.05$)

Table 5.1 Recovery of PAHs over 24 hour dosing period in glass and plastic 96-well plates

Time	Glass (%)				Plastic (%)			
	FLU[1]	**B(a)A[1]**	**CHR[1]**	**B(a)P[1]**	**FLU[1]**	**B(a)A[1]**	**CHR[1]**	**B(a)P[1]**
1 hour	75.4 (23.5)	80.0 (9.37)	27.8 (13.1)	89.6 (20.0)	88.6 (20.4)	90.0 (22.6)	27.8 (19.2)	87.3 (13.6)
2 hour	60.9 (10.9)	78.2 (12.3)	17.4 (8.00)	54.6 (16.0)	77.6 (7.25)	84.3 (11.5)	31.3 (6.82)	83.4 (15.4)
4 hour	52.9 (25.4)	62.4 (11.5)	19.3 (12.0)	57.3 (36.9)	59.4 (15.8)	71.1 (11.6)	27.7 (3.98)	56.9 (12.9)
8 hour	NA	NA	NA	NA	29.0 (4.46)	74.9 (7.81)	13.4 (1.77)	69.3 (15.2)
24 hour	NA	NA	NA	NA	43.0 (29.1)	41.6 (12.4)	19.3 (2.60)	52.3 (26.7)

[1]Abbreviations are as follows: FLU is fluoranthene, B(a)A is benzo(a)anthracene, CHR is chrysene, and B(a)P is benzo(a)pyrene. Reported value is the average of five replicates with the standard deviation in parentheses.
Recovery was calculated as the total PAH recovered from ~100 μL media divided by the total amount of PAH added (1μM).

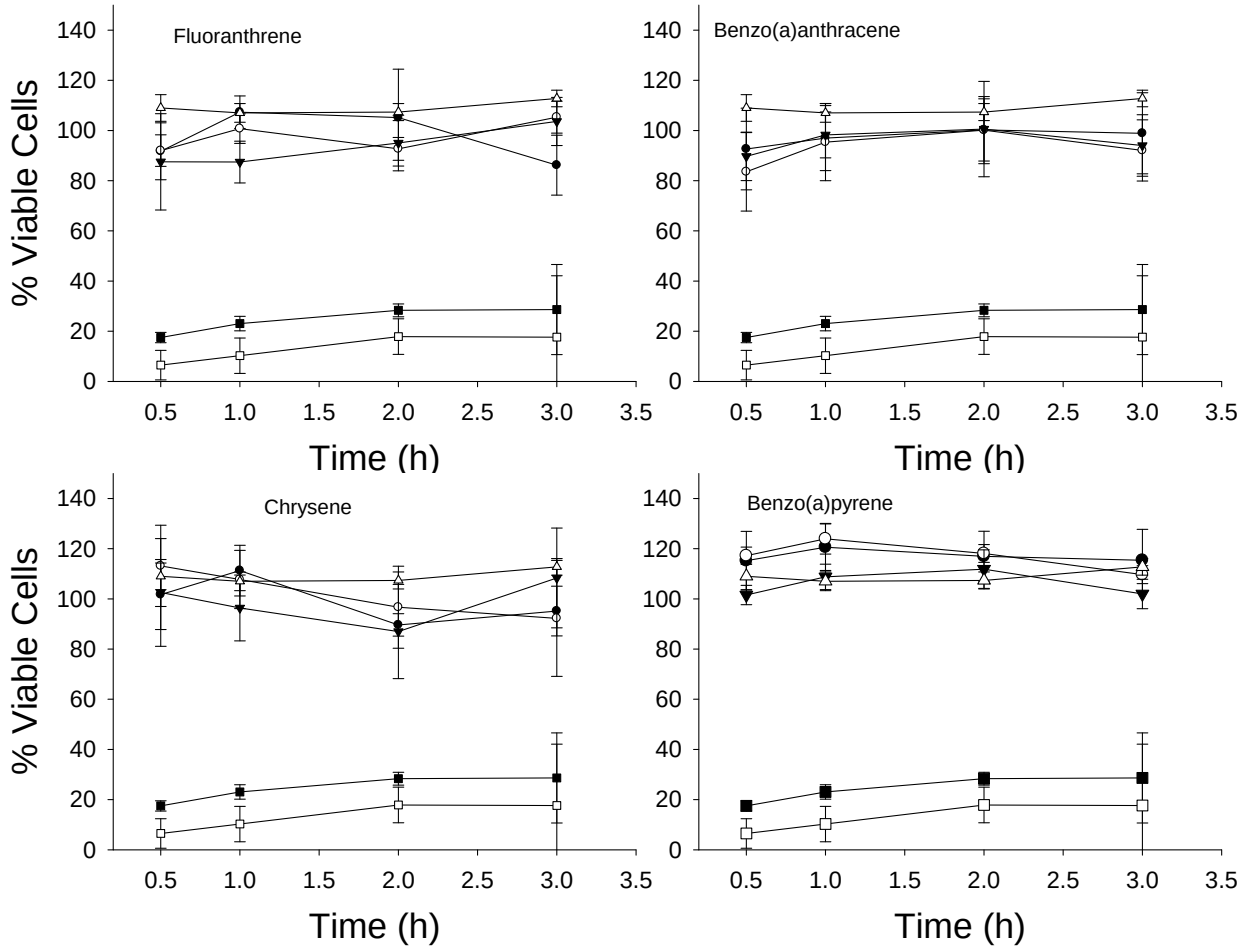

Figure 5.1 WST-1 cytotoxicity of PAHs to IPEC-J2 cells. Cells were dosed with the following treatments 0.2 µM (●), 1 µM (◌), 10 µM (▼), DMSO control (△), 0.01% triton (□), and 0.001% triton (■) (n = 3 and each treatment consists of six replicate samples). ANOVA tables indicate that 0.01% triton (□) and 0.001% triton (■) are significantly different from the other treatment groups, but not from each other.

PAH Metabolism

The amount of benzo(a)anthracene remaining from the benzo(a)anthracene/fluoranthene mixture at 2 hours was the only mixture that was significantly different ($P<0.05$) from solo benzo(a)anthracene exposure (**Figure 5.2**).The remaining benzo(a)anthracene after 2 hour exposure was 65 ± 9.0% (mean ± standard deviation) for solo benzo(a)anthracene, 54 ± 9.1% for benzo(a)anthracene/fluoranthene, 64 ± 13% for benzo(a)anthracene/chrysene, 59 ± 18% for

benzo(a)anthracene/fluoranthene/chrysene and 64 ± 15% for benzo(a)anthracene/benzo(a)pyrene. The remaining benzo(a)pyrene after 2 hour exposure was 71 ± 6.9% for solo benzo(a)pyrene exposure and 69 ± 12% for benzo(a)pyrene/benzo(a)anthracene mixture. Notably, the total PAH recovered has been corrected to PAH recovery from parallel abiotic control experiments.

PAH Binding to Cellular Components

Three PAH mixtures, benzo(a)anthracene/fluoranthene, benzo(a)anthracene/chrysene, and benzo(a)anthracene/fluoranthene/chrysene at 2 hours resulted in significantly ($P<0.05$) less binding to cellular components than solo benzo(a)anthracene (**Figure 5.3**). The average partitioning of benzo(a)anthracene into cellular components (amount in cells divided by amount in media) after 2 hour incubation was 0.74 ± 0.46 for solo benzo(a)anthracene, , 0.47 ± 0.13for benzo(a)anthracene/fluoranthene, 0.36 ± 0.16 for benzo(a)anthracene/chrysene, 0.45 ± 0.17 for benzo(a)anthracene/fluoranthene/chrysene, and 0.64 ± 0.43. Benzo(a)pyrene/benzo(a)anthracene mixture was significantly different from solo benzo(a)pyrene after 2 hour incubation (**Figure 5.3**). The average partitioning of benzo(a)pyrene into cellular components after 2 hour incubation was 0.23 ± 0.20 for benzo(a)pyrene solo and 0.68 ± 0.58 for benzo(a)pyrene/benzo(a)anthracene.

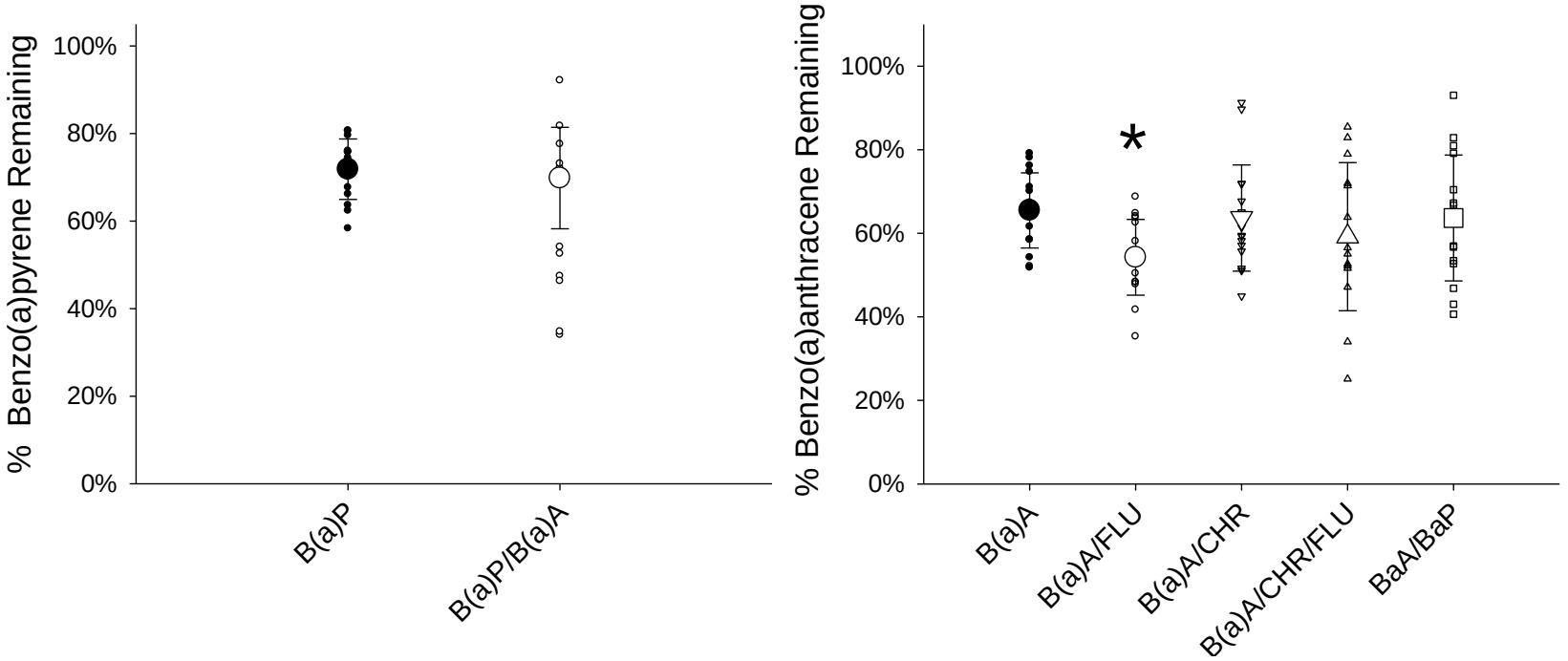

Figure 5.2 Percentage of benzo(a)pyrene (left) or benzo(a)anthracene (right) remaining in cells and media after 2 hour incubation. `*`denotes a significant difference using Students t-test with Bonferroni correction ($p < 0.05$) compared to single compound exposure. Comparisons were made to the recovery of single compound mixtures at the given time point. Small symbols represent the value of individual replicates while the large symbols represents the mean (n = 15) and error bars are the standard deviation of this mean. The percentage of PAH remaining was calculated as the total amount recovered divided by the total dose. The total amount recovered was corrected to parallel abiotic control experiments. .Abbreviations are as follows: Flu is fluoranthene, B(a)A is benzo(a)anthracene, Chr is chrysene, and B(a)P is benzo(a)pyrene.

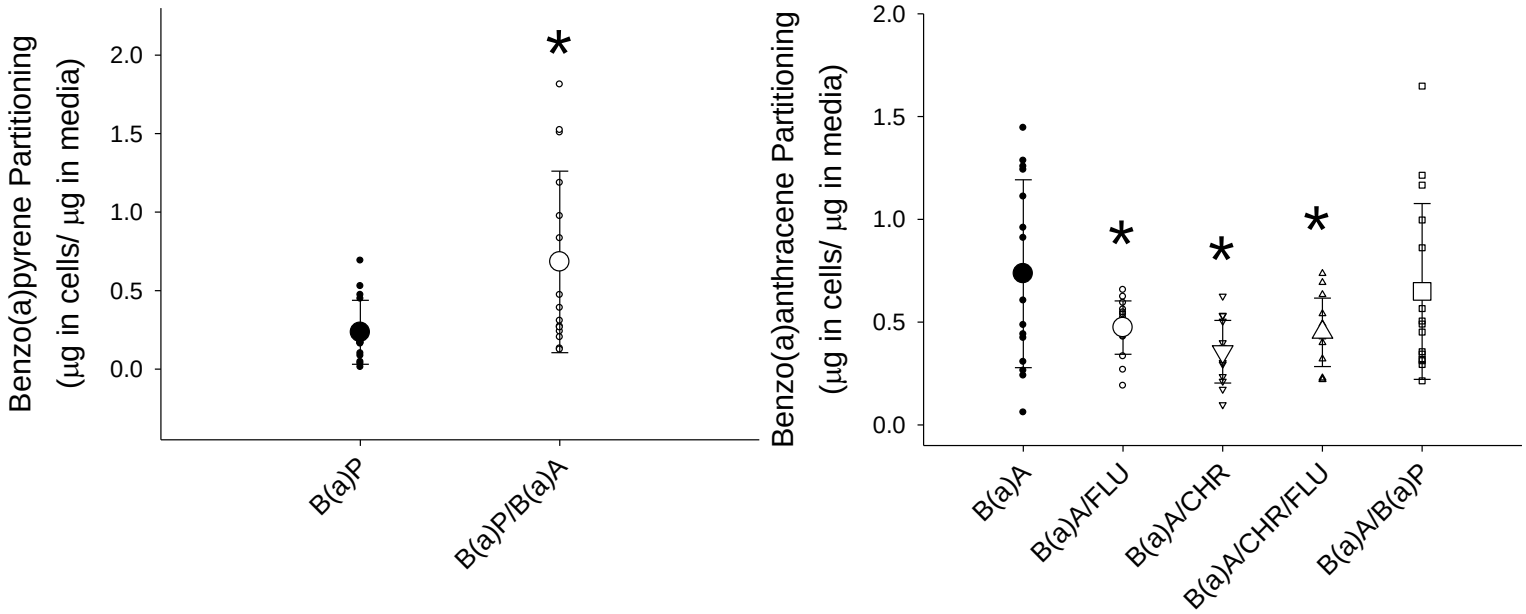

Figure 5.3 Partitioning of benzo(a)pyrene (left) and benzo(a)anthracene (right) between cells and media based on PAH mixture after 2 hour incubation. `*`denotes a significant difference using Students t-test with Bonferroni correction ($p < 0.05$) compared to single compound exposure. Significant difference was compared the partitioning of single a compound at the given time point. Small symbols represent the value of individual replicates while the large symbols represents the mean (n = 15) and error bars are the standard deviation of this mean. The total amount recovered was corrected to parallel abiotic control experiments. Abbreviations are as follows: Flu is fluoranthene, B(a)A is benzo(a)anthracene, Chr is chrysene, and B(a)P is benzo(a)pyrene.

5.6 Discussion

The original goal was to determine if cellular exposure to simple PAH mixtures can help explain the differences in bioaccessibility and bioavailability reported by James et al. (2016) and James et al. (2018). Whereas, the statistical modelling by James et al. (2018) predicted that increased free fluoranthene would increase benzo(a)anthracene bioavailability, here it was found that fluoranthene co-exposure with benzo(a)anthracene decreased the amount of remaining benzo(a)anthracene (**Figure 5.2**), thus not likely to increase the bioavailable fraction of parent compound. Notable, when cells were exposed to a fluoranthene/chrysene/benzo(a)anthracene mixture, benzo(a)anthracene metabolism is not significantly different from solo benzo(a)anthracene exposure (**Figure 5.2)**. The results here suggest that PAH kinetics and dynamics may not be confidently predicted with simple mixtures of one to three compounds. Larsson et al. (2012) investigated the differences in the relative potency of individual PAHs to PAH mixtures with as many as 15 PAHs mixed together for a luciferase bioassay. Larsson et al. (2012), found good agreement in most PAH mixtures using a concentration addition model of individual PAHs but noted that as the number of PAHs in the mixture increased, predictions had a higher tendency to deviate from predicted values. Although researchers have acknowledged the influence of PAH interactions, the mixtures are oftentimes limited to a binary (Merchant et al. 1992; Tarantini et al. 2011) or trinary scale (Chun et al. 2002).

PAH interactions were unique to the mixture they were in. For example, while a benzo(a)pyrene/benzo(a)anthracene mixture resulted in an increase of benzo(a)pyrene partitioning to cellular components, the mixture does not affect partitioning of benzo(a)anthracene to cellular components (**Figure 5.3)**. In contrast, benzo(a)anthracene mixtures with either or both fluoranthene and chrysene resulted in a significant decrease of partitioning to cellular components, although only a benzo(a)anthracene/fluoranthene mixture

resulted in a significant increase in benzo(a)anthracene metabolism (**Figure 5.2)**. Notably, PAH binding affinity to receptors and receptor induction are both PAH dependent (Bosveld et al. 2002; Kamps and Safe 1987; Larsson et al. 2012; Piskorskapliszczynska et al. 1986; Topinka et al. 2008).

There are many complicating factors for PAH exposure to organisms. Exposure to environmental PAHs typically occurs as mixture of PAHs, of which there are numerous parent, akly-, nitro-, and oxidative-PAHs, as well the metabolites of the aforementioned PAHs that will influence PAH exposure through the numerous potential interactions with either each other (White et al. 1997; White et al. 1999) or with cellular responses (Shimada et al. 2008).Species, tissue and cell specificity for induction of metabolism and cell binding may further influence the unique cellular response (Iwanari et al. 2002; Shimada et al. 2003; Vondracek et al. 2017). In an attempt to minimize these complications only simple PAH mixtures of 1-3 parent PAH compounds were used in this study. Ideally, PAH mixtures would be dominated by primary interactions, i.e. one or two other PAHs as predicted by James et al. (2018). However this ideal scenario does not appear to be the likely for biochemical responses. An intestinal porcine enterocyte cell line (IPEC-J2) was used to generate comparable results to previous research by James et al. (2016) and James et al. (2018), where bioavailability was determined from landrace female juvenile swine, 8-9 weeks old. Notably, IPEC-J2 cells were isolated from the jejunum of unsuckled newborn mixed breed piglets (Berschneider 1989; Vergauwen 2015). The discrepancy between mixed breed vs landrace swine, as well as newborn (< 1 day) vs juvenile (8-9 weeks) may also contribute to varying results. Lastly, whereas a swine jejunal cell line was used to measure metabolism of PAHs, whole organism exposure may also have significant

metabolic contributions from the liver, duodenal, ileal and colon cells which likely influence PAH exposure.

Exposure time was limited to 2 hours and plastic 96-well plates were favored over glass 96-well plates. Exposure of 4 hours led to PAH recovery at best of 71 ± 11 % but typically between 50 -60% (**Table 5.1**). Although 2 hour exposure time may not be optimum for metabolic activation, Barranco et al. (2017) found that 6 hours was enough to illicit maximum response from CYP1A1 in zebrafish embryos. Intestinal transit times through the stomach and small intestine average approximately 5 hours (Madsen et al. 1992) and PAH bioaccessibility models are based on physiological conditions transit times range between 4 to 18 hours (Oomen et al. 2002; Van de Wiele et al. 2007). Although longer exposure likely result in greater relative metabolism, they may not be representative of mammalian exposure.

Disappearance of parent PAHs is primarily due to three processes: metabolism by IPEC-J2 cells, evaporation, and adsorption/absorption to the sides of the walls. To account for the evaporative losses and adsorption/absorption of PAHs in 96-well plates, all PAHs were corrected to the relative recovery of PAHs from 100 µL media. Theoretically, metabolism of PAHs by IPEC-J2 cells should be the primary process responsible for the disappearance of each PAH. Direct measurement of PAH metabolites would be ideal, however PAHs typically undergo multiple steps of metabolism, see review by Ramesh et al. (2004), and there are numerous individual metabolites which further complicates measuring rates of PAH metabolism. One method to simplify the measurement of multiple metabolites is to conjugate groups of metabolites with sulfate or glucuronic acid and simply measure for the entire group (Autrup 1979). In the present study we attempted to use physiological relevant concentrations of parent PAH, 0.2 µM, and although cytotoxicity and recovery at 0.2 µM was acceptable (data not

shown), the analytical sensitivity would not allow for detection of significant differences between metabolism at such low concentrations, thus a concentration of 1 μM was used.

PAH binding to cellular components and PAH metabolism can be significantly affected by PAH mixture. In support of the hypothesis, a benzo(a)anthracene/benzo(a)pyrene mixture increased the amount of free benzo(a)pyrene. In contrast, various mixtures of fluoranthene, chrysene, and benzo(a)anthracene does not increase the available benzo(a)anthracene as predicted by James et. (2018). Unfortunately, simple PAH mixtures of 2-3 PAHs are unlikely to predict the interactions from complex PAH mixtures present in environmental matrixes. Our work supports previous findings (Larsson et al. 2012), where although simple mixtures can be reliably predicted, predictions deviate as mixture complexity increases. Future work investigating cellular responses to PAHs should consider a variety of complex mixtures to attain a more accurate biochemical response.

6 SYNTHESIS

Human health risk assessment for oral absorption of soil-borne PAHs currently use a default conservative estimate of 100%. This default estimate naturally leads to overestimation of human risk. Estimating oral PAH soil bioavailability from animal models are costly, time consuming and ethically impractical, hence the development of *in vitro* bioaccessibility models to circumvent these challenges. Currently, the major issue with using *in vitro* bioaccessibility models is that they have not been validated to accurately predict the bioavailability across many soils from across the world, therefore leading to inaccurate estimates of human exposure. Without *in vitro* or *in vivo* models, PAH soil absorption, exposure assessment and subsequent risk assessment are likely to be overestimated. These overestimations may cause unnecessary concern for the public as well as unnecessary remediation goals. Therefore, the primary goal of this research was to develop an *in vitro* bioaccessibility model that improves the prediction of *in vivo* bioavailability. The principle goals of this research was to further investigate factors influencing PAH bioavailability as it relates to PAH soil desorption, PAH interactions, energetic input of *in vitro* models, and cellular responses to PAH mixtures. Overall the global objective was improving *in vitro* predictions of *in vivo* bioavailability.

6.1 Principle Findings

The PAH bioavailability varied significantly across soils, while it was found that PAH mixture will influence desorption of PAHs from soil and relative rates of metabolism, affecting exposure via bioavailability of parent compound. From 14 soils, individual PAH concentrations ranged from ~1-750 µg g^{-}, bioavailability was as high 87% and in contrast, bioavailability from some soils/PAHs was undetectable, i.e. 0% (**Table 3.1 and Table A1**). The average bioavailability of all PAHs was between ~1-15%, while the median bioavailability was ~2-30%

(**Table 3.1 and Table A1**). Although partitioning, as measured by fugacity, could not explain exposure between soils (**Figure 3.2**), it does explain exposure between PAHs (**Figure 3.3**). When accounting for energetic input and PAH interactions within an *in vitro* digestion model, *in vitro* bioaccessibile predictions of *in vivo* bioavailability were improved to significant correlations ($p < 0.05$) with r^2 values of ~ 0.65 (**Figure 4.3**). Although the observed effects of PAH mixture on PAH metabolism does not support statistical predictions, metabolism due to PAH mixture was a significant factor that affects parent PAH bioavailability (**Figure 5.2**). The overall research demonstrates that PAH interactions were an integral aspect to PAH partitioning, metabolism, bioaccessibility, and bioavailability.

A major obstacle for determining factors for PAH soil bioavailability is that many soil properties inter-correlate, particularly to PAH soil concentration (**Figure 3.1 and Figure 3.2**). PAH soil concentration is typically the denominator for calculating bioavailability, therefore any property correlated to PAH bioavailability may simply be a result of correlating to soil concentration. To analyze the numerous inter-correlations SEM was used to illuminate the relationships between the multiple predictor variables (**Figure 3.2; Table 3.2**). SEM revealed that benzo(a)pyrene was the only PAH where fugacity capacity and organic carbon content predict benzo(a)pyrene exposure (AUC48) independent of benzo(a)pyrene soil concentration (**Figure 3.2**). PAH exposure averaged across soils can be predicted by fugacity with a slope of 0.33 and r^2 of 0.66 ($p < 0.005$) (**Figure 3.3**).

Energetic input and PAH interactions were essential components to creating an *in vitro* bioaccessibility to mimic *in vivo* bioavailability. By introducing a new shaking method which has a lower kinetic energy input, PAH desorption from soil was significantly reduced (**Figure 4.2**). Furthermore, the high energy FOREhST model had moderate correlations (r^2's ~0.4-0.6) to

PAH soil concentration (**Figure 4.1**), but as stated previously, correlating to soil concentration typically does not correlate to bioavailability. Through a series of statistical analysis performed by COIA, SEM, and general linear modeling, improved predictions of *in vivo* exposure of benzo(a)pyrene and benzo(a)anthracene were made with the *in vitro* FOREhST model. PAH partitioning from PAH mixtures was not influenced uniformly, as **Figure 4.4** demonstrates how PAH mixtures (up to 4 PAHs) influence partitioning of various PAHs. The general linear model predicting benzo(a)pyrene exposure was $B(a)P_{AUC48} \sim B(a)A_{FOR} + B(A)P_{FOR}$, while the general linear model for benzo(a)anthracene exposure was $B(a)A_{AUC48} \sim B(a)A_{FOR} + FLU_{FOR} + CHR_{FOR}$ **(Figure 4.3)**. Confirming the statistical modelling, spiked benzo(a)anthracene in FOREhST fluids with soil resulted in increased bioaccessbile benzo(a)pyrene, while in contrast spiked fluoranthene in FOREhST fluids with soil did not result in any significant difference of bioaccessible benzo(a)anthracene (**Figure 4.5**). Interestingly, spiked benzo(a)anthracene influenced bioaccessible benzo(a)pyrene, whereas exposure of IPEC-J2 cells to a mixture of benzo(a)anthracene and benzo(a)pyrene does not alter metabolism of benzo(a)pyrene (**Figure 5.2**). Conversely, where spiked fluoranthene did not affect bioaccessible benzo(a)anthracene, IPEC-J2 cells exposed to a mixture of fluoranthene and benzo(a)anthracene resulted in a significant increase of benzo(a)anthracene metabolism (**Figure 5.2**).

In summary, improved predictions of *in vivo* PAH bioavailability from *in vitro* PAH bioaccessibility can be made by accounting for the interactions of PAH mixtures. In the research presented here, benzo(a)pyrene partitioning, bioaccessibility and bioavailability was primarily influenced by benzo(a)anthracene. In contrast, while statistical modelling predicted that fluoranthene would affect benzo(a)anthracene bioavailability/bioaccessibility, no experimental

evidence was found to improve predictions, however fluoranthene did affect the metabolism and cellular partitioning of benzo(a)anthracene.

6.2 Future Directions

The results generated here indicate that PAH interactions will influence exposure, and by accounting for PAH interactions improved predictions of exposure can be made. To further improve *in vitro* predictions of *in vivo* bioavailability research regarding the complexities of PAH metabolism as it relates to PAH mixtures consisting of numerous, i.e. 10-plus, PAH compounds is needed. To further complicate complex PAH mixtures is co-exposure of PAHs with other environmental contaminants, such as metals, pesticides, dioxins, petroleum hydrocarbons, and PCBs. The aforementioned contaminants may further interact and influence PAH exposure and are routinely found in soil. Determining the myriad of contaminants present in every single soil is a nigh impossible task and therefore is not an enviable option. However, cell exposure to bioaccessible extracts, as performed by Oomen et al. (2001) and Vasiluk et al. (2007), may provide a realistic exposure scenario to ascertain the unique interactions between numerous contaminants. The work of Oomen et al. (2001) and Vasiluk et al. (2007) used the *in vitro* PBET model, which is similar to the FOREhST model, to extract contaminants from soil and expose caco-2 cells to measure the absorption from cells. Although Oomen et al. (2001) and Vasiluk et al. (2007) were only looking at a single contaminant, the cell line was exposed to the entirety of soil components solubilized into PBET fluids. Thus any potential biochemical interactions influencing metabolism, transportation and binding were accounted for.

Metabolic contributions from additional cell lines derived from varying species and tissues could be used to further understand PAH exposure. The research here investigated bioavailability/exposure to juvenile swine, as a model for human exposure, and compared to

porcine jejunal cells (IPEC-J2) to investigate the biochemical PAH interactions. To further explore PAH biochemical interactions, additional relevant and high priority species include swine, rodent and human. The majority of *in vivo* bioavailability research has been performed with rodents (Culp et al. 1998; Juhasz et al. 2014b; Ramesh et al. 2004; Roberts et al. 2007), while in this thesis, swine was the model organism (Casteel et al. 1997). As metabolism is known vary between species, it is imperative to differentiate and evaluate the extent of differences between species. If differences between species are evaluated, identifying patterns and trends between multiple studies across species would provide a larger database which can potential clarify any observed disparity. For example, the mouse AhR is 10 times more sensitive than the human Ahr to TCDD (Flaveny and Perdew 2009) while the swine AhR is comparable to the human AhR for benzo(a)pyrene and TCDD (Lesca et al. 1994).

In terms of tissue discrepancy, CYP enzyme induction has also been found to be dependent upon both tissue and cell type (Iwanari et al. 2002; Shimada et al. 2003; Vondracek et al. 2017). In this thesis, jejunal cells were used to investigate PAH interactions influecning partitioning and metabolism. For PAHs that are orally absorbed, the foremost tissues of concern include the liver, small intestines and large intestines. The liver has the largest capacity for metabolism of PAHs, while the small and large intestines are the first tissues in contact that have an apprepeciable ability to metabolize PAHs (Ding and Kaminsky 2003). Given that PAHs mixtures influence PAH partitioning, the partitioning may illicit a different biochemical response based on tissue type. Therefore, the relative partitioning/metabolic response from multiple tissues would likely provide a more holistic view to further our understanding of PAH exposure.

Overall, fututre directions to improve *in vitro* predictions of *in vivo* PAH soil bioavailability include evaluating complex chemical mixtures naturally present in soil,

differences between animal models regarding exposure to mixtures and lastly, differenes between tissue/cell types to PAH mixtures.

REFERENCES

Androutsopoulos VP, Tsatsakis AM, Spandidos DA. 2009. Cytochrome p450 cyp1a1: Wider roles in cancer progression and prevention. BMC Cancer 9.

Arlt VM, Stiborova M, Henderson CJ, Thiemann M, Frei E, Aimova D, Singh R, Da Costa GG, Schmitz OJ Farmer PB, Wolf CR, Phillips DH. 2008. Metabolic activation of benzo a pyrene *in vitro* by hepatic cytochrome p450 contrasts with detoxification *in vivo*: Experiments with hepatic cytochrome p450 reductase null mice. Carcinogenesis 29:656-665.

ATSDR (Agency for Toxic Substances and Disease Registry). 1995. Toxicological profile for polycyclic aromatic hydrocarbons. Washington:U.S. Department of Health and Human Services.

Autrup H. 1979. Separation of water-soluble metabolites of benzo(a)pyrene formed by cultured human-colon. Biochemical Pharmacology 28:1727-1730.

Band PR, Le ND, Fang R, Deschamps M. 2002. Carcinogenic and endocrine disrupting effects of cigarette smoke and risk of breast cancer. Lancet 360:1044-1049.

Bansal V, Kim KH. 2015. Review of pah contamination in food products and their health hazards. Environment International 84:26-38.

Barranco A, Escudero L, Landaluze JS, Rainieri S. 2017. Detection of exposure effects of mixtures of heavy polycyclic aromatic hydrocarbons in zebrafish embryos. Journal of Applied Toxicology 37:253-264.

Basta NT, Foster JN, Dayton EA, Rodriguez RR, Casteel SW. 2007. The effect of dosing vehicle on arsenic bioaccessibility in smelter-contaminated soils. Journal of Environmental

Science and Health Part a-Toxic/Hazardous Substances & Environmental Engineering 42:1275-1281.

Berridge MV, Tan AS, McCoy KD, Wang R. 1996. The biochemical and cellular basis of cell proliferation assays that use tetrazolium salts. Biochemica 4:14-19.

Berschneider H. 1989. Development of normal cultured small intestinal epithelial cell lines which transport na and cl. Gastroenterology 96:A41.

Bessette EE, Fasco MJ, Pentecost BT, Kaminsky LS. 2005. Mechanisms of arsenite-mediated decreases in benzo k fluoranthene-induced human cytochrome p4501a1 levels in hepg2 cells. Drug Metabolism and Disposition 33:312-320.

Boffetta P, Jourenkova N, Gustavsson P. 1997. Cancer risk from occupational and environmental exposure to polycyclic aromatic hydrocarbons. Cancer Causes & Control 8:444-472.

Bosveld ATC, de Bie PAF, van den Brink NW, Jongepier H, Klomp AV. 2002. *In vitro* erod induction equivalency factors for the 10 pahs generally monitored in risk assessment studies in the netherlands. Chemosphere 49:75-83.

Brandt HCA, Watson WP. 2003. Monitoring human occupational and environmental exposures to polycyclic aromatic compounds. Annals of Occupational Hygiene 47:349-378.

Brosnahan AJ, Brown DR. 2012. Porcine ipec-j2 intestinal epithelial cells in microbiological investigations. Veterinary Microbiology 156:229-237.

Buchet JP, Lauwerys R, Roels H. 1981. Urinary-excretion of inorganic arsenic and its metabolites after repeated ingestion of sodium metaarsenite by volunteers. International Archives of Occupational and Environmental Health 48:111-118.

Budinsky RA, Rowlands JC, Casteel S, Fent G, Cushing CA, Newsted J, Giesy JP, Ruby MV, Aylward LL. 2008. A pilot study of oral bioavailability of dioxins and furans from

contaminated soils: Impact of differential hepatic enzyme activity and species differences. Chemosphere 70:1774-1786.

Buesen R, Mock M, Seidel A, Jacob J, Lampen A. 2002. Interaction between metabolism and transport of benzo a pyrene and its metabolites in enterocytes. Toxicology and Applied Pharmacology 183:168-178.

Buesen R, Mock M, Nau H, Seidel S, Jacob J, Lampen A. 2003. Human intestinal caco-2 cells display active transport of benzo a pyrene metabolites. Chemico-Biological Interactions 142:201-221.

Burgess RM, Lohmann R. 2004. Role of black carbon in the partitioning and bioavailability of organic pollutants. Environmental Toxicology and Chemistry 23:2531-2533.

Busbee DL, Norman JO, Ziprin RL. 1990. Comparative uptake, vascular transport, and cellular internalization of aflatoxin-b1 and benzo(a)pyrene. Archives of Toxicology 64:285-290.

Cachada A, Pereira R, Ferreira da Silva E, Duarte AC. 2014. The prediction of pahs bioavailability in soils using chemical methods: State of the art and future challenges. Science of the Total Environment 472:463-480.

Casteel SW, Cowart RP, Weis CP, Henningsen GM, Hoffman E, Brattin WJ, Guzman RE, Starost MF, Payne JT, Stockham SL, Becker SV, Brexler JW, Turk JR. 1997. Bioavailability of lead to juvenile swine dosed with soil from the smuggler mountain npl site of aspen, colorado. Fundamental and Applied Toxicology 36:177-187.

Cavalieri EL, Rogan EG. 1995. Central role of radical cations in metabolic activation of polycyclic aromatic hydrocarbons. Xenobiotica 25:677-688.

Cave MR, Wragg J, Harrison I, Vane CH, Van de Wiele T, De Groeve E, Nathanail CP, Ashmore M, Thomas R, Robinson J, Daly P. 2010. Comparison of batch mode and

dynamic physiologically based bioaccessibility tests for pahs in soil samples. Environmental Science & Technology 44:2654-2660.

Cave MR, Vane CH, Kim A, Moss-Hayes VL, Wragg J, Richardson CL, Harrison H, Nathanail CP, Thomas R, Wills G. 2014. Measurement and modelling of the ingestion bioaccessibility of polyaromatic hydrocarbons in soils. Environmental Technology & Innovation.

Cavret S, Feidt C. 2005. Intestinal metabolism of par *in vitro* demonstration and study of its impact on pah transfer through the intestinal epithelium. Environmental Research 98:22-32.

CCME (Canandian Council of Ministers of the Environment). 2010. Canadian soil quality guidelines for the protection of environmental and human health: Carcinogenic and other pahs. Winnipeg, Canada.

Cencic A, Langerholc T. 2010. Functional cell models of the gut and their applications in food microbiology a review. International Journal of Food Microbiology 141:S4-S14.

Chiou CT, McGroddy SE, Kile DE. 1998. Partition characteristics of polycyclic aromatic hydrocarbons on soils and sediments. Environmental Science & Technology 32:264-269.

Chun CL, Lee JJ, Park JW. 2002. Solubilization of pah mixtures by three different anionic surfactants. Environmental Pollution 118:307-313.

Cooper DA, Berry DA, Spendel VA, Kiorpes AL, Peters JC. 1997. The domestic pig as a model for evaluating olestra's nutritional effects. Journal of Nutrition 127:S1555-S1565.

Cornelissen G, Gustafsson O, Bucheli TD, Jonker MTO, Koelmans AA, Van Noort PCM. 2005. Extensive sorption of organic compounds to black carbon, coal, and kerogen in sediments

and soils: Mechanisms and consequences for distribution, bioaccumulation, and biodegradation. Environmental Science & Technology 39:6881-6895.

Crampon M, Bureau F, Akpa-Vinceslas M, Bodilis J, Machour N, Le Derf F, Portet-Koltalo F. 2014. Correlations between pah bioavailability, degrading bacteria, and soil characteristics during pah biodegradation in five diffusely contaminated dissimilar soils. Environmental Science and Pollution Research 21:8133-8145.

Cui XY, Xiang P, He RW, Juhasz A, Ma LQ. 2016. Advances in *in vitro* methods to evaluate oral bioaccessibility of pahs and pbdes in environmental matrices. Chemosphere 150:378-389.

Culp SJ, Gaylor DW, Sheldon WG, Goldstein LS, Beland FA. 1998. A comparison of the tumors induced by coal tar and benzo a pyrene in a 2-year bioassay. Carcinogenesis 19:117-124.

Ding XX, Kaminsky LS. 2003. Human extrahepatic cytochromes p450: Function in xenobiotic metabolism and tissue-selective chemical toxicity in the respiratory and gastrointestinal tracts. Annual Review of Pharmacology and Toxicology 43:149-173.

Doledec S, Chessel D. 1994. Co-inertia analysis - an alternative method for studying species environment relationships. Freshwater Biology 31:277-294.

Domingo JL, Nadal M. 2015. Human dietary exposure to polycyclic aromatic hydrocarbons: A review of the scientific literature. Food and Chemical Toxicology 86:144-153.

Dray S, Chessel D, Thioulouse J. 2003. Co-inertia analysis and the linking of ecological data tables. Ecology 84:3078-3089.

Dray S, Dufour AB. 2007. The ade4 package: Implementing the duality diagram for ecologists. Journal of Statistical Software 22:1-20.

Drexler JW, Brattin WJ. 2007. An *in vitro* procedure for estimation of lead relative bioavailability: With validation. Human and Ecological Risk Assessment 13:383-401.

Duan L, Naidu R. 2013. Effect of ionic strength and index cation on the sorption of phenanthrene. Water Air and Soil Pollution 224:1700.

Duan L, Palanisami T, Liu Y, Dong Z, Mallavarapu M, Kuchel T, Semple KT, Naidu R. 2014. Effects of ageing and soil properties on the oral bioavailability of benzo a pyrene using a swine model. Environment International 70:192-202.

Ekstrom C. 2014. Package MESS: Miscellaneous esoteric statistical scripts.

Enell A, Reichenberg F, Ewald G, Warfvinge P. 2005. Desorption kinetics studies on pah-contaminated soil under varying temperatures. Chemosphere 61:1529-1538.

Flaveny CA, Perdew GH. 2009. Transgenic humanized ahr mouse reveals differences between human and mouse ahr ligand selectivity. *Molecular and cellular pharmacology* 1:119-123.

Galarneau E. 2008. Source specificity and atmospheric processing of airborne pahs: Implications for source apportionment. Atmospheric Environment 42:8139-8149.

Galvan N, Teske DE, Zhou GD, Moorthy B, MacWilliams PS, Czuprynski CJ, Jefcoate CR. 2005. Induction of cyp1a1 and cyp1b1 in liver and lung by benzo(a)pyrene and 7,12-dimethylbenz(a)anthracene do not affect distribution of polycyclic hydrocarbons to target tissue: Role of ahr and cyp1b1 in bone marrow cytotoxicity. Toxicology and Applied Pharmacology 202:244-257.

Gilbert D, Mayer P, Pedersen M, Vinggaard AM. 2015. Endocrine activity of persistent organic pollutants accumulated in human silicone implants - dosing *in vitro* assays by partitioning from silicone. Environment International 84:107-114.

Gobas F, McCorquodale JR, Haffner GD. 1993. Intestinal-absorption and biomagnification of organochlorines. Environmental Toxicology and Chemistry 12:567-576.

Gonzalez-Vallina R, Wang H, Zhan RG, Berschneider HM, Lee RM, Davidson NO, Black DD. 1996. Lipoprotein and apolipoprotein secretion by a newborn piglet intestinal cell line (ipec-1). American Journal of Physiology-Gastrointestinal and Liver Physiology 271:G249-G259.

Gouliarmou V, Mayer P. 2012. Sorptive bioaccessibility extraction (sbe) of soils: Combining a mobilization medium with an absorption sink. Environmental Science & Technology 46:10682-10689.

Gouliarmou V, Smith KEC, de Jonge LW, Mayer P. 2012. Measuring binding and speciation of hydrophobic organic chemicals at controlled freely dissolved concentrations and without phase separation. Analytical Chemistry 84:1601-1608.

Gouliarmou V, Collins CD, Christiansen E, Mayer P. 2013. Sorptive physiologically based extraction of contaminated solid matrices: Incorporating silicone rod as absorption sink for hydrophobic organic contaminants. Environmental Science & technology 47:941-948.

Hamel SC, Buckley B, Lioy PJ. 1998. Bioaccessibility of metals in soils for different liquid to solid ratios in synthetic gastric fluid. Environmental Science & Technology 32:358-362.

Hansen T, Borlak J, Bader A. 2000. Cytochrome p450 enzyme activity and protein expression in primary porcine enterocyte and hepatocyte cultures. Xenobiotica 30:27-46.

Hardin JA, Hinoshita F, Sherr DH. 1992. Mechanisms by which benzo a pyrene, an environmental carcinogen, suppresses b-cell lymphopoiesis. Toxicology and Applied Pharmacology 117:155-164.

Harvey RG. 1996. Mechanisms of carcinogenesis of polycyclic aromatic hydrocarbons. Polycyclic Aromatic Compounds 9:1-23.

Hawthorne SB, Grabanski CB, Miller DJ. 2006. Measured partitioning coefficients for parent and alkyl polycyclic aromatic hydrocarbons in 114 historically contaminated sediments: Part 1. K-oc values. Environmental Toxicology and Chemistry 25:2901-2911.

Hessel S, Lampen A. 2010. All-trans retinoic acid enhances the transport of phase ii metabolites of benzo a pyrene by inducing the breast cancer resistance protein expression in caco-2 cells. Toxicology Letters 197:151-155.

Hessel S, John A, Seidel A, Lampen A. 2013. Multidrug resistance-associated proteins are involved in the transport of the glutathione conjugates of the ultimate carcinogen of benzo a pyrene in human caco-2 cells. Archives of Toxicology 87:269-280.

Hurdzan CM, Basta NT, Hatcher PG, Tuovinen OH. 2008. Phenanthrene release from natural organic matter surrogates under simulated human gastrointestinal conditions. Ecotoxicology and Environmental Safety 69:525-530.

Ikegami K, Tagawa K, Narisawa S, Osawa T. 2003. Suitability of the cynomolgus monkey as an animal model for drug absorption studies of oral dosage forms from the viewpoint of gastrointestinal physiology. Biological & Pharmaceutical Bulletin 26:1442-1447.

Ioannides C, Lewis DFV. 2004. Cytochromes p450 in the bioactivation of chemicals. Current Topics in Medicinal Chemistry 4:1767-1788.

Iwanari M, Nakajima M, Kizu R, Hayakawa K, Yokoi T. 2002. Induction of cyp1a1, cyp1a2, and cyp1b1 mrnas by nitropolycyclic aromatic hydrocarbons in various human tissue-derived cells: Chemical-, cytochrome p450 isoform-, and cell-specific differences. Archives of Toxicology 76:287-298.

James K, Peters RE, Laird BD, Ma WK, Wickstrom M, Stephenson GL, Siciliano SD. 2011. Human exposure assessment: A case study of 8 pah contaminated soils using *in vitro* digestors and the juvenile swine model. Environmental Science & Technology 45:4586-4593.

James K, Farrell RE, Siciliano SD. 2012. Comparison of human exposure pathways in an urban brownfield: Reduced risk from paving roads. Environmental Toxicology and Chemistry 31:2423-2430.

James K, Peters RE, Cave MR, Wickstrom M, Lamb EG, Siciliano SD. 2016. Predicting polycyclic aromatic hydrocarbon bioavailability to mammals from incidentally ingested soils using partitioning and fugacity. Environmental Science & Technology 50:1338-1346.

James K, Peters ers RE, Cave MR, Wickstrom M, Siciliano SD. 2018. In vitro prediction of polycyclic aromatic hydrocarbon bioavailability of 14 different incidentally ingested soils in juvenile swine. Science of The Total Environment 618:682-689.

Juhasz AL, Smith E, Weber J, Naidu R, Rees M, Rofe A, Kuchel T, Sansom L. 2008. Effect of soil ageing on *in vivo* arsenic bioavailability in two dissimilar soils. Chemosphere 71:2180-2186.

Juhasz AL, Smith E, Nelson C, Thomas DJ, Bradham K. 2014a. Variability associated with as *in vivo-in vitro* correlations when using different bioaccessibility methodologies. Environmental Science & Technology 48:11646-11653.

Juhasz AL, Weber J, Stevenson G, Slee D, Gancarz D, Rofe A, Smith E. 2014b. *In vivo* measurement, *in vitro* estimation and fugacity prediction of pah bioavailability in post-remediated creosote-contaminated soil. Science of the Total Environment 473:147-154.

Juhasz AL, Tang W, Smith E. 2016. Using *in vitro* bioaccessibility to refine estimates of human exposure to pahs via incidental soil ingestion. Environmental Research 145:145-153.

Kaminsky L. 2006. The role of trace metals in cytochrome p4501 regulation. Drug Metabolism Reviews 38:227-234.

Kamps C, Safe S. 1987. Binding of polynuclear aromatic-hydrocarbons to the rat 4s cytosolic binding-protein - structure-activity-relationships. Cancer Letters 34:129-137.

Kararli TT. 1995. Comparison of the gastrointestinal anatomy, physiology, and biochemistry of humans and commonly used laboratory-animals. Biopharmaceutics & Drug Disposition 16:351-380.

Kawamoto K, MacLeod M, Mackay D. 2001. Evaluation and comparison of multimedia mass balance models of chemical fate: Application of euses and chemcan to 68 chemicals in japan. Chemosphere 44:599-612.

Kelly BC, Gobas F, McLachlan MS. 2004. Intestinal absorption and biomagnification of organic contaminants in fish, wildlife, and humans. Environmental Toxicology and Chemistry 23: 2324-2336.

Kim KH, Jahan SA, Kabir E, Brown RJC. 2013. A review of airborne polycyclic aromatic hydrocarbons (pahs) and their human health effects. Environment International 60:71-80.

Kramer NI, Busser FJM, Oosterwijk MTT, Schirmer K, Escher BI, Hermens JLM. 2010. Development of a partition-controlled dosing system for cell assays. Chemical Research in Toxicology 23:1806-1814.

Laher JM, Chernenko GA, Barrowman JA. 1983. Studies of the absorption and enterohepatic circulation of 7,12-dimethylbenz a anthracene in the rat. Canadian Journal of Physiology and Pharmacology 61:1368-1373.

Laird BD, Van de Wiele TR, Corriveau MC, Jamieson HE, Parsons MB, Verstraete W, Siciliano SD. 2007. Gastrointestinal microbes increase arsenic bioaccessibility of ingested mine tailings using the simulator of the human intestinal microbial ecosystem. Environmental Science & Technology 41:5542-5547.

Lamb EG, Shirtliffe SJ, May WE. 2011. Structural equation modeling in the plant sciences: An example using yield components in oat. Canadian Journal of Plant Science 91:603-619.

Lampen A, Ebert B, Stumkat L, Jacob J, Seidel A. 2004. Induction of gene expression of xenobiotic metabolism enzymes and abc-transport proteins by pah and a reconstituted pah mixture in human caco-2 cells. Biochimica Et Biophysica Acta-Gene Structure and Expression 1681:38-46.

Langerholc T, Maragkoudakis PA, Wollgast J, Gradisnik L, Cencic A. 2011. Novel and established intestinal cell line models - an indispensable tool in food science and nutrition. Trends in Food Science & Technology 22:S11-S20.

Larsson M, Orbe D, Engwall M. 2012. Exposure time-dependent effects on the relative potencies and additivity of pahs in the ah receptor-based h4iie-luc bioassay. Environmental Toxicology and Chemistry 31:1149-1157.

Lesca P, Witkamp R, Maurel P, Galtier P. 1994. The pig as a model for studying ah receptor and other pah-binding proteins inman. Biochemical and Biophysical Research Communications 200:475-481.

Li A, Jang JK, Scheff PA. 2003. Application of epa cmb8.2 model for source apportionment of sediment pahs in lake calumet, chicago. Environmental Science & Technology 37:2958-2965.

Li C, Cui XY, Fan YY, Teng Y, Nan ZR, Ma LQ. 2015. Tenax as sorption sink for *in vitro* bioaccessibility measurement of polycyclic aromatic hydrocarbons in soils. Environmental Pollution 196:47-52.

Liu G, Bi RT, Wang SJ, Li FS, Guo GL. 2013. The use of spatial autocorrelation analysis to identify pahs pollution hotspots at an industrially contaminated site. Environmental Monitoring and Assessment 185:9549-9558.

Mackay D. 1979. Finding fugacity feasible. Environmental Science & Technology 13 (10): 1218-1223.

Mackay D, Patterson S. 1981. Calculating fugacity. Environmental Science & Technology 15 (9): 1006-1014.

Mackay D, Patterson S. 1982. Fugacity revisited - The fugacity approach to environmental transport. Environmental Science & Technology 16 (12): A654-A660.

Mackay D, Fraser A. 2000. Bioaccumulation of persistent organic chemicals: Mechanisms and models. Environmental Pollution 110:375-391.

Mackay D. 2001. Multimedia environmental models : The fugacity approach. Boca Raton, Florida.

Mackay D. 2004. Finding fugacity feasible, fruitfulm and fun. Enivronmental Toxicology and Chemistry 23: 2282-2289.

Mackay D, Shiu W, Ma K, Lee S, Shiu WY, Ma KC, Lee SC. 2006. In Handbook of physical-chemical properties and environmental fate for organic chemicals. Lewis/CRC: Boca Raton, Florida, 2001.

MacLeod M, Mackay D. 1999. An assessment of the environmental fate and exposure of benzene and the chlorobenzenes in canada. Chemosphere 38:1777-1796.

MacLeod M, Woodfine DG, Mackay D, McKone T, Bennett D, Maddalena R. 2001. BETR north america: A regionally segmented multimedia contaminant fate model for north america. Environmental Science and Pollution Research 8: 156.

Madsen JL. 1992. Effects of gender, age, and body-mass index on gastrointestinal transit times. Digestive Diseases and Sciences 37:1548-1553.

Mariani V, Palermo S, Fiorentini S, Lanubile A, Giuffra E. 2009. Gene expression study of two widely used pig intestinal epithelial cell lines: IPEC-J2 and IPI-2I. Veterinary Immunology and Immunopathology 131:278-284.

Marriott PJ, Carpenter PD, Brady PH, McCormick MJ, Griffiths AJ, Hatvani TSG, Rasdell SG. 1993. Optimization of fluorescence detection for polyaromatic hydrocarbon determination by using high-performance liquid-chromatography. Journal of Liquid Chromatography 16:3229-3247.

Mathieu MC, Lapierre I, Brault K, Raymond M. 2001. Aromatic hydrocarbon receptor (AhR) ·AhR nuclear translocator- and p53-mediated induction of the murine multidrug resistance mdr1 gene by 3-methylcholanthrene and benzo(a)pyrene in hepatoma cells. Journal of Biological Chemistry 276:4819-4827.

Merchant M, Wang X, Kamps C, Rosengren R, Morrison V, Safe S. 1992. Mechanism of benzo a pyrene-induced cyp1a-1 gene-expression in mouse hepa 1c1c7 cells - role of the nuclear 6s-protein and 4s-protein. Archives of Biochemistry and Biophysics 292:250-257.

Miller ER, Ullrey DE. 1987. The pig as a model for human-nutrition. Annual Review of Nutrition 7:361-382.

Minekus M, Marteau P, Havenaar R, Huisintveld JHJ. 1995. A multicompartmental dynamic computer-controlled model simulating the stomach and small-intestine. Atla-Alternatives to Laboratory Animals 23:197-209.

Minhas JK, Vasiluk L, Pinto LJ, Gobas F, Moore MM. 2006. Mobilization of chrysene from soil in a model digestive system. Environmental Toxicology and Chemistry 25:1729-1737.

Miyata M, Furukawa M, Takahashi K, Gonzalez FJ, Yamazoe Y. 2001. Mechanism of 7,12-dimethylbenz alpha anthracene-induced immunotoxicity: Role of metabolic activation at the target organ. Japanese Journal of Pharmacology 86:302-309.

Nebert DW, Dieter MZ. 2000. The evolution of drug metabolism. Pharmacology 61:124-135.

Oomen AG, Sips A, Groten JP, Sijm D, Tolls J. 2000. Mobilization of pcbs and lindane from soil during *in vitro* digestion and their distribution among bile salt micelles and proteins of human digestive fluid and the soil. Environmental Science & Technology 34:297-303.

Oomen AG, Tolls J, Kruidenier M, Bosgra SSD, Sips A, Groten JP. 2001. Availability of polychlorinated biphenyls (pcbs) and lindane for uptake by intestinal caco-2 cells. Environmental Health Perspectives 109:731-737.

Oomen AG, Hack A, Minekus M, Zeijdner E, Cornelis C, Schoeters G, Verstraete W, Van dde Wiele T, Wragg J, Rompleberg CJM, Sips A, Van Wijnen JH. 2002. Comparison of five *in vitro* digestion models to study the bioaccessibility of soil contaminants. Environmental Science & Technology 36:3326-3334.

Osborne JW, Waters E. 2002. Four assumptions of multiple regression that researchers should always test.Practical Assessment, Research and Evaluation 8:1-9.

Page DS, Boehm PD, Douglas GS, Bence AE, Burns WA, Mankiewicz PJ. 1999. Pyrogenic polycyclic aromatic hydrocarbons in sediments record past human activity: A case study in prince william sound, alaska. Marine Pollution Bulletin 38:247-260.

Patterson JK, Lei XG, Miller DD. 2008. The pig as an experimental model for elucidating the mechanisms governing dietary influence on mineral absorption. Experimental Biology and Medicine 233:651-664.

Penning TM, Burczynski ME, Hung CF, McCoull KD, Palackal NT, Tsuruda LS. 1999. Dihydrodiol dehydrogenases and polycyclic aromatic hydrocarbon activation: Generation of reactive and redox active o-quinones. Chemical Research in Toxicology 12:1-18.

Peters RE, Wickstrom M, Siciliano SD. 2015. The bioavailability of polycyclic aromatic hydrocarbons from different dose media after single and sub-chronic exposure in juvenile swine. Science of the Total Environment 506:308-314.

Phillips DH. 1999. Polycyclic aromatic hydrocarbons in the diet. Mutation Research-Genetic Toxicology and Environmental Mutagenesis 443:139-147.

Pignatello JJ, Xing BS. 1996. Mechanisms of slow sorption of organic chemicals to natural particles. Environmental Science & Technology 30:1-11.

Piskorska-Pliszczynska J, Keys B, Safe S, Newman MS. 1986. The cytosolic receptor-binding affinities and ahh induction potencies of 29 polynuclear aromatic-hydrocarbons. Toxicology Letters 34:67-74.

Prak DJL, Pritchard PH. 2002. Solubilization of polycyclic aromatic hydrocarbon mixtures in micellar nonionic surfactant solutions. Water Research 36:3463-3472.

R Core Team. 2013. R: A language and environment for statistical computing. Vienna, Austria:R Foundation for Statistical Computing.

Rahman A, Barrowman JA, Rahimtula A. 1986. The influence of bile on the bioavailability of polynuclear aromatic-hydrocarbons from the rat intestine. Canadian Journal of Physiology and Pharmacology 64:1214-1218.

Raha A, Reddy V, Houser W, Bresnick E. 1990. Binding characteristics of 4s pah-binding protein and ah receptor from rats and mice. Journal of Toxicology and Environmental Health 29:339-355.

Ramesh A, Walker SA, Hood DB, Guillen MD, Schneider K, Weyand EH. 2004. Bioavailability and risk assessment of orally ingested polycyclic aromatic hydrocarbons. International Journal of Toxicology 23:301-333.

Ravindra K, Wauters E, Van Grieken R. 2008. Variation in particulate pahs levels and their relation with the transboundary movement of the air masses. Science of the Total Environment 396:100-110.

Rees M, Sansom L, Rofe A, Juhasz AL, Smith E, Weber J, Naidu R, Kuchel T. 2009. Principles and application of an *in vivo* swine assay for the determination of arsenic bioavailability in contaminated matrices. Environmental Geochemistry and Health 31:167-177.

Reichenberg F, Mayer P. 2006. Two complementary sides of bioavailability: Accessibility and chemical activity of organic contaminants in sediments and soils. Environmental Toxicology and Chemistry 25:1239-1245.

Richardson GM, Bright DA, Dodd M. 2006. Do current standards of practice in canada measure what is relevant to human exposure at contaminated sites? Ii: Oral bioaccessibility of contaminants in soil. Human and Ecological Risk Assessment 12:606-616.

Roberts SM, Munson JW, Lowney YW, Ruby MV. 2007. Relative oral bioavailability of arsenic from contaminated soils measured in the cynomolgus monkey. Toxicological Sciences 95:281-288.

Roos PH, Tschirbs S, Welge P, Hack A, Theegarten D, Mogilevski G, Wilhelm M. 2002. Induction of cytochrome p450 1a1 in multiple organs of minipigs after oral exposure to soils contaminated with polycyclic aromatic hydrocarbons (PAH). Archives of Toxicology 76:326-334.

Rosseel Y. 2012. Lavaan: An r package for structural equation modeling. Journal of Statistical Software 48:1-36.

Rowlands JC, Gustafsson JA. 1997. Aryl hydrocarbon receptor-mediated signal transduction. Critical Reviews in Toxicology 27:109-134.

Ruby MV, Davis A, Link TE, Schoof R, Chaney RL, Freeman GB, Bergstrom P. 1993. Development of an in-vitro screening-test to evaluate the in-vivo bioaccessibility of ingested mine-waste lead. Environmental Science & Technology 27:2870-2877.

Ruby MV, Davis A, Schoof R, Eberle S, Sellstone CM. 1996. Estimation of lead and arsenic bioavailability using a physiologically based extraction test. Environmental Science & Technology 30:422-430.

Ruby MV, Schoof R, Brattin W, Goldade M, Post G, Harnois M, Mosby DE, Casteel SW, Berti W, Carpenter M, Edwards D, Cragin D, Chappell W. 1999. Advances in evaluating the oral bioavailability of inorganics in soil for use in human health risk assessment. Environmental Science & Technology 33:3697-3705.

Ruby MV, Fehling KA, Paustenbach DJ, Landenberger BD, Holsapple MP. 2002. Oral bioaccessibility of dioxins/furans at low concentrations (50-350 ppt toxicity equivalent) in soil. Environmental Science & Technology 36:4905-4911.

Ruby MV, Lowney YW, Bunge AL, Roberts SM, Gomez-Eyles JL, Ghosh U, Kissel JC, Tomlinson P, Menzie C. 2016. Oral bioavailability, bioaccessibility, and dermal absorption of pahs from soil-state of the science. Environmental Science & Technology 50:2151-2164.

Schierack P, Nordhoff M, Pollmann M, Weyrauch KD, Amasheh S, Lodemann U, Jores J, Tachu B, Kleta S, Blikslager A, Tedin K, Wieler LH. 2006. Characterization of a porcine intestinal epithelial cell line for *in vitro* studies of microbial pathogenesis in swine. Histochemistry and Cell Biology 125:293-305.

Schreiber R, Altenburger R, Paschke A, Kuster E. 2008. How to deal with lipophilic and volatile organic substances in microtiter plate assays. Environmental Toxicology and Chemistry 27:1676-1682.

Schroder JL, Basta NT, Casteel SW, Evans TJ, Payton ME, Si J. 2004. Validation of the *in vitro* gastrointestinal (ivg) method to estimate relative bioavailable lead in contaminated soils. Journal of Environmental Quality 33:513-521.

Semple KT, Morriss AWJ, Paton GI. 2003. Bioavailability of hydrophobic organic contaminants in soils: Fundamental concepts and techniques for analysis. European Journal of Soil Science 54:809-818.

Sergent T, Ribonnet L, Kolosova A, Garsou S, Schaut A, De Saeger S, Van Peteghem C, Larondelle Y, Pussemier L, Schneider Y. 2008. Molecular and cellular effects of food

contaminants and secondary plant components and their plausible interactions at the intestinal level. Food and Chemical Toxicology 46:813-841.

Shimada T, Sugie A, Shindo M, Nakajima T, Azuma E, Hashimoto M, Inoue K. 2003. Tissue-specific induction of cytochromes p450 1a1 and 1b1 by polycyclic aromatic hydrocarbons and polychlorinated biphenyls in engineered c57bl/6j mice of arylhydrocarbon receptor gene. Toxicology and Applied Pharmacology 187:1-10.

Shimada T, Guengerich FP. 2006. Inhibition of human cytochrome p450 1a1-, 1a2-, and 1b1-mediated activation of procarcinogens to genotoxic metabolites by polycyclic aromatic hydrocarbons. Chemical Research in Toxicology 19:288-294.

Shimada T, Muryama N, Tanaka K, Takenaka S, Imai Y, Hopkins NE, Foroozesh MK, Alworth WL, Yamazaki H, Guengerich FP, Komori M. 2008. Interaction of polycyclic aromatic hydrocarbons with human cytochrome p450 1b1 in inhibiting catalytic activity. Chemical Research in Toxicology 21:2313-2323.

Siciliano SD, James K, Zhang GY, Schafer AN, Peak JD. 2009. Adhesion and enrichment of metals on human hands from contaminated soil at an arctic urban brownfield. Environmental Science & Technology 43:6385-6390.

Singh R, Sram RJ, Binkova B, Kalina I, Popov TA, Georgieva T, Garte S, Taioli E, Farmer PB. 2007. The relationship between biomarkers of oxidative dna damage, polycyclic aromatic hydrocarbon dna adducts, antioxidant status and genetic susceptibility following exposure to environmental air pollution in humans. Mutation Research-Fundamental and Molecular Mechanisms of Mutagenesis 620:83-92.

Smith E, Kempson IM, Juhasz AL, Weber J, Rofe A, Gancarz D, Naidu R, McLaren RG, Graefe M. 2011. *In vivo-in vitro* and xanes spectroscopy assessments of lead bioavailability in contaminated periurban solis. Environmental Science & Technology 45:6145-6152.

Spink DC, Katz BH, Hussain MM, Spink BC, Wu SJ, Liu N, Pause R, Kaminsky LS. 2002. Induction of cyp1a1 and cyp1b1 in t-47d human breast cancer cells by benzo a pyrene is diminished by arsenite. Drug Metabolism and Disposition 30:262-269.

Spink DC, Wu SJ, Spink BC, Hussain MM, Vakhania DD, Pentecost BT, Kaminsky LS. 2008. Induction of cyp1a1 and cyp1b1 by benzo(k)fluoranthene and benzo(a)pyrene in t-47d human breast cancer cells: Roles of pah interactions and pah metabolites. Toxicology and Applied Pharmacology 226:213-224.

Tang L, Tang XY, Zhu YG, Zheng MH, Miao QL. 2005. Contamination of polycyclic aromatic hydrocarbons (pahs) in urban soils in beijing, china. Environment International 31:822-828.

Tang XY, Tang L, Zhu YG, Xing BS, Duan J, Zheng MH. 2006. Assessment of the bioaccessibility of polycyclic aromatic hydrocarbons in soils from beijing using an *in vitro* test. Environmental Pollution 140:279-285.

Tanneberger K, Rico-Rico A, Kramer NI, Busser FJM, Hermens JLM, Schirmer K. 2010. Effects of solvents and dosing procedure on chemical toxicity in cell-based *in vitro* assays. Environmental Science & Technology 44:4775-4781.

Tarantini A, Maitre A, Lefebvre E, Marques M, Rajhi A, Douki T. 2011. Polycyclic aromatic hydrocarbons in binary mixtures modulate the efficiency of benzo a pyrene to form dna adducts in human cells. Toxicology 279:36-44.

Thioulouse J. 2011. Simultaneous analysis of a sequence of paired ecological tables: A comparison of several methods. Annals of Applied Statistics 5:2300-2325.

Tilston EL, Gibson GR, Collins CD. 2011a. Colon extended physiologically based extraction test (ce-pbet) increases bioaccessibility of soil-bound pah. Environmental Science & Technology 45:5301-5308.

Tilston EL, Gibson GR, Collins CD. 2011b. Colon extended physiologically based extraction test (ce-pbet) increases bioaccessibility of soil-bound pah. Environmental Science & Technology 45:5301-5308.

Tobiszewski M, Namiesnik J. 2012. Pah diagnostic ratios for the identification of pollution emission sources. Environmental Pollution 162:110-119.

Toose L, Woodfine DG, MacLeod M, Mackay D, Gouin J. 2004. Betr-world: A geographically explicit model of chemical fate: Application to transport of alpha-hch to the arctic. Environmental Pollution 128:223-240.

Topinka J, Marvanova S, Vondracek J, Sevastyanova O, Novakova Z, Krcmar P, Pencikova K, Machala M. 2008. Dna adducts formation and induction of apoptosis in rat liver epithelial 'stem-like' cells exposed to carcinogenic polycyclic aromatic hydrocarbons. Mutation Research-Fundamental and Molecular Mechanisms of Mutagenesis 638:122-132.

Uno S, Dalton TP, Derkenne S, Curran CP, Miller ML, Shertzer HG, Nebert DW. 2004. Oral exposure to benzo a pyrene in the mouse: Detoxication by inducible cytochrome p450 is more important than metabolic activation. Molecular Pharmacology 65:1225-1237.

Vakharia DD, Liu N, Pause R, Fasco M, Bessette E, Zhang QY, Kaminsky LS. 2001. Polycyclic aromatic hydrocarbon/metal mixtures: Effect on pah induction of cyp1a1 in human hepg2 cells. Drug Metabolism and Disposition 29:999-1006.

Van de Wiele TR, Verstraete W, Siciliano SD. 2004. Polycyclic aromatic hydrocarbon release from a soil matrix in the *in vitro* gastrointestinal tract. Journal of Environmental Quality 33:1343-1353.

Van de Wiele TR, Oomen AG, Wragg J, Cave M, Minekus M, Hack A, Cornelis C, Rompelberg CJM, De Zwart LL, Klinck B, Van Wijen J, Verstraete W, Sips A. 2007. Comparison of five *in vitro* digestion models to *in vivo* experimental results: Lead bioaccessibility in the human gastrointestinal tract. Journal of Environmental Science & Health Part a-Toxic/Hazardous Substances & Environmental Engineering 42:1203-1211.

Van Grevenynghe J, Rion S, Le Ferrec E, Le Vee M, Amiot L, Fauchet R, Fardel O. 2003. Polycyclic aromatic hydrocarbons inhibit differentiation of human monocytes into macrophages. Journal of Immunology 170:2374-2381.

Van Schooten FJ, Moonen EJC, vanderWal L, Levels P, Kleinjans JCS. 1997. Determination of polycyclic aromatic hydrocarbons (pah) and their metabolites in blood, feces, and urine of rats orally exposed to pah contaminated soils. Archives of Environmental Contamination and Toxicology 33:317-322.

Vasiluk L, Pinto LJ, Walji ZA, Tsang WS, Gobas F, Eickhoff C, Moore MM. 2007. Benzo a pyrene bioavailability from pristine soil and contaminated sediment assessed using two *in vitro* models. Environmental Toxicology and Chemistry 26:387-393.

Venables WN, Ripley BD. 2002. Random and mixed effects. In: Modern applied statistics with s:Springer, 271-300.

Vergauwen H. 2015. The ipec-j2 cell line. In: The impact of food bioactives on health:Springer, 125-134.

Vergauwen H, Tambuyzer B, Jennes K, Degroote J, Wang W, De Smet S, Michiels J, Van Ginneken C. 2015. Trolox and ascorbic acid reduce direct and indirect oxidative stress in the ipec-j2 cells, an *in vitro* model for the porcine gastrointestinal tract. Plos One 10.

Versantvoort C, Rompelberg C. 2004. Development and applicability of an *in vitro* digestion model in assessing the bioaccessibility of contaminants from food. RIVM rapport 320102002.

Vondracek J, Pencikova K, Neca J, Ciganek M, Grycova A, Dvorak Z, Machala M. 2017. Assessment of the aryl hydrocarbon receptor-mediated activities of polycyclic aromatic hydrocarbons in a human cell-based reporter gene assay. Environmental Pollution 220:307-316.

Voparil IM, Mayer LM, Place AR. 2003. Interactions among contaminants and nutritional lipids during mobilization by digestive fluids of marine invertebrates. Environmental Science & Technology 37:3117-3122.

Wania F, Breivik K, Persson NJ, McLachlan MS. 2006. Cozmo-pop 2 - a fugacity-based dynamic multi-compartmental mass balance model of the fate of persistent organic pollutants. Environmental Modelling & Software 21:868-884.

White JC, Kelsey JW, Hatzinger PB, Alexander M. 1997. Factors affecting sequestration and bioavailability of phenanthrene in soils. Environmental Toxicology and Chemistry 16:2040-2045.

White JC, Alexander M, Pignatello JJ. 1999. Enhancing the bioavailability of organic compounds sequestered in soil and aquifer solids. Environmental Toxicology and Chemistry 18:182-187.

White KL, Lysy HH, Holsapple MP. 1985. Immunosuppression by polycyclic aromatic-hydrocarbons - a structure-activity relationship in b6c3f1 and dba/2 mice. Immunopharmacology 9:155-164.

Wilcke W. 2000. Polycyclic aromatic hydrocarbons (pahs) in soil - a review. Journal of Plant Nutrition and Soil Science-Zeitschrift Fur Pflanzenernahrung Und Bodenkunde 163:229-248.

Wild SR, Jones KC. 1995. Polynuclear aromatic-hydrocarbons in the united-kingdom environment - a preliminary source inventory and budget. Environmental Pollution 88:91-108.

Willett KL, Wassenberg D, Lienesch L, Reichert W, Di Giulio RT. 2001. In vivo and in vitro inhibition of CYP1A-dependent activity in Fundulus heteroclitus by the polynuclear aromatic hydrocarbon fluoranthene. Toxicology and Applied Pharmacology 177:264-271.

Wu SJ, Spink DC, Spink BC, Kaminsky LS. 2003. Quantitation of cyp1a1 and 1b1 mrna in polycyclic aromatic hydrocarbon-treated human t-47d and hepg2 cells by a modified bdna assay using fluorescence detection. Analytical Biochemistry 312:162-166.

Yebra-Pimentel I, Fernandez-Gonzalez R, Martinez-Carballo E, Simal-Gandara J. 2015. A critical review about the health risk assessment of pahs and their metabolites in foods. Critical Reviews in Food Science and Nutrition 55:1383-1405.

Yunker MB, Macdonald RW, Vingarzan R, Mitchell RH, Goyette D, Sylvestre S. 2002. Pahs in the fraser river basin: A critical appraisal of pah ratios as indicators of pah source and composition. Organic Geochemistry 33:489-515.

Zhang J, Sequaris JM, Narres HD, Vereecken H, Klumpp E. 2010. Effect of organic carbon and mineral surface on the pyrene sorption and distribution in yangtze river sediments. Chemosphere 80:1321-1327.

Zhang XL, Tao S, Liu WX, Yang Y, Zuo Q, Liu SZ. 2005. Source diagnostics of polycyclic aromatic hydrocarbons based on species ratios: A multimedia approach. Environmental Science & Technology 39:9109-9114.

APPENDIX A

CHAPTER 3 SUPPLEMENTAL INFORMATION

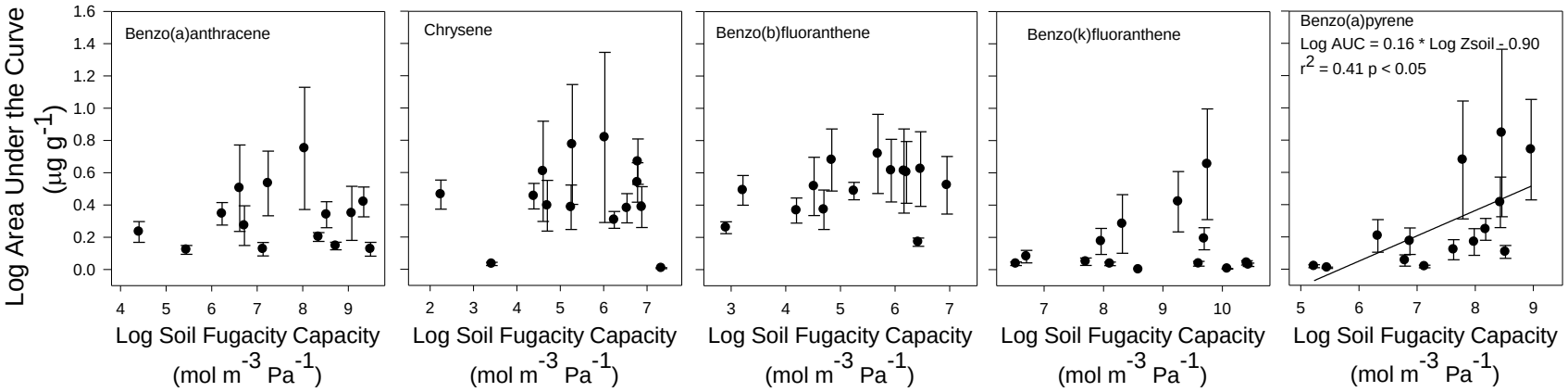

Figure A1. Comparison between Area under the Curve (µg PAHs recovered in plasma per gram of soil over a 48 hour time period) and soil fugacity capacity of five PAHs. Data points represent the average (n = 6) and error bars represent the standard error of the mean for Area under the Curve.

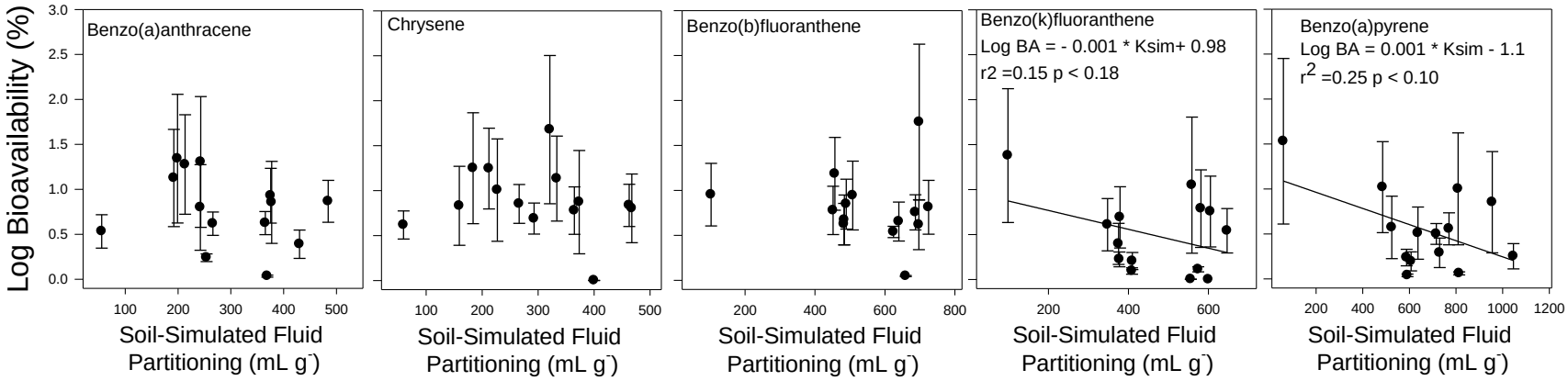

Figure A2. Comparison of the bioavailability for 5 PAHs against partitioning into simulated fluids for 14 soils historically contaminated with petroleum hydrocarbons. Data points represent the mean (n =6) of mammalian bioavailability and (n=3) estimates of K_{sim}. Bioavailability was calculated as the quotient of Area under the Curve (μg PAHs recovered in plasma per gram of soil over a 48 hour time period) divided by the total amount of PAHs in the dosed soil. Error bars represent the standard error of the mean and were obscured for K_{sim}.

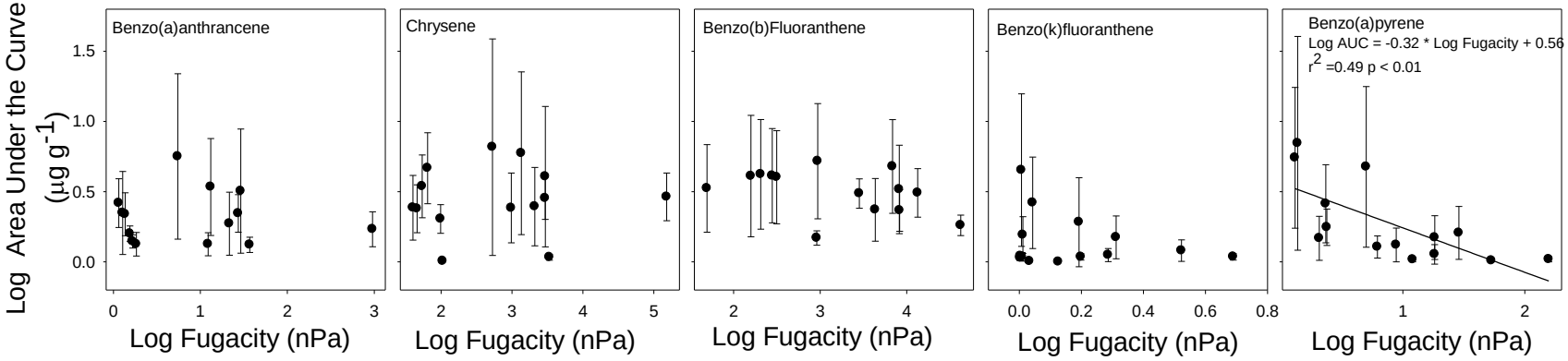

Figure A3. Comparison between Area under the Curve (µg PAHs recovered in plasma per gram of soil over a 48 hour time period) and fugacity of five polyaromatic hydrocarbons. Fugacity units are reported in nano-fugacity or 10^{-9} Pa and was calculated from soil concentration and soil fugacity capacity. Data points represent the average (n = 6) and error bars represent the standard error of the mean for Area under the Curve.

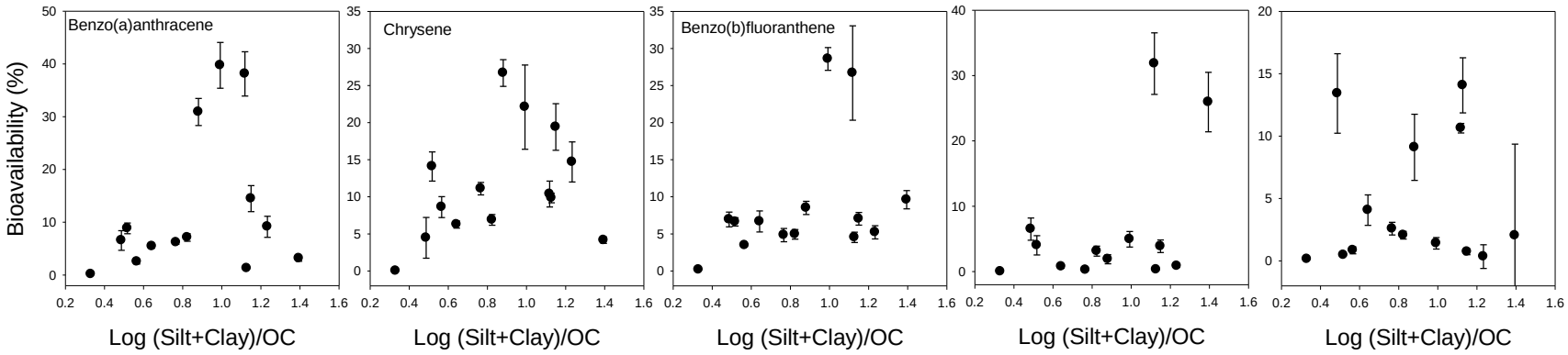

Figure A4. Correlation between bioavailability and (Silt + Clay)/TOC in soils for five PAHs. Bioavailability was calculated as the quotient of Area under the Curve (μg polyaromatic hydrocarbons recovered in plasma per gram of soil over a 48 hour time period) divided by the total amount of polyaromatic hydrocarbons in the dosed soil.

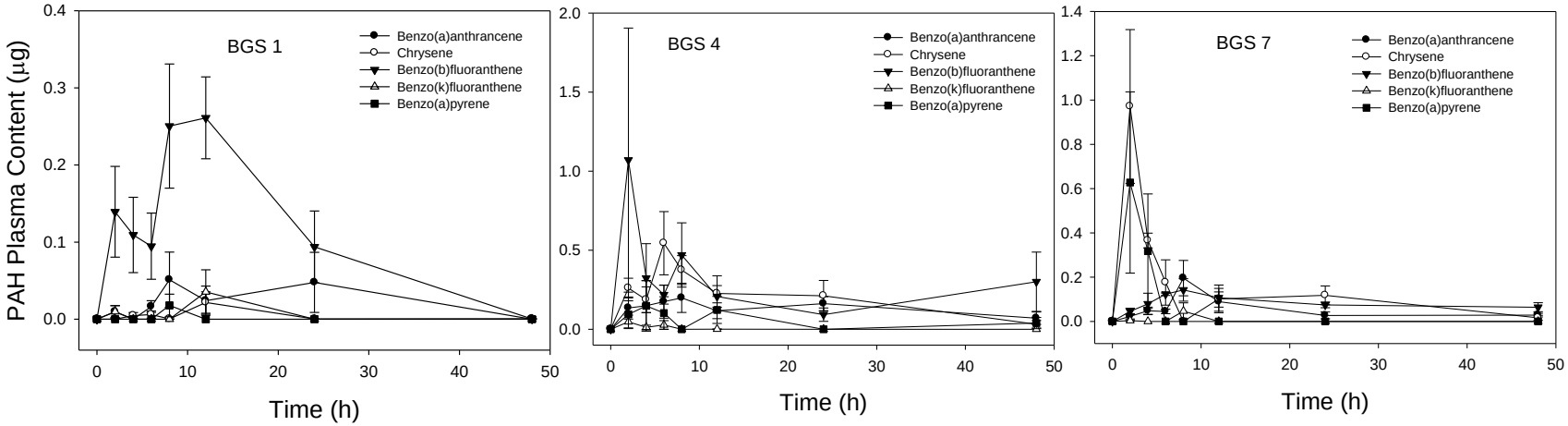

Figure A5. Time course of PAH plasma concentration following oral ingestion of three PAH contaminated soils over 48 hours

Table A1. Physiochemical properties and additional PAH bioavailability of soils used in this study

Soil	Soil Concentration (µg/g)						Bioavailability (%)					
	ANT[1]	FLU[1]	PYR[1]	DIB[1]	B(g)P[1]	IND[1]	ANT[1]	FLU[1]	PYR[1]	DIB[1]	B(g)P[1]	IND[1]
BGS1	1.6	1.2	2.7	ND	3.1	1.0	16	12	13	-	20	0
BGS2	11	53	76	47	48	35	1.7	0.3	0.07	0	0.06	0
BGS3	11	69	77	40	37	35	5.2	1.0	0.5	9.9	-	0
BGS4	11	149	125	61	64	48	55	3.9	4.1	1.5	2.0	3.2
BGS5	5.7	88	53	20	23	22	31	4.2	14	2.7	2.2	4.1
BGS6	4.9	63	56	21	25	20	33	2.5	5.3	0.1	0.6	4.3
BGS7	3.3	28	23	14	18	18	38	30.9	25	9.9	0.7	2.1
BGS8	4.1	121	76	24	28	30	87	2.5	10	0.1	0.9	17
BGS9	2.7	30	32	20	25	19	14	0	9.7	0.8	1.1	0
BGS10	17	289	300	32	49	37	16	1.7	2.3	0.06	0.3	0.3
BGS11	11	136	184	41	46	39	16	2.6	2.2	1.8	2.2	0.1
BGS12	140	758	582	170	166	125	0.2	0	0.2	0	0.07	0
WP1	27	213	117	7.0	5.7	5.6	24	0.3	1.2	9.3	14	2.6
GW2	1	5.5	4.6	7.4	4.3	2.2	85	39.7	7.4	0	30	16
COT1	0.01	ND	0.02	ND	0.04	ND	100	-	100	-	100	-
COT2	0.01	0.01	0.02	ND	ND	ND	100	100	100	-	-	-
COT3	ND	ND	0.05	ND	ND	ND	-	-	100	-	-	-
COT4	0.01	0.01	<LOQ	ND	0.01	ND	100	0	-	-	100	-
COT5	0.01	ND	ND	ND	0.01	ND	100	-	-	-	0	-
Average[2]	18	143	122	39	39	31	30	7.3	6.8	2.8	6.3	3.5
Geometric Mean[2]	7	62	59	27	24	19	15	3.0	3.0	1.1	1.6	2.5
Standard Deviation[2]	36	195	154	43	41	31	27	12	7.1	4.0	14	5.6

[1]Abbreviations are as follows: ANT is anthracene, FLU is fluoranthene, PYR is pyrene, DIB is dibenzo(ah)anthracene, B(g)P is benzo(ghi)perylene, and IND is indeno(123-cd)pyrene

[2]The average, geometric mean and standard deviation values for bioavailability do not include the 5 COT soils

ND indicates a non-detection of PAH in soil

<LOQ indicates a value below the limit of quantification

Table A2. Log Soil-Water Partitioning Coefficients (K_d) of PAHs between Soils

Soil	ANT[1]	FLU[1]	PYR[1]	B(a)A[1]	CHR[1]	B(b)F[1]	B(k)F[1]	B(a)P[1]	DIB[1]	B(g)P[1]	IND[1]
BGS 1	2.24 (0.06)	1.65 (0.03)	1.74 (0.03)	1.51 (0.03)	1.49 (0.02)	1.55 (0.03)	1.52 (0.02)	1.55 (0.03)	NA	1.68 (0.04)	1.66 (0.02)
BGS 2	3.96 (0.11)	3.87 (0.11)	3.09 (3.27)	3.17 (0.09)	3.31 (1.09)	3.57 (0.09)	3.39 (0.12)	3.72 (0.18)	4.08 (0.02)	4.02 (0.18)	3.45 (0.04)
BGS 3	1.28 (0.04)	1.76 (0.09)	4.81 (0.09)	4.57 (0.07)	4.59 (0.06)	4.53 (0.13)	4.50 (0.07)	4.27 (0.07)	1.05 (0.16)	4.60 (0.05)	4.23 (0.14)
BGS 4	3.78 (0.21)	4.82 (0.01)	4.71 (0.02)	5.38 (0.12)	4.84 (0.28)	4.79 (0.15)	5.22 (0.07)	4.52 (0.04)	NA	5.37 (0.11)	4.17 (1.13)
BGS 5	2.92 (0.04)	2.62 (0.01)	2.51 (0.05)	2.66 (0.02)	2.66 (0.04)	2.84 (0.03)	2.76 (0.06)	2.88 (0.03)	3.00 (0.09)	2.85 (0.01)	2.83 (0.02)
BGS 6	0.66 (0.03)	4.44 (0.07)	4.58 (0.11)	4.39 (0.01)	4.30 (0.01)	4.25 (0.08)	4.41 (0.11)	4.07 (0.13)	NA	4.67 (0.13)	4.20 (0.36)
BGS 7	2.98 (0.12)	2.53 (0.09)	2.21 (0.09)	2.27 (0.09)	2.45 (0.09)	2.52 (0.08)	2.51 (0.10)	2.42 (0.12)	2.76 (0.11)	2.72 (0.09)	2.64 (0.06)
BGS 8	3.33 (0.23)	3.40 (0.08)	3.34 (0.06)	3.29 (0.10)	3.33 (0.10)	3.16 (0.24)	3.12 (0.29)	3.22 (0.34)	4.29 (0.54)	3.92 (0.39)	3.54 (0.23)
BGS 9	3.49 (0.30)	3.30 (0.12)	3.32 (0.15)	2.76 (0.23)	2.76 (0.21)	3.02 (0.14)	2.91 (0.13)	2.97 (0.10)	3.13 (0.11)	3.22 (0.11)	3.17 (0.09)
BGS 10	4.11 (0.16)	4.67 (0.16)	4.47 (0.16)	4.08 (0.23)	4.08 (0.22)	4.01 (0.21)	4.06 (0.16)	3.88 (0.07)	4.55 (0.15)	4.56 (0.04)	0.72 (0.06)
BGS 11	4.19 (0.16)	4.59 (0.07)	4.63 (0.08)	4.77 (0.11)	4.84 (0.12)	5.27 (0.14)	5.24 (0.14)	5.05 (0.13)	NA	0.40 (0.15)	NA
BGS 12	5.94 (0.57)	5.32 (0.09)	5.35 (0.14)	5.53 (0.11)	5.39 (0.11)	4.75 (0.09)	4.89 (0.14)	4.61 (0.26)	5.00 (0.28)	5.09 (0.26)	5.44 (0.50)
WP1	4.46 (0.08)	3.02 (0.04)	5.53 (0.06)	5.12 (0.26)	4.94 (0.22)	4.49 (0.35)	4.55 (0.43)	4.55 (0.23)	NA	NA	NA
GW5	4.02 (0.06)	0.65 (0.07)	0.52 (0.03)	0.58 (0.03)	0.48 (0.02)	1.25 (0.16)	1.35 (0.14)	1.34 (0.15)	0.96 (0.20)	0.44 (0.02)	1.99 (0.25)

[1]Abbreviations are as follows: ANT is anthracene, FLU is fluoranthene, PYR is pyrene, B(a)A is benzo(a)anthracene, CHR is chrysene, B(b)F is benzo(b)fluoranthene, B(k)F is benzo(k)fluoranthene, B(a)P is benzo(a)pyrene, DIB is dibenzo(ah)anthracene, B(g)P is benzo(ghi)perylene, and IND is indeno(123,cd)pyrene

Values in parentheses indicate the standard deviation from 3 measurements

NA – No estimate available

Table A3. Log Soil-Simulated Fluid Partitioning Coefficients (K_{sim}) of PAHs between Soils

Soil	ANT[1]	FLU[1]	PYR[1]	B(a)A[1]	CHR[1]	B(b)F[1]	B(k)F[1]	B(a)P[1]	DIB[1]	B(g)P[1]	IND[1]
BGS 1	2.89 (0.36)	0.74 (0.43)	1.96 (0.03)	2.30 (0.06)	2.20 (0.04)	2.84 (0.10)	2.77 (0.08)	2.84 (0.56)	NA	2.93 (0.05)	NA
BGS 2	2.38 (0.06)	2.24 (0.08)	2.30 (0.04)	2.63 (0.05)	2.67 (0.05)	2.80 (0.03)	2.78 (0.03)	2.78 (0.04)	2.96 (0.04)	2.96 (0.03)	2.87 (0.06)
BGS 3	2.37 (0.10)	2.28 (0.11)	2.35 (0.14)	2.67 (0.15)	2.65 (0.17)	2.79 (0.16)	2.80 (0.14)	2.83 (0.018)	3.07 (0.16)	2.99 (0.15)	2.84 (0.15)
BGS 4	2.22 (0.17)	2.13 (0.21)	2.22 (0.19)	2.53 (0.18)	2.53 (0.18)	2.82 (0.17)	2.73 (0.17)	2.87 (0.016)	3.03 (0.16)	3.00 (0.14)	2.92 (0.16)
BGS 5	2.01 (0.09)	1.86 (0.12)	1.74 (0.13)	2.28 (0.10)	2.26 (0.11)	2.65 (0.09)	2.54 (0.10)	2.76 (0.10)	2.84 (0.06)	2.90 (0.10)	2.74 (0.15)
BGS 6	2.27 (0.10)	2.10 (0.11)	2.17 (0.11)	2.41 (0.14)	2.45 (0.14)	2.69 (0.15)	2.60 (0.11)	2.70 (0.16)	2.77 (0.12)	2.79 (0.12)	2.70 (0.11)
BGS 7	2.73 (0.15)	1.96 (0.14)	2.08 (0.14)	2.32 (0.12)	2.31 (0.14)	2.68 (0.10)	2.56 (0.13)	2.97 (0.012)	2.80 (0.09)	2.87 (0.07)	2.94 (0.18)
BGS 8	2.25 (0.15)	2.11 (0.10)	2.09 (0.11)	2.57 (0.08)	2.52 (0.08)	2.84 (0.05)	2.78 (0.06)	2.90 (0.04)	2.98 (0.09)	2.95 (0.06)	3.01 (0.11)
BGS 9	2.40 (0.29)	1.93 (0.25)	2.10 (0.21)	2.37 (0.14)	2.34 (0.15)	2.68 (0.12)	2.57 (0.10)	2.78 (0.16)	2.71 (0.06)	2.87 (0.10)	2.75 (0.08)
BGS 10	2.30 (0.10)	2.33 (0.14)	2.23 (0.04)	2.58 (0.04)	2.57 (0.04)	2.86 (0.05)	2.76 (0.006)	2.91 (0.06)	3.04 (0.10)	3.04 (0.08)	2.91 (0.10)
BGS 11	2.07 (0.03)	2.01 (0.11)	2.08 (0.11)	2.39 (0.13)	2.39 (0.13)	2.67 (0.14)	2.60 (0.013)	2.67 (0.13)	2.84 (0.12)	2.87 (0.14)	2.80 (0.14)
BGS 12	2.32 (0.34)	2.23 (0.13)	2.24 (0.10)	2.56 (0.06)	2.60 (0.07)	2.82 (0.04)	2.74 (0.034	2.77 (0.04)	2.88 (0.03)	2.93 (0.03)	2.83 (0.04)
WP1	1.08 (0.20)	1.51 (0.07)	1.38 (0.08)	1.74 (0.012)	1.77 (0.12)	2.01 (0.12)	1.99 (0.0311	1.59 (0.58)	2.15 (0.18)	2.15 (0.13)	2.17 (0.12)
GW5	2.36 (0.10)	2.06 (0.23)	2.09 (0.08)	2.38 (0.11)	2.50 (0.12)	2.58 (0.35)	2.58 (0.08)	2.84 (0.17)	NA	2.73 (0.21)	NA

[1]Abbreviations are as follows: ANT is anthracene, FLU is fluoranthene, PYR is pyrene, B(a)A is benzo(a)anthracene, CHR is chrysene, B(b)F is benzo(b)fluoranthene, B(k)F is benzo(k)fluoranthene, B(a)P is benzo(a)pyrene, DIB is dibenzo(ah)anthracene, B(g)P is benzo(ghi)perylene, and IND is indeno(123,cd)pyrene

Values in parentheses indicate the standard deviation from 3 measurements

NA – No estimate available

Table A4. Summary of Collinear Data from Structure Equation Modelling

PAH[1]	Model Parameters			Significant Relationship[2]	P value	Coefficient	Standardized Coefficient
	Chi-square	DF	P-Value				
ANT	3.3	2	0.20	Z_{soil} predicts [Soil]	0.010	0.17	0.51
				TOC predicts [Soil]	0.022	0.71	0.45
				[Soil] predicts AUC	0.087	-0.17	-0.45
				Z_{soil} predicts AUC	0.79	0.008	0.064
				K_{sim} predicts AUC	0.002	-1.055	-0.61
				TOC predicts AUC	0.87	0.023	0.037
FLU	4.8	2	0.10	Z_{soil} predicts [Soil]	0.001	0.31	0.71
				TOC predicts [Soil]	0.18	0.49	0.24
				[Soil] predicts AUC	0.24	0.29	0.41
				Z_{soil} predicts AUC	0.047	-0.2	-0.66
				K_{sim} predicts AUC	0.19	0.14	0.41
				TOC predicts AUC	0.45	-0.35	-0.24
PYR	2.7	2	0.25	Z_{soil} predicts [Soil]	0.001	0.31	0.83
				TOC predicts [Soil]	0.034	0.53	0.28
				[Soil] predicts AUC	0.33	0.30	0.49
				Z_{soil} predicts AUC	0.41	-0.090	-0.39
				K_{sim} predicts AUC	0.17	0.25	0.4
				TOC predicts AUC	0.26	-0.43	-0.37
B(a)A	3.4	2	0.18	Z_{soil} predicts [Soil]	0.001	0.26	0.80
				TOC predicts [Soil]	0.035	0.51	0.30
				[Soil] predicts AUC	0.14	0.25	0.65
				Z_{soil} predicts AUC	0.39	-0.046	-0.37
				K_{sim} predicts AUC	0.25	0.056	0.33
				TOC predicts AUC	0.072	-0.38	-0.57
CHR	3.2	2	0.20	Z_{soil} predicts [Soil]	0.001	0.25	0.79
				TOC predicts [Soil]	0.004	0.60	0.37
				[Soil] predicts AUC	0.069	0.44	0.86
				Z_{soil} predicts AUC	0.21	-0.090	-0.22
				K_{sim} predicts AUC	0.31	0.62	0.31
				TOC predicts AUC	0.078	-0.58	-0.70
B(b)F	3.7	2	0.15	Z_{soil} predicts [Soil]	0.001	0.24	0.69
				TOC predicts [Soil]	0.001	0.81	0.55
				[Soil] predicts AUC	0.41	-0.13	-0.30
				Z_{soil} predicts AUC	0.009	0.12	0.82
				K_{sim} predicts AUC	0.04	0.043	0.42
				TOC predicts AUC	0.12	-0.27	-0.44

Table A4 continued.

B(k)F	3.0	2	0.22	Z_{soil} predicts [Soil]	0.001	0.20	0.69
				TOC predicts [Soil]	0.001	0.66	0.50
				[Soil] predicts AUC	0.96	0.014	0.02
				Z_{soil} predicts AUC	0.33	0.063	0.34
				K_{sim} predicts AUC	0.67	-0.016	-0.10
				TOC predicts AUC	0.14	-0.39	-0.46
B(a)P	3.0	2	0.23	Z_{soil} predicts [Soil]	0.001	0.24	0.67
				TOC predicts [Soil]	0.001	0.74	0.51
				[Soil] predicts AUC	0.91	0.019	0.024
				Z_{soil} predicts AUC	0.001	0.21	0.78
				K_{sim} predicts AUC	0.88	0.004	-0.029
				TOC predicts AUC	0.010	-0.51	-0.46
DIB	7.9	2	0.02	Z_{soil} predicts [Soil]	0.52	0.014	0.14
				TOC predicts [Soil]	0.002	0.79	0.65
				[Soil] predicts AUC	0.43	-0.26	-0.25
				Z_{soil} predicts AUC	0.085	-0.045	-0.43
				K_{sim} predicts AUC	0.095	0.12	0.43
				TOC predicts AUC	0.70	-0.16	-0.13
B(g)P	9.5	2	0.01	Z_{soil} predicts [Soil]	0.024	0.11	0.46
				TOC predicts [Soil]	0.012	0.68	0.51
				[Soil] predicts AUC	0.93	-0.0.24	-0.031
				Z_{soil} predicts AUC	0.65	-0.035	-0.20
				K_{sim} predicts AUC	0.31	0.070	0.44
				TOC predicts AUC	0.90	-0.046	-0.045
IND	6.7	2	0.04	Z_{soil} predicts [Soil]	0.89	0.006	0.033
				TOC predicts [Soil]	0.006	0.61	0.65
				[Soil] predicts AUC	0.23	-0.48	-0.40
				Z_{soil} predicts AUC	0.24	0.083	0.36
				K_{sim} predicts AUC	0.041	0.10	0.71
				TOC predicts AUC	0.75	-0.13	-0.12

[1]Abbreviations are as follows: ANT is anthracene, FLU is fluoranthene, PYR is pyrene, B(a)A is benzo(a)anthracene, CHR is chrysene, B(b)F is benzo(b)fluoranthene, B(k)F is benzo(k)fluoranthene, B(a)P is benzo(a)pyrene, DIB is dibenzo(ah)anthracene, B(g)P is benzo(ghi)perylene, and IND is indeno(123,cd)pyrene

[2]Abbreviations are as follows: Z_{soil} is the soil fugacity capacity, [Soil] is the soil PAH concentration, OC is the soil organic carbon, and AUC is the area under the curve (exposure)

Table A5. P-values from ANOVA comparison of IV AUC`s for weeks one, three, four and five

PAH[1]	Week vs Week	P value
B(a)A	One-Three	0.99
	One-Four	0.91
	One-Five	0.98
	Three-Four	0.98
	Three-Five	0.99
	Four-Five	0.98
CHR	One-Three	0.99
	One-Four	0.94
	One-Five	0.98
	Three-Four	0.99
	Three-Five	0.93
	Four-Five	0.63
B(b)F	One-Three	0.83
	One-Four	0.84
	One-Five	0.96
	Three-Four	0.87
	Three-Five	0.53
	Four-Five	0.96
B(k)F	One-Three	0.97
	One-Four	0.93
	One-Five	0.66
	Three-Four	0.99
	Three-Five	0.47
	Four-Five	0.14
B(a)P	One-Three	0.99
	One-Four	0.93
	One-Five	0.80
	Three-Four	0.99
	Three-Five	0.97
	Four-Five	0.98

Table A6. P-values from ANOVA comparison of WP1 soil AUC`s for weeks one, four and five.

PAH[1]	Week vs Week	P value
B(a)A	One-Four	0.58
	One-Five	0.80
	Four-Five	0.93
CHR	One-Four	0.5
	One-Five	0.92
	Four-Five	0.30
B(b)F	One-Four	0.90
	One-Five	0.64
	Four-Five	0.88
B(k)F	One-Four	0.0001
	One-Five	0.0001
	Four-Five	0.97
B(a)P	One-Four	0.26
	One-Five	0.12
	Four-Five	0.88

Table A7. Soil Locations

Soil	Site
BGS1	Isle of Wight, UK
BGS2	Near Stonehouse, UK
BGS3	Near Stonehouse, UK
BGS4	Isle of Wight, UK
BGS5	Isle of Wight, UK
BGS6	Isle of Wight, UK
BGS7	Isle of Wight, UK
BGS8	Isle of Wight, UK
BGS9	Isle of Wight, UK
BGS10	Sheffield, UK
BGS11	Sheffield, UK
BGS12	Gasworks site, UK
WP1	Holmsund, Sweden
GW2	Gothenburg, Sweden
COT1	Saskatchewan, Canada
COT2	Saskatchewan, Canada
COT3	Saskatchewan, Canada
COT4	Saskatchewan, Canada
COT5	Saskatchewan, Canada

APPENDIX B

CHAPTER 4 SUPPLEMENTAL INFOMRATION

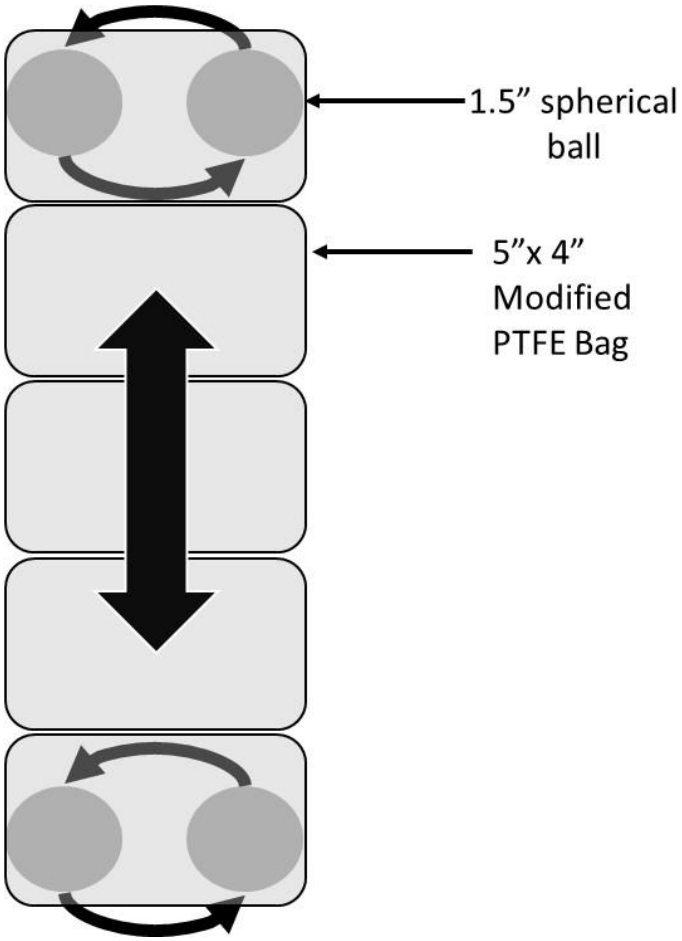

Figure B1. Diagram of the low energy FOREhST massaging method. In the method, 2-1.5” rotating spherical balls move up and down the length of 5 modified polytetrafluoroethylene (PTFE) bags (5”x4”).

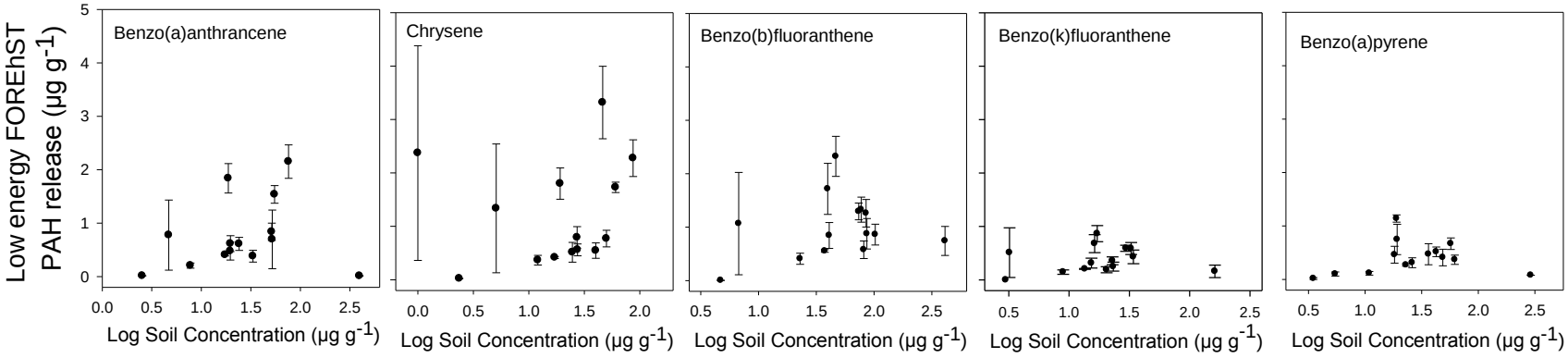

Figure B2. Comparison between low energy FOREhST PAH release and soil concentration of five PAHs in 14 soils historically contaminated with hydrocarbons. Data points represent the mean (n=3) for FOREhST PAH release and error bars represent the standard error of this mean.

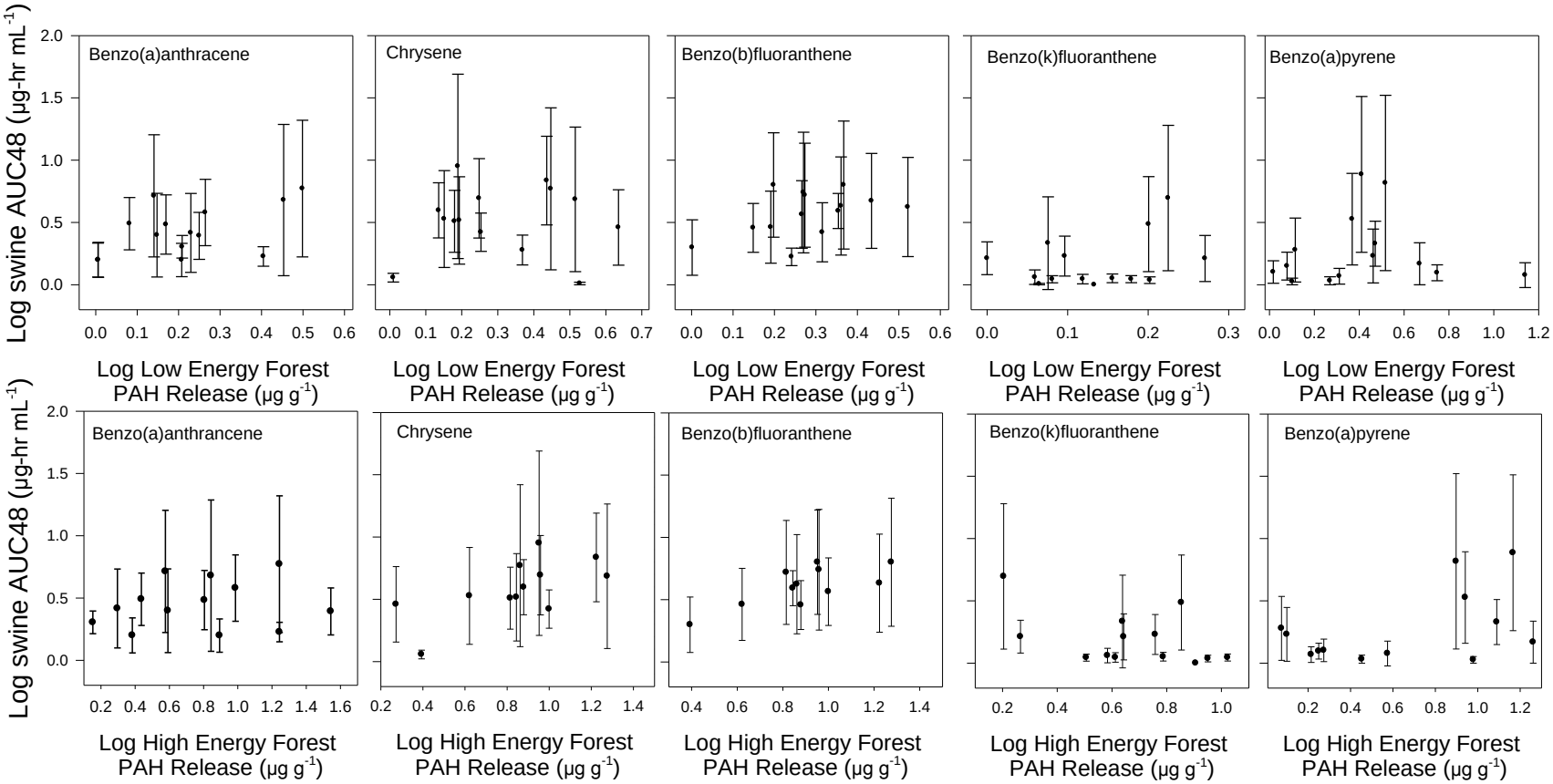

Figure B3. Comparison of Area Under the Curve (AUC) against Low energy FORE(h)ST PAH release (top) and high energy FOREhST release (bot) of 5 PAHs in 14 soils historically contaminated with hydrocarbons. Data points represent the mean (n = 6) of mammalian exposure (AUC48) measured in µg PAH per gram of soil and (n=3) estimates of *in vitro* FORE(h)ST PAH release. Error bars represent the standard error of the mean.

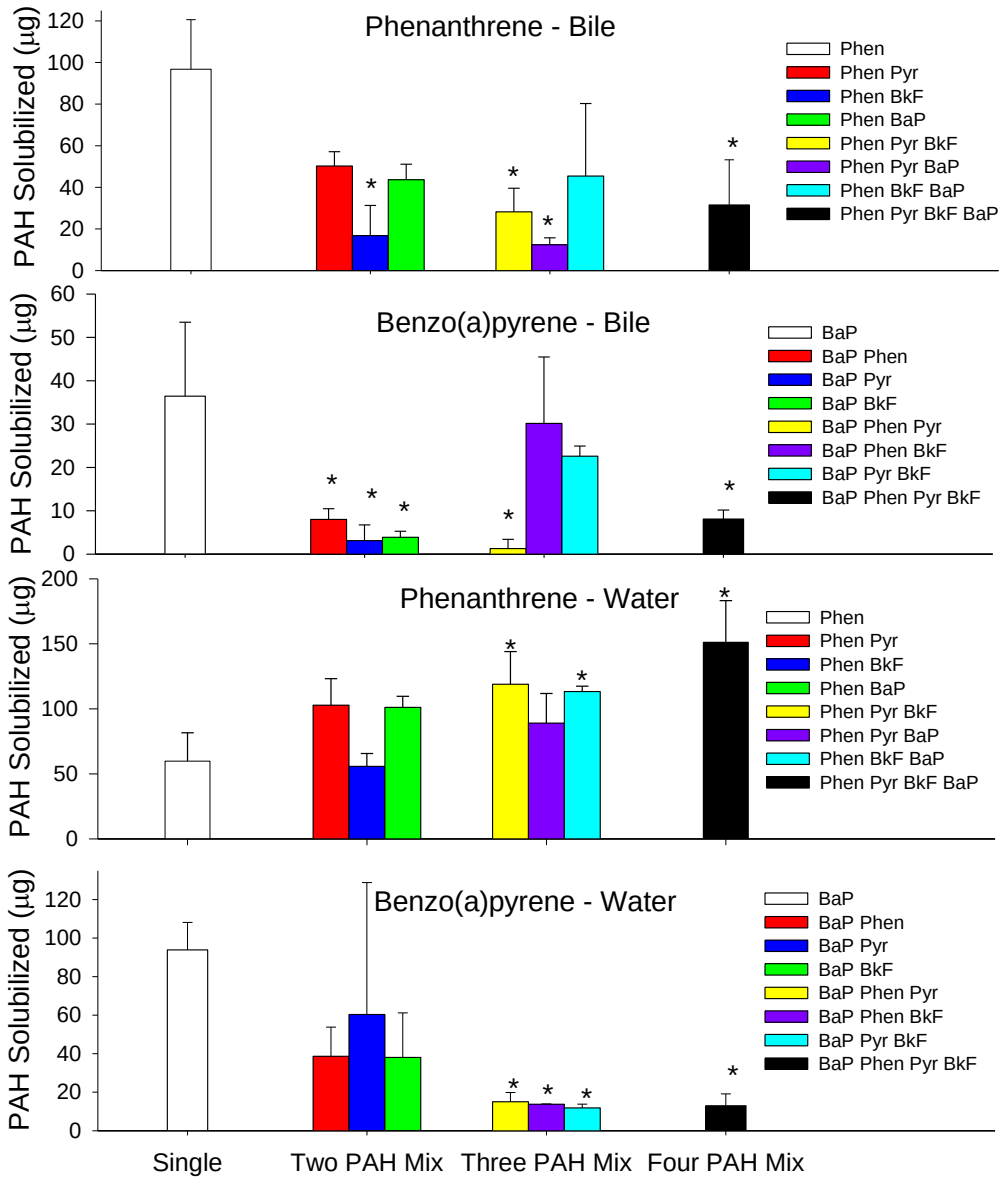

Figure B4. Comparison of phenanthrene and benzo(a)pyrene solubility in both bile (top 2 panels) and water (bottom 2 panels) from single compound to multiple compound mixtures. Significant difference is indicating by '*' at $p < 0.05$. Abbreviations are as follows: Phen is phenanthrene, Pyr is pyrene, BkF is benzo(k)fluoranthene, and B(a)P is benzo(a)pyrene.

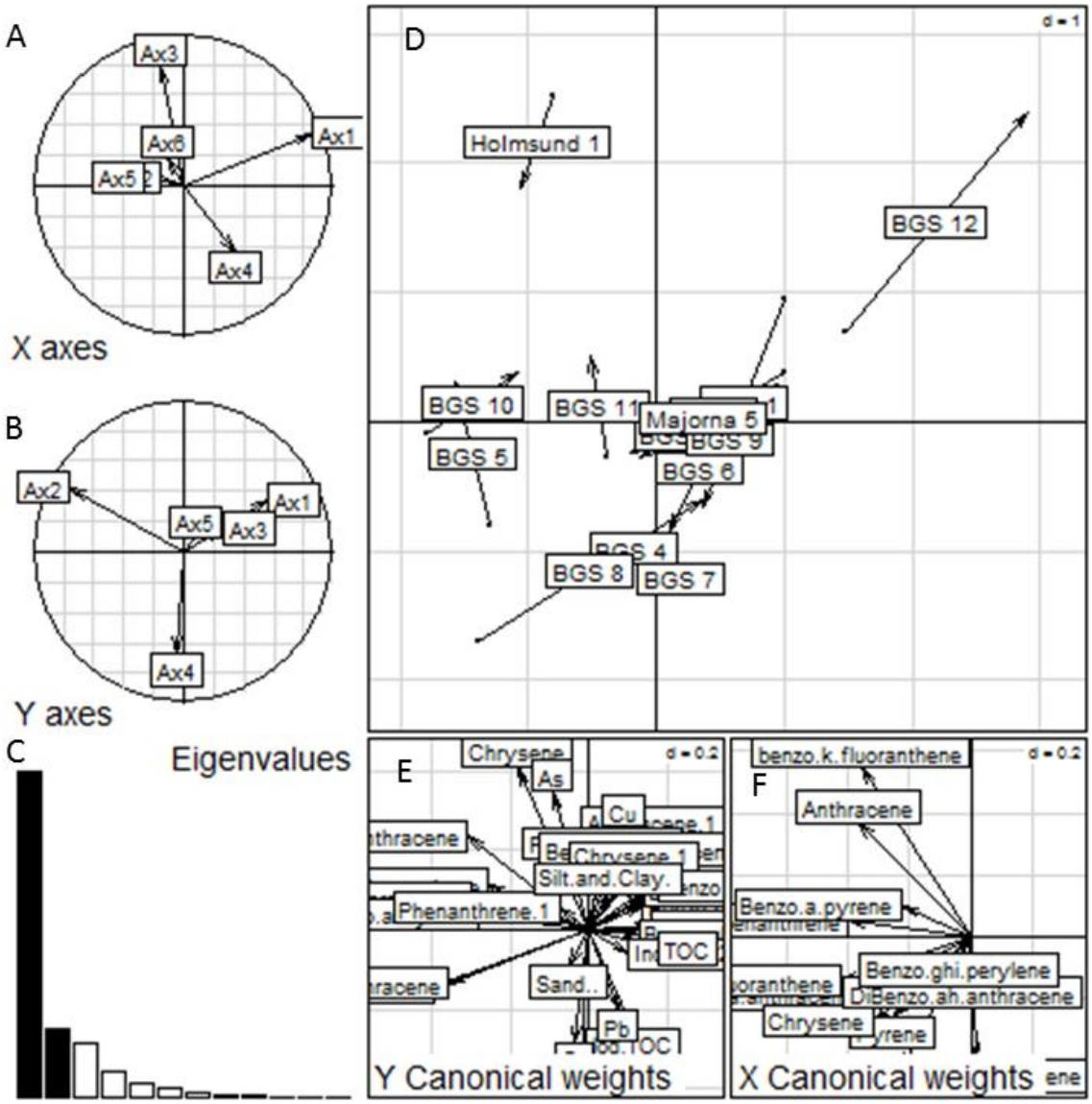

Figure B5. Output of co-inertia analysis. A) Components of the standardized principal component analysis of the PAH bioavailability data set projected on to the co-inertia axes. B) Components of the standardized principal component analysis on the predictor variable (PAH bioaccessibility and soil properties) data set projected on to the co-inertia axes. C) Histogram of the eigenvalues. D) Standardized co-inertia scores of the bioavailability (A) and predictor variable data sets (B) projected on to the co-inertia axes. E) Canonical weights of predictor variables F) canonical weights of PAH bioavailability

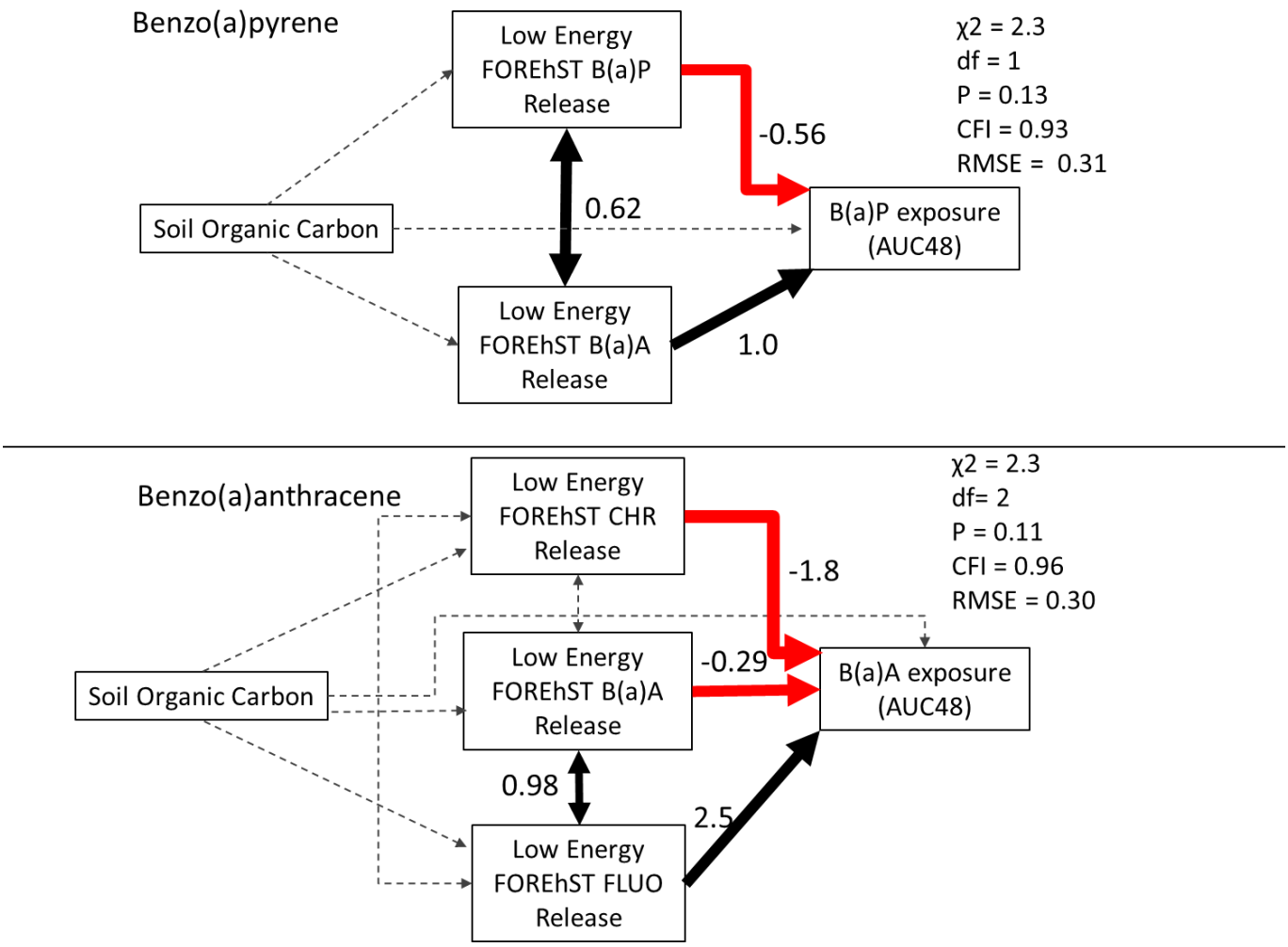

Figure B6. SEM diagram of the relationships between Soil Organic Carbon, FOREhST release of multiple PAHs, and PAH exposure. Single headed arrows indicate that a change in the variable at the tail causes a direct change to the variable at the head. Double headed arrows indicate non-directed causality. Dashed lines indicate a non-significant (P>0.05) path, whereas black arrows indicate a positive relationship and red arrows indicate a negative relationship. Arrow width corresponds to the strength of the relationship between variables with standardized coefficients provided for significant paths.

Table B1. Physiochemical properties of 14 soils used in this study

	Particle Size (%)				Soil Concentration (µg/g)										
	Sand	Silt + Clay	OC[a]	pH	ANT[b]	FLU[b]	PYR[b]	B(a)A[b]	CHR[b]	B(b)F[b]	B(k)F[b]	B(a)P[b]	DIB[b]	B(g)P[b]	IND[b]
BGS1	84	16	1.3	6.7	1.6	1.2	2.7	1.5	1.4	3.7	2.0	2.5	ND	3.1	1.0
BGS2	77	23	8.8	6.7	11	53	76	23	27	84	22	56	47	48	35
BGS3	54	46	8.2	6.5	11	69	77	19	24	86	22	35	40	37	35
BGS4	67	33	6.8	n/a	11	149	125	50	49	101	33	61	61	64	48
BGS5	57	43	3.3	n/a	5.7	88	53	18	18	46	16	18	20	23	22
BGS6	59	41	12	6.5	4.9	63	56	19	26	40	14	17	21	25	20
BGS7	49	51	7.8	6.6	3.3	28	23	6.8	11	22	8	10	14	18	18
BGS8	70	30	13	2.0	4.1	121	76	32	39	80	19	25	24	28	30
BGS9	38	62	3.9	6.2	2.7	30	32	16	16	36	13	22	20	25	19
BGS10	90	10	4.8	6.3	17	289	300	75	86	77	32	41	32	49	37
BGS11	39	61	4.9	6.3	11	136	184	54	60	73	29	48	41	46	39
BGS12	63	37	33	n/a	140	758	582	390	340	410	160	290	170	166	125
WP1	42	58	2.4	5.7	27	213	117	51	45	39	15	18	7.0	5.7	5.6
GW2	59	41	4.6	6.7	1	5.5	4.6	3.7	4.0	5.7	2.2	4.5	7.4	4.3	2.2

[a]Organic carbon reported as percent (w/w).

[b]Abbreviations are as follows: ANT is anthracene, FLU is fluoranthene, PYR is pyrene, B(a)A is benzo(a)anthracene, CHR is chrysene, B(b)F is benzo(b)fluoranthene, B(k)F is benzo(k)fluoranthene, B(a)P is benzo(a)pyrene, DIB is dibenzo(ah)anthracene, B(g)P is benzo(ghi)perylene, and IND is indeno(123,cd)pyrene

ND indicates a non-detection of PAH in soil

Table B2. PAH bioavailability (%) of 14 soils used in this study

Soil	ANT[a]	FLU[a]	PYR[a]	B(a)A[a]	CHR[a]	B(b)F[a]	B(k)F[a]	B(a)P[a]	B(a)A[a]	DIB[a]	B(g)P[a]	IND[a]
BGS1	16	12	13	21.0	5.8	56.6	10.2	0.8	21.0	-	20	0
BGS2	1.7	0.3	0.07	1.5	5.4	2.5	0.0	0.6	1.5	0	0.06	0
BGS3	5.2	1.0	0.5	6.4	5.9	3.5	2.5	2.2	6.4	9.9	-	0
BGS4	55	3.9	4.1	3.2	5.0	3.2	0.3	2.6	3.2	1.5	2.0	3.2
BGS5	31	4.2	14	12.4	16.8	5.0	3.1	0.7	12.4	2.7	2.2	4.1
BGS6	33	2.5	5.3	3.2	3.9	7.8	0.6	2.7	3.2	0.1	0.6	4.3
BGS7	38	30.9	25	17.9	16.6	6.0	1.5	6.1	17.9	9.9	0.7	2.1
BGS8	87	2.5	10	7.5	12.6	4.7	4.7	0.2	7.5	0.1	0.9	17
BGS9	14	0	9.7	5.3	9.2	3.7	0.7	2.2	5.3	0.8	1.1	0
BGS10	16	1.7	2.3	6.2	6.5	5.5	5.2	9.0	6.2	0.06	0.3	0.3
BGS11	16	2.6	2.2	0.7	6.1	3.2	0.2	9.5	0.7	1.8	2.2	0.1
BGS12	0.2	0	0.2	0.1	0.004	0.1	0.01	0.1	0.1	0	0.07	0
WP1	24	0.3	1.2	2.4	3.2	8.0	22.9	33.0	2.4	9.3	14	2.6
GW2	85	39.7	7.4	19.2	46.7	14.3	3.9	1.0	19.2	0	30	16

[a]Abbreviations are as follows: ANT is anthracene, FLU is fluoranthene, PYR is pyrene, B(a)A is benzo(a)anthracene, CHR is chrysene, B(b)F is benzo(b)fluoranthene, B(k)F is benzo(k)fluoranthene, B(a)P is benzo(a)pyrene, DIB is dibenzo(ah)anthracene, B(g)P is benzo(ghi)perylene, and IND is indeno(123,cd)pyrene

Table B3. Soil PAH release in the low energy FOREhST model across 14 soils

Soil	ANT[a]	FLU[a]	PYR[a]	B(a)A[a]	CHR[a]	B(b)F[a]	B(k)F[a]	B(a)P[a]	DIB[a]	B(g)P[a]	IND[a]
BGS1	0.0062 (0.0035)	0.10 (0.0040)	0.035 (0.0047)	0.015 (0.0023)	0.023 (0.0066)	0.0037 (0.00003)	NA	0.017 (0.030)	0.00076 (0.0013)	NA	0.00018 (0.00032)
BGS2	0.25 (0.060)	2.1 (0.62)	2.4 (0.68)	0.61 (0.21)	0.56 (0.19)	1.26 (0.45)	0.36 (0.13)	0.67 (0.19)	0.63 (0.16)	0.40 (0.16)	0.34 (0.13)
BGS3	0.17 (0.11)	1.9 (0.98)	1.4 (0.69)	0.48 (0.29)	0.51 (0.32)	0.88 (0.49)	0.25 (0.15)	0.47 (0.34)	0.52 (0.33)	0.32 (0.20)	0.25 (0.14)
BGS4	0.11 (0.026)	5.1 (1.2)	3.2 (0.85)	0.84 0.28)	0.77 (0.27)	0.86 (0.34)	0.43 (0.22)	0.37 (0.15)	0.53 (0.22)	0.38 (0.16)	0.33 (0.14)
BGS5	0.33 (0.044)	9.2 (2.5)	3.2 (2.6)	1.8 (0.48)	1.8 (0.51)	2.3 (0.65)	0.87 (0.26)	1.1 (0.12)	1.5 (0.33)	1.2 (0.29)	0.97 (0.30)
BGS6	0.11 (0.033)	3.0 (0.95)	2.3 (0.81)	0.62 (0.26)	0.79 (0.35)	0.85 (0.42)	0.31 (0.16)	0.46 (0.27)	0.50 (0.26)	0.43 (0.23)	0.38 (0.20)
BGS7	0.021 (0.012)	1.5 (0.57)	0.92 (0.37)	0.21 (0.083)	0.37 (0.16)	0.41 (0.18)	0.15 (0.071)	0.11 (0.060)	0.24 (0.11)	0.25 (0.11)	0.18 (0.081)
BGS8	0.045 (0.028)	2.3 (0.83)	1.1 (0.52)	0.38 (0.19)	0.55 (0.25)	0.58 (0.28)	0.19 (0.098)	0.31 (0.16)	0.31 (0.16)	0.22 (0.114)	0.19 (0.088)
BGS9	0.040 (0.0059)	1.4 (0.12)	0.98 (0.082)	0.41 (0.032)	0.42 (0.032)	0.55 (0.042)	0.20 (0.014)	0.27 (0.039)	0.31 (0.026)	0.23 (0.017)	0.20 (0.015)
BGS10	0.364 (0.096	13 (2.3)	0.00099 (0.0017)	2.2 (0.54)	2.3 (0.59)	1.33 (0.40)	0.59 (0.19)	0.52 (0.16)	0.58 (0.18)	0.52 (0.17)	0.48 (0.14)
BGS11	0.15 (0.081)	6.9 (0.20)	0.043 (0.019)	1.5 (0.29)	1.7 0.17)	1.3 (0.27)	0.59 (0.099)	0.41 (0.27)	0.60 (0.15)	0.52 (0.12)	0.53 (0.096)
BGS12	ND	ND	ND	0.012 (0.013)	2.4 (3.5)	0.74 (0.47)	0.16 (0.20)	0.078 (0.0013)	5.0 (1.3)	3.7 (1.2)	3.3 (1.0)
WP1	0.37 (0.65)	4.0 (6.9)	0.029 (0.050)	0.70 (0.95)	3.3 (1.2)	1.7 (0.83)	0.68 0.29)	0.75 (0.49)	0.24 (0.12)	0.14 (0.085)	0.15 (0.082)
GW2	0.083 (0.081)	3.0 (4.7)	1.8 (2.8)	0.78 (1.1)	1.3 (2.1)	1.1 (1.7)	0.51 (0.80)	0.10 (0.067)	0.74 (1.1)	0.37 (0.54)	0.38 (0.60)

[a]Abbreviations are as follows: ANT is anthracene, FLU is fluoranthene, PYR is pyrene, B(a)A is benzo(a)anthracene, CHR is chrysene, B(b)F is benzo(b)fluoranthene, B(k)F is benzo(k)fluoranthene, B(a)P is benzo(a)pyrene, DIB is dibenzo(ah)anthracene, B(g)P is benzo(ghi)perylene, and IND is indeno(123,cd)pyrene

Values in parentheses indicate the standard deviation from 3 measurements

NA – No estimate available

Table B4. Soil PAH release in the high energy FOREhST model across 13 soils

Soil	ANT[a]	FLU[a]	PYR[a]	B(a)A[a]	CHR[a]	B(b)F[a]	B(k)F[a]	B(a)P[a]	DIB[a]	B(g)P[a]	IND[a]
BGS1	4.9 (3.0)	3.3 (2.2)	2.0 (2.1)	1.4 (1.0)	1.5 (0.89)	1.9 (1.3)	0.84 (0.53)	0.88 (0.92)	1.3 (0.87)	1.3 (0.79)	1.0 (0.64)
BGS2	29 (6.4)	24 (5.9)	25 (6.6)	6.8 (1.7)	6.0 (1.5)	25 (6.0)	7.1 (1.7)	17 (4.2)	19 (4.5)	16 (3.7)	12 (2.6)
BGS3	25 (2.9)	15 (1.9)	24 (2.7)	5.4 (0.69)	5.5 (0.62)	18 (2.4)	4.7 (0.63)	11 (1.3)	13 (1.9)	11 (1.5)	8.7 (1.1)
BGS4	39 (34)	26 (23)	24 (21)	8.7 (7.5)	8.1 (7.0)	14 (12)	5.1 (4.4)	7.7 (6.7)	9.4 (6.4)	8.5 (7.4)	6.5 (5.5)
BGS5	34 (4.4)	23 (2.9)	12 (2.0)	6.0 (0.85)	6.3 (0.84)	7.9 (1.1)	3.4 (0.43)	2.8 (0.70)	5.1 (0.60)	4.9 (0.63)	3.9 (0.54)
BGS6	30 (3.6)	14 (1.2)	4.1 (5.5)	0.42 (0.66)	9.0 (0.99)	8.2 (0.83)	3.1 (0.28)	0.26 (0.064)	6.4 (0.65)	5.5 (0.54)	4.5 (0.39)
BGS7	22 (20)	12 (9.8)	0.98 (1.7)	1.7 (1.6)	6.6 (5.8)	5.9 (4.7)	2.8 (2.4)	0.19 (0.17)	4.1 (3.1)	4.2 (2.7)	3.4 (2.2)
BGS8	25 (14)	14 (6.9)	1.6 (1.4)	2.8 (3.3)	8.0 (4.1)	7.4 (37)	3.4 (1.7)	0.64 (0.80)	5.0 (2.0)	4.5 (1.6)	3.7 (1.3)
BGS9	10 (1.8)	6 (1.1)	3.7 (0.84)	2.9 (0.72)	3.2 (0.52)	5.1 (1.2)	2.2 (0.41)	1.8 (1.0)	3.4 (0.74)	3.6 (0.73)	2.8 (0.62)
BGS10	82 (8.5)	74 (9.0)	28 (21)	17 (2.5)	18 (2.1)	14 (1.9)	6.1 (0.66)	6.9 (2.1)	8.8 (1.3)	8.4 (1.1)	7.3 (0.78)
BGS11	55 (2.6)	57 (2.6)	33 (1.6)	17 (0.75)	16 (0.70)	19 (0.83)	7.9 (0.33)	14 (0.66)	13 (0.62)	12 (0.34)	10 (0.40)
BGS12	NA	NA	NA	NA	NA	NA	NA	NA	NA	NA	NA
WP1	149 (14)	96 (9.2)	113 (17)	34 (4.0)	31 (3.3)	23 (3.0)	9.5 (1.2)	8.5 (1.8)	5.9 (0.74)	5.6 (0.82)	3.1 (0.39)
GW2	2.3 (1.1)	1.4 (0.68)	2.6 (1.7)	0.98 (0.52)	0.87 (0.45)	1.2 (0.69)	0.60 (0.32)	0.78 (0.50)	1.3 (0.76)	1.1 (0.61)	0.28 (0.30)

[a]Abbreviations are as follows: ANT is anthracene, FLU is fluoranthene, PYR is pyrene, B(a)A is benzo(a)anthracene, CHR is chrysene, B(b)F is benzo(b)fluoranthene, B(k)F is benzo(k)fluoranthene, B(a)P is benzo(a)pyrene, DIB is dibenzo(ah)anthracene, B(g)P is benzo(ghi)perylene, and IND is indeno(123,cd)pyrene

Values in parentheses indicate the standard deviation from 3 measurements

NA – No estimate available

Table B5. PCA of PAH exposure (AUC48)

	PC1	PC2	PC3	PC4	PC5	PC6
Phenanthrene	-0.12	-0.17	-0.09	0.20	-0.79	-0.36
Anthracene	-0.29	0.07	0.55	0.091	0.065	0.15
Fluoranthene	-0.28	-0.12	-0.33	0.29	0.039	0.70
Pyrene	-0.42	-0.19	-0.20	-0.0056	-0.10	0.11
Benzo(a)anthracene	-0.41	0.053	-0.053	-0.031	-0.25	0.071
Chrysene	-0.41	0.0076	-0.18	-0.15	0.14	-0.26
Benzo(b)fluoranthene	-0.38	0.30	0.071	-0.037	0.13	-0.26
Benzo(k)fluoranthene	-0.19	0.16	0.62	0.25	-0.12	0.12
Benzo(a)pyrene	-0.18	0.08	-0.22	0.60	0.43	-0.40
Dibenzo(ah)anthracene	0.035	0.62	-0.21	-0.0018	-0.17	0.21
Benzo(ghi)perylene	0.061	0.64	-0.15	-0.06	-0.13	-0.016
Indeno(123-cd)pyrene	-0.31	-0.05	-0.00071	-0.64	0.11	-0.032
Standard deviation	2.12	1.48	1.31	1.10	1.06	0.800
Proportion of Variance	0.376	0.183	0.144	0.101	0.093	0.053
Cumulative Proportion	0.376	0.559	0.702	0.803	0.897	0.949

Table B6. PCA of predictor variables, including PAH bioaccessibility and soil properties

	PC1	PC2	PC3	PC4	PC5
FOREhST Phenanthrene	-0.077	-0.26	-0.32	0.018	-0.066
FOREhST Anthracene	-0.053	-0.35	0.13	-0.0076	0.076
FOREhST Fluoranthene	-0.038	-0.30	0.26	0.11	-0.24
FOREhST Pyrene	-0.068	-0.047	-0.093	0.55	0.28
FOREhST Benzo(a)anthracene	-0.048	-0.32	0.20	0.10	-0.22
FOREhST Chrysene	0.098	-0.30	-0.034	-0.20	-0.16
FOREhST Benzo(b)fluoranthene	-0.014	-0.38	-0.064	0.066	0.091
FOREhST Benzo(k)fluoranthene	-0.046	-0.38	-0.038	0.070	-0.077
FOREhST Benzo(a)pyrene	-0.058	-0.33	-0.032	0.14	0.29
FOREhST Dibenzo(ah)anthracene	0.24	-0.037	-0.055	0.0047	0.098
FOREhST Benzo(ghi)perylene	0.24	-0.050	-0.050	0.018	0.080
FOREhST Indeno(123-cd)pyrene	0.24	-0.047	-0.050	0.0032	0.051
Soil Phenanthrene	0.19	-0.11	0.29	-0.034	-0.17
Soil Anthracene	0.25	-0.013	-0.049	-0.092	0.044
Soil Fluoranthene	0.24	-0.073	0.042	-0.074	-0.047
Soil Pyrene	0.24	-0.081	0.094	-0.057	-0.13
Soil Benzo(a)anthracene	0.25	-0.014	-0.013	-0.065	-0.013
Soil Chrysene	0.25	-0.021	0.0072	-0.057	-0.041
Soil Benzo(b)fluoranthene	0.25	0.0012	-0.024	0.021	0.071
Soil Benzo(k)fluoranthene	0.25	-0.0086	-0.021	-0.0062	0.022
Soil Benzo(a)pyrene	0.25	0.0067	-0.031	0.0053	0.046
Soil Dibenzo(ah)anthracene	0.24	0.0054	-0.036	0.10	0.048
Soil Benzo(ghi)perylene	0.24	-0.0011	0.0089	0.11	0.0063
Soil Indeno(123-cd)pyrene	0.24	-0.0045	-0.0056	0.11	0.017
Soil organic carbon	0.23	0.085	-0.068	0.087	0.010
Log Soil organic carbon	0.19	0.085	-0.090	0.25	-0.081
Sand	0.028	0.048	0.54	0.14	0.14
Silt and Clay	-0.027	-0.050	-0.54	-0.13	-0.14
As	0.042	-0.24	-0.16	-0.036	0.46
Cr	-0.047	0.071	-0.11	0.37	-0.35
Cu	0.054	-0.099	-0.14	-0.0031	-0.45
Pb	0.051	0.068	-0.095	0.55	-0.14
Standard deviation	3.98	2.53	1.68	1.49	1.27
Proportion of Variance	0.494	0.201	0.088	0.070	0.0500
Cumulative Proportion	0.494	0.695	0.783	0.853	0.903

Table B7. Summary of Canonical Weights from Co-Inertia Modelling

Predictive Factor	X Canonical Weight	Y Canonical Weight	Strength[a]
FOREhST Chrysene	-0.181	0.407	0.446
FOREhST Fluoranthene	-0.396	-0.144	0.421
FOREhST Anthracene	-0.308	0.235	0.388
FOREhST Benzo(a)anthracene	-0.356	-0.136	0.381
Soil [As]	-0.092	0.348	0.360
FOREhST Pyrene	-0.0162	-0.349	0.349
FOREhST Benzo(k)fluoranthene	-0.299	0.0815	0.310
Soil [Cr]	-0.0380	-0.285	0.287
Soil [Anthracene]	0.165	0.232	0.285
FOREhST Benzo(a)pyrene	-0.281	0.0376	0.284
FOREhST Benzo(b)fluoranthene	-0.258	0.112	0.281
Log Soil Organic Carbon	0.114	-0.252	0.277
Soil [Cu]	0.0855	0.259	0.273
Soil [Pb]	0.0756	-0.202	0.216
Soil [Benzo(a)anthracene]	0.134	0.163	0.211
Soil [Benzo(a)pyrene]	0.176	0.109	0.207
Soil Organic Carbon	0.180	-0.0476	0.186
FOREhST Dibenzo(ah)anthracene	0.160	0.0902	0.184
Soil [Chrysene]	0.114	0.142	0.182
Soil [Fluoranthene]	0.0323	0.179	0.182
Soil [Benzo(k)fluoranthene]	0.140	0.0987	0.171
FOREhST Phenanthrene	-0.161	0.0556	0.170
FOREhST Indeno(123-cd)pyrene	0.146	0.0839	0.168
Soil [Dibenzo(ah)anthracene]	0.158	0.0103	0.159
FOREhST Benzo(ghi)perylene	0.139	0.0647	0.153
Soil [Benzo(b)fluoranthene]	0.137	0.0589	0.149
Soil [Pyrene]	0.0216	0.132	0.134
Soil [Benzo(ghi)perylene]	0.130	-0.0143	0.130
Soil [Indeno(123-cd)pyrene]	0.103	-0.0622	0.120
Sand	-0.0509	-0.0913	0.105
Silt and Clay	0.0496	0.0891	0.102
Soil [Phenanthrene]	-0.0750	0.0541	0.0925

[a] Strength calculated as the square root of the sum of the squares for the X and Y canonical weights (Strength = $\sqrt{(\text{X canonical weight}^2 + \text{Y canonical weight}^2)}$).

Table B8. Summary of Collinear Data from Structure Equation Modelling

PAH	Model Parameters					Significant Relationship	P-value	Coefficient	Standardized Coefficient
	Chi-square	DF	P-Value	CFI	RMSE				
B(a)A	4.5	2	0.11	0.96	0.30	$B(a)A_{FOR}$ predicts AUC	0.01	-4.1	-1.8
						CHR_{FOR} predicts AUC	0.088	-0.45	-0.29
						FLU_{FOR} predicts AUC	0.001	1.1	2.5
						OC predicts AUC	0.62	0.014	0.075
						OC predicts $B(a)A_{FOR}$	0.40	-0.004	-0.048
						$B(a)A_{FOR}$ -FLU_{FOR} covariance	0.01	2.1	0.98
B(a)P	2.3	1	0.13	0.93	0.31	$B(a)P_{FOR}$ predicts AUC	0.03	-4.1	-0.56
						$B(a)A_{FOR}$ predicts AUC	0.001	3.5	1.0
						OC predicts AUC	0.62	0.021	0.075
						OC predicts $B(a)P_{FOR}$	0.74	-0.003	-0.070
						$B(a)P_{FOR}$ -$B(a)A_{FOR}$ covariance	0.05	0.112	0.62

Abbreviations are as follows: FLU is fluoranthene, B(a)A is benzo(a)anthracene, CHR is chrysene, B(a)P is benzo(a)pyrene, FOR represents the bioaccessible fraction of a PAH from low energy FOREhST model, and OC is the soil organic carbon

APPENDIX C

CHAPTER 5 SUPPLEMENTAL INFOMRATION

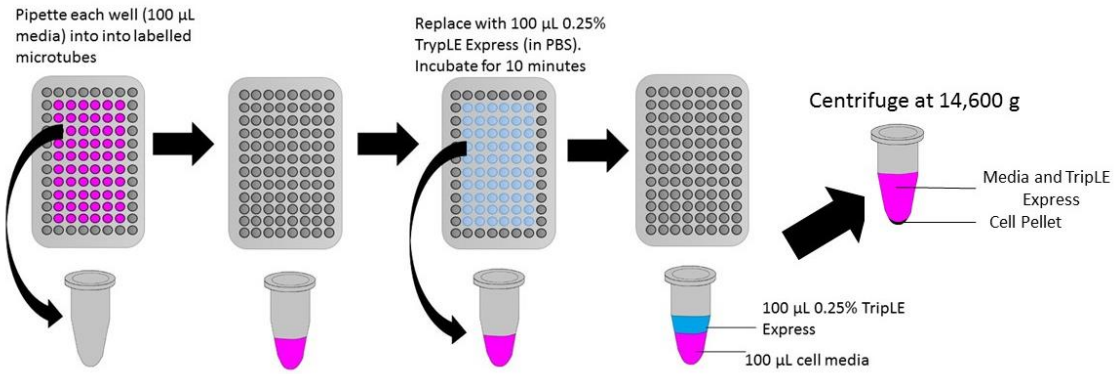

Figure C1. Diagram of PAH recovery from plastic 96-well plates. After incubation, media was removed into microtube. To each well, 100 µL of 0.25% TrypLE Express was added and incubated for 10 minutes. TrypLE Express was removed and added to corresponding mircotube prior to centrifugation.

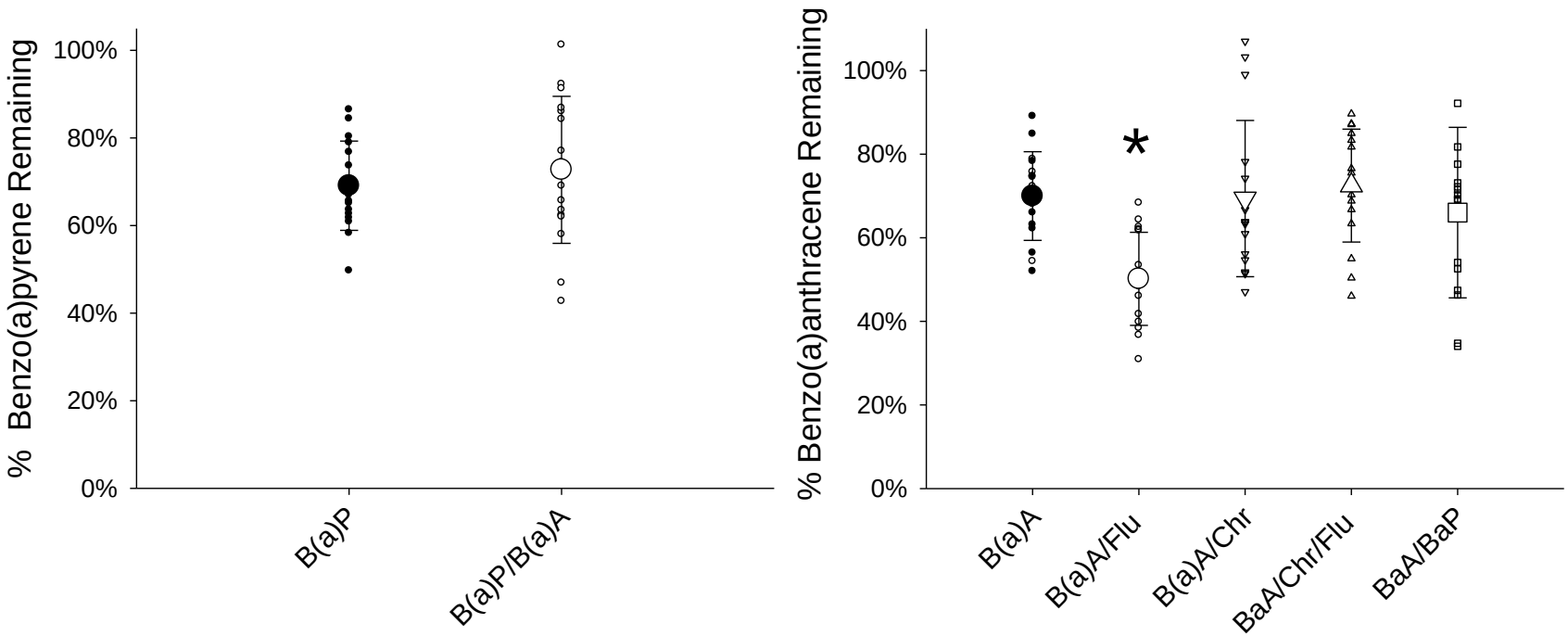

Figure C2. Percentage of benzo(a)pyrene (left) or benzo(a)anthracene (right) remaining in cells and media after incubation 1 hour incubation. `*`denotes a significant difference at $p < 0.05$. Comparisons were made to the recovery of single compound mixtures at the given time point. Small symbols represent the value of individual replicates while the large symbols represents the mean (n = 15) and error bars were the standard deviation of this mean. The percentage of PAH remaining was calculated as the total amount recovered divided by the total dose. The total amount recovered was corrected to parallel abiotic control experiments. .Abbreviations are as follows: Flu is fluoranthene, B(a)A is benzo(a)anthracene, Chr is chrysene, and B(a)P is benzo(a)pyrene.

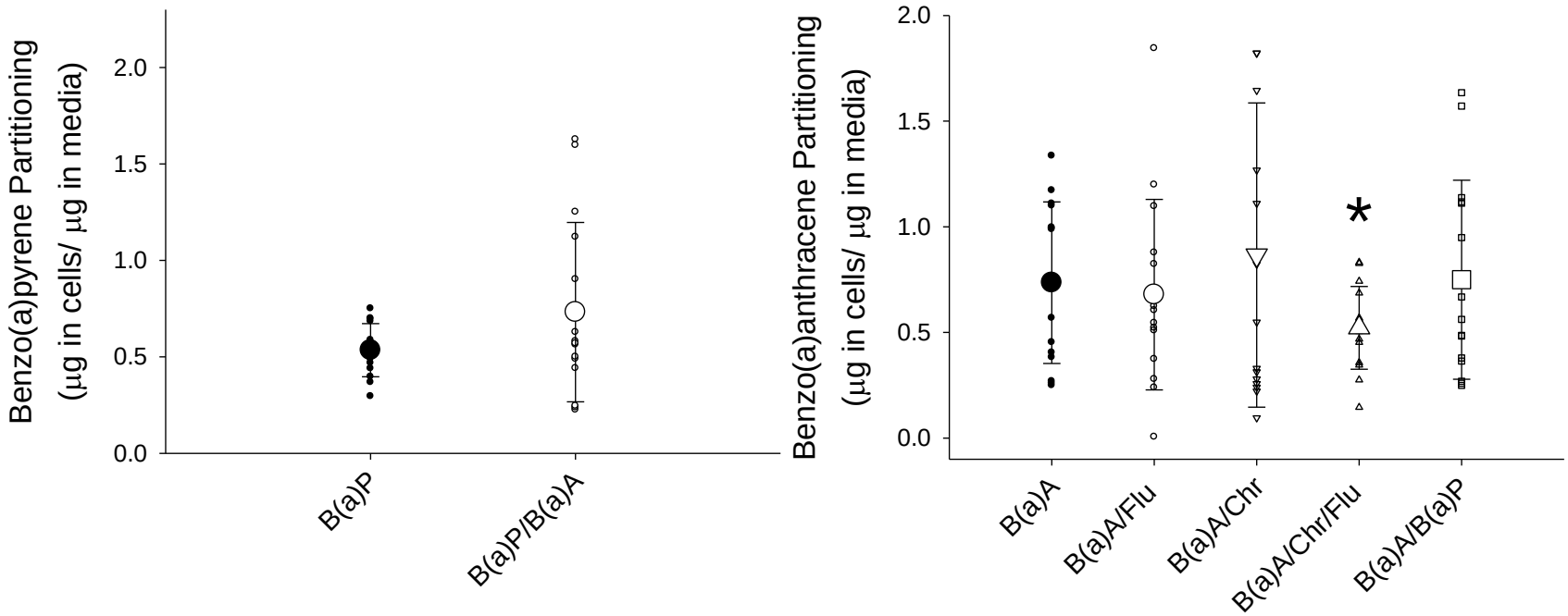

Figure C3. Partitioning of benzo(a)pyrene (left) and benzo(a)anthracene (right) between cells and media based on PAH mixture after 1 hour incubation. `*`denotes a significant difference at $p < 0.05$. Significant difference was compared the partitioning of single a compound at the given time point. Small symbols represent the value of individual replicates while the large symbols represents the mean (n = 15) and error bars were the standard deviation of this mean. The total amount recovered was corrected to parallel abiotic control experiments. Abbreviations are as follows: Flu is fluoranthene, B(a)A is benzo(a)anthracene, Chr is chrysene, and B(a)P is benzo(a)pyrene.